GOLDEN RIDGE RESOURCES

2011 Assessment Report

Elko Project, Yukon Canada

Comprised of: Cow 1-38 claims (YD 08099-08100, YD 08575-08610), Elko 1-67 claims (YD 58651-58717) and Elko 68-177 (YD 110388-110497)

NTS 106D/06 and 106D/07
Mayo Mining District
Yukon Territory, Canada
64º18'N Lat., 135º02'W Long

For Work Performed During:
August 8th to 12th, 2011

By
Golden Ridge Resources
110-2300 Carrington Rd
West Kelowna, BC, V4T 2N6

On Behalf of Registered Owners:
Cathro Resource Corp.
And
Cazador Resources Ltd.

Report Prepared By:
Kevin E Piepgrass
February 14, 2012

Table of Contents

1.0 SUMMARY AND INTRODUCTION 1

2.0 PROJECT LOCATION AND LAND STATUS 1

3.0 ACCESS 8

4.0 PREVIOUS WORK 9

5.0 REGIONAL GEOLOGY AND MINERAL DEPOSITS 9

6.0 REGIONAL GEOPHYSICS 10

7.0 2011 WORK PROGRAM 13

8.0 RESULTS AND INTERPRETATION 13

9.0 SUMMARY AND RECOMMENDATIONS 16

10.0 STATEMENT OF EXPENDITURES 17

11.0 STATEMENT OF QUALIFICATIONS 18

12.0 REFERENCES 19

FIGURE 1 ELKO PROPERTY LOCATION MAP 2
FIGURE 2 ELKO CLAIM MAP 8
FIGURE 3 ELKO REGIONAL GEOLOGY 11
FIGURE 4 ELKO REGIONAL TOTAL FIELD AEROMAGNETICS (FROM YUKON GEOLOGICAL SURVEY) 12
FIGURE 5 ELKO APPARENT RESISTIVITY, 7200 COPLANAR 14
FIGURE 6 ELKO RESIDUAL MAGNETIC FIELD 15

TABLE 1 ELKO PROPERTY LIST OF CLAIMS 3
TABLE 2 RECOMMENDED BUDGET FOR 2012 17

1. SUMMARY AND INTRODUCTION

A DIGHEM V electromagnetic/resistivity/magnetic survey, conducted by Fugro Airborne Surveys Corp, was flown over the Elko property between August 8th and August 12th 2011. The objective of the 2011 program was to follow up on encouraging geochemical sampling completed from 2010. The survey was successful in delineating several conductive and magnetic trends similar in orientation to that of the known Rau Trend.

2. PROJECT LOCATION AND LAND STATUS

The Elko property (Figure 1) is located approximately 45 km NNE of Keno City in the Mayo Mining Division on NTS map sheet 106D/06 (approximately 64º18'N, l35º02'W).

The project area includes the Elko quartz claim groups Elko 1 – 67 and Elko 68 – 177 and the Cow 1-38 quartz claim group. The total area of the project claim groups is approximately 4350 Ha (Table 1; Figure 2). The claims are held in the name of Michael S. Cathro, Adam R. Travis and Cathro Resources Corp.

Golden Ridge Resources has entered into an option agreement allowing them to earn 100% interest of the Elko property over a four year period.

The property is not subject to any land restrictions.

Figure 1 Elko property location map

Table 1 Elko property list of claims

Grant #	Claim Name	Claim #	ClaimOwner
YD08099	Cow	1	Adam R. Travis - 100%
YD08100	Cow	2	Adam R. Travis - 100%
YD08575	Cow	3	Adam R. Travis - 100%
YD08576	Cow	4	Adam R. Travis - 100%
YD08577	Cow	5	Adam R. Travis - 100%
YD08578	Cow	6	Adam R. Travis - 100%
YD08579	Cow	7	Adam R. Travis - 100%
YD08580	Cow	8	Adam R. Travis - 100%
YD08581	Cow	9	Adam R. Travis - 100%
YD08582	Cow	10	Adam R. Travis - 100%
YD08583	Cow	11	Adam R. Travis - 100%
YD08584	Cow	12	Adam R. Travis - 100%
YD08585	Cow	13	Adam R. Travis - 100%
YD08586	Cow	14	Adam R. Travis - 100%
YD08587	Cow	15	Adam R. Travis - 100%
YD08588	Cow	16	Adam R. Travis - 100%
YD08589	Cow	17	Adam R. Travis - 100%
YD08590	Cow	18	Adam R. Travis - 100%
YD08591	Cow	19	Adam R. Travis - 100%
YD08592	Cow	20	Adam R. Travis - 100%
YD08593	Cow	21	Adam R. Travis - 100%
YD08594	Cow	22	Adam R. Travis - 100%
YD08595	Cow	23	Adam R. Travis - 100%
YD08596	Cow	24	Adam R. Travis - 100%
YD08597	Cow	25	Adam R. Travis - 100%
YD08598	Cow	26	Adam R. Travis - 100%
YD08599	Cow	27	Adam R. Travis - 100%
YD08600	Cow	28	Adam R. Travis - 100%
YD08601	Cow	29	Adam R. Travis - 100%
YD08602	Cow	30	Adam R. Travis - 100%
YD08603	Cow	31	Adam R. Travis - 100%
YD08604	Cow	32	Adam R. Travis - 100%
YD08605	Cow	33	Adam R. Travis - 100%
YD08606	Cow	34	Adam R. Travis - 100%
YD08607	Cow	35	Adam R. Travis - 100%
YD08608	Cow	36	Adam R. Travis – 100%
YD08609	Cow	37	Adam R. Travis – 100%
YD08610	Cow	38	Adam R. Travis – 100%
YD58651	Elko	1	Michael S. Cathro – 100%
YD58652	Elko	2	Michael S. Cathro – 100%
YD58653	Elko	3	Michael S. Cathro – 100%
YD58654	Elko	4	Michael S. Cathro – 100%

Grant #	Claim Name	Claim #	ClaimOwner
YD58655	Elko	5	Michael S. Cathro – 100%
YD58656	Elko	6	Michael S. Cathro – 100%
YD58657	Elko	7	Michael S. Cathro – 100%
YD58658	Elko	8	Michael S. Cathro – 100%
YD58659	Elko	9	Michael S. Cathro – 100%
YD58660	Elko	10	Michael S. Cathro – 100%
YD58661	Elko	11	Michael S. Cathro – 100%
YD58662	Elko	12	Michael S. Cathro – 100%
YD58663	Elko	13	Michael S. Cathro – 100%
YD58664	Elko	14	Michael S. Cathro – 100%
YD58665	Elko	15	Michael S. Cathro – 100%
YD58666	Elko	16	Michael S. Cathro – 100%
YD58667	Elko	17	Michael S. Cathro – 100%
YD58668	Elko	18	Michael S. Cathro – 100%
YD58669	Elko	19	Michael S. Cathro – 100%
YD58670	Elko	20	Michael S. Cathro – 100%
YD58671	Elko	21	Michael S. Cathro – 100%
YD58672	Elko	22	Michael S. Cathro – 100%
YD58673	Elko	23	Michael S. Cathro – 100%
YD58674	Elko	24	Michael S. Cathro – 100%
YD58675	Elko	25	Michael S. Cathro – 100%
YD58676	Elko	26	Michael S. Cathro – 100%
YD58677	Elko	27	Michael S. Cathro – 100%
YD58678	Elko	28	Michael S. Cathro – 100%
YD58679	Elko	29	Michael S. Cathro – 100%
YD58680	Elko	30	Michael S. Cathro – 100%
YD58681	Elko	31	Michael S. Cathro – 100%
YD58682	Elko	32	Michael S. Cathro – 100%
YD58683	Elko	33	Michael S. Cathro – 100%
YD58684	Elko	34	Michael S. Cathro – 100%
YD58685	Elko	35	Michael S. Cathro – 100%
YD58686	Elko	36	Michael S. Cathro – 100%
YD58687	Elko	37	Michael S. Cathro – 100%
YD58688	Elko	38	Michael S. Cathro – 100%
YD58689	Elko	39	Michael S. Cathro – 100%
YD58690	Elko	40	Michael S. Cathro – 100%
YD58691	Elko	41	Michael S. Cathro – 100%
YD58692	Elko	42	Michael S. Cathro – 100%
YD58693	Elko	43	Michael S. Cathro – 100%
YD58694	Elko	44	Michael S. Cathro – 100%
YD58695	Elko	45	Michael S. Cathro – 100%
YD58696	Elko	46	Michael S. Cathro – 100%
YD58697	Elko	47	Michael S. Cathro – 100%
YD58698	Elko	48	Michael S. Cathro – 100%

Grant #	Claim Name	Claim #	ClaimOwner
YD58699	Elko	49	Michael S. Cathro – 100%
YD58700	Elko	50	Michael S. Cathro – 100%
YD58701	Elko	51	Michael S. Cathro – 100%
YD58702	Elko	52	Michael S. Cathro – 100%
YD58703	Elko	53	Michael S. Cathro – 100%
YD58704	Elko	54	Michael S. Cathro – 100%
YD58705	Elko	55	Michael S. Cathro – 100%
YD58706	Elko	56	Michael S. Cathro – 100%
YD58707	Elko	57	Michael S. Cathro – 100%
YD58708	Elko	58	Michael S. Cathro – 100%
YD58709	Elko	59	Michael S. Cathro – 100%
YD58710	Elko	60	Michael S. Cathro – 100%
YD58711	Elko	61	Michael S. Cathro – 100%
YD58712	Elko	62	Michael S. Cathro – 100%
YD58713	Elko	63	Michael S. Cathro – 100%
YD58714	Elko	64	Michael S. Cathro – 100%
YD58715	Elko	65	Michael S. Cathro – 100%
YD58716	Elko	66	Michael S. Cathro – 100%
YD58717	Elko	67	Michael S. Cathro – 100%
YD110388	Elko	68	Cathro Resource Corp. - 100%
YD110389	Elko	69	Cathro Resource Corp. - 100%
YD110390	Elko	70	Cathro Resource Corp. - 100%
YD110391	Elko	71	Cathro Resource Corp. - 100%
YD110392	Elko	72	Cathro Resource Corp. - 100%
YD110393	Elko	73	Cathro Resource Corp. - 100%
YD110394	Elko	74	Cathro Resource Corp. - 100%
YD110395	Elko	75	Cathro Resource Corp. - 100%
YD110396	Elko	76	Cathro Resource Corp. - 100%
YD110397	Elko	77	Cathro Resource Corp. - 100%
YD110398	Elko	78	Cathro Resource Corp. - 100%
YD110399	Elko	79	Cathro Resource Corp. - 100%
YD110400	Elko	80	Cathro Resource Corp. - 100%
YD110401	Elko	81	Cathro Resource Corp. - 100%
YD110402	Elko	82	Cathro Resource Corp. - 100%
YD110403	Elko	83	Cathro Resource Corp. - 100%
YD110404	Elko	84	Cathro Resource Corp. - 100%
YD110405	Elko	85	Cathro Resource Corp. - 100%
YD110406	Elko	86	Cathro Resource Corp. - 100%
YD110407	Elko	87	Cathro Resource Corp. - 100%
YD110408	Elko	88	Cathro Resource Corp. - 100%
YD110409	Elko	89	Cathro Resource Corp. - 100%
YD110410	Elko	90	Cathro Resource Corp. - 100%
YD110411	Elko	91	Cathro Resource Corp. - 100%
YD110412	Elko	92	Cathro Resource Corp. - 100%

Grant #	Claim Name	Claim #	ClaimOwner
YD110413	Elko	93	Cathro Resource Corp. - 100%
YD110414	Elko	94	Cathro Resource Corp. - 100%
YD110415	Elko	95	Cathro Resource Corp. - 100%
YD110416	Elko	96	Cathro Resource Corp. - 100%
YD110417	Elko	97	Cathro Resource Corp. - 100%
YD110418	Elko	98	Cathro Resource Corp. - 100%
YD110419	Elko	99	Cathro Resource Corp. - 100%
YD110420	Elko	100	Cathro Resource Corp. - 100%
YD110421	Elko	101	Cathro Resource Corp. - 100%
YD110422	Elko	102	Cathro Resource Corp. - 100%
YD110423	Elko	103	Cathro Resource Corp. - 100%
YD110424	Elko	104	Cathro Resource Corp. - 100%
YD110425	Elko	105	Cathro Resource Corp. - 100%
YD110426	Elko	106	Cathro Resource Corp. - 100%
YD110427	Elko	107	Cathro Resource Corp. - 100%
YD110428	Elko	108	Cathro Resource Corp. - 100%
YD110429	Elko	109	Cathro Resource Corp. - 100%
YD110430	Elko	110	Cathro Resource Corp. - 100%
YD110431	Elko	111	Cathro Resource Corp. - 100%
YD110432	Elko	112	Cathro Resource Corp. - 100%
YD110433	Elko	113	Cathro Resource Corp. - 100%
YD110434	Elko	114	Cathro Resource Corp. - 100%
YD110435	Elko	115	Cathro Resource Corp. - 100%
YD110436	Elko	116	Cathro Resource Corp. - 100%
YD110437	Elko	117	Cathro Resource Corp. - 100%
YD110438	Elko	118	Cathro Resource Corp. - 100%
YD110439	Elko	119	Cathro Resource Corp. - 100%
YD110440	Elko	120	Cathro Resource Corp. - 100%
YD110441	Elko	121	Cathro Resource Corp. - 100%
YD110442	Elko	122	Cathro Resource Corp. - 100%
YD110443	Elko	123	Cathro Resource Corp. - 100%
YD110444	Elko	124	Cathro Resource Corp. - 100%
YD110445	Elko	125	Cathro Resource Corp. - 100%
YD110446	Elko	126	Cathro Resource Corp. - 100%
YD110447	Elko	127	Cathro Resource Corp. - 100%
YD110448	Elko	128	Cathro Resource Corp. - 100%
YD110449	Elko	129	Cathro Resource Corp. - 100%
YD110450	Elko	130	Cathro Resource Corp. - 100%
YD110451	Elko	131	Cathro Resource Corp. - 100%
YD110452	Elko	132	Cathro Resource Corp. - 100%
YD110453	Elko	133	Cathro Resource Corp. - 100%
YD110454	Elko	134	Cathro Resource Corp. - 100%
YD110455	Elko	135	Cathro Resource Corp. - 100%
YD110456	Elko	136	Cathro Resource Corp. - 100%

Grant #	Claim Name	Claim #	ClaimOwner
YD110457	Elko	137	Cathro Resource Corp. - 100%
YD110458	Elko	138	Cathro Resource Corp. - 100%
YD110459	Elko	139	Cathro Resource Corp. - 100%
YD110460	Elko	140	Cathro Resource Corp. - 100%
YD110461	Elko	141	Cathro Resource Corp. - 100%
YD110462	Elko	142	Cathro Resource Corp. - 100%
YD110463	Elko	143	Cathro Resource Corp. - 100%
YD110464	Elko	144	Cathro Resource Corp. - 100%
YD110465	Elko	145	Cathro Resource Corp. - 100%
YD110466	Elko	146	Cathro Resource Corp. - 100%
YD110467	Elko	147	Cathro Resource Corp. - 100%
YD110468	Elko	148	Cathro Resource Corp. - 100%
YD110469	Elko	149	Cathro Resource Corp. - 100%
YD110470	Elko	150	Cathro Resource Corp. - 100%
YD110471	Elko	151	Cathro Resource Corp. - 100%
YD110472	Elko	152	Cathro Resource Corp. - 100%
YD110473	Elko	153	Cathro Resource Corp. - 100%
YD110474	Elko	154	Cathro Resource Corp. - 100%
YD110475	Elko	155	Cathro Resource Corp. - 100%
YD110476	Elko	156	Cathro Resource Corp. - 100%
YD110477	Elko	157	Cathro Resource Corp. - 100%
YD110478	Elko	158	Cathro Resource Corp. - 100%
YD110479	Elko	159	Cathro Resource Corp. - 100%
YD110480	Elko	160	Cathro Resource Corp. - 100%
YD110481	Elko	161	Cathro Resource Corp. - 100%
YD110482	Elko	162	Cathro Resource Corp. - 100%
YD110483	Elko	163	Cathro Resource Corp. - 100%
YD110484	Elko	164	Cathro Resource Corp. - 100%
YD110485	Elko	165	Cathro Resource Corp. - 100%
YD110486	Elko	166	Cathro Resource Corp. - 100%
YD110487	Elko	167	Cathro Resource Corp. - 100%
YD110488	Elko	168	Cathro Resource Corp. - 100%
YD110489	Elko	169	Cathro Resource Corp. - 100%
YD110490	Elko	170	Cathro Resource Corp. - 100%
YD110491	Elko	171	Cathro Resource Corp. - 100%
YD110492	Elko	172	Cathro Resource Corp. - 100%
YD110493	Elko	173	Cathro Resource Corp. - 100%
YD110494	Elko	174	Cathro Resource Corp. - 100%
YD110495	Elko	175	Cathro Resource Corp. - 100%
YD110496	Elko	176	Cathro Resource Corp. - 100%
YD110497	Elko	177	Cathro Resource Corp. - 100%

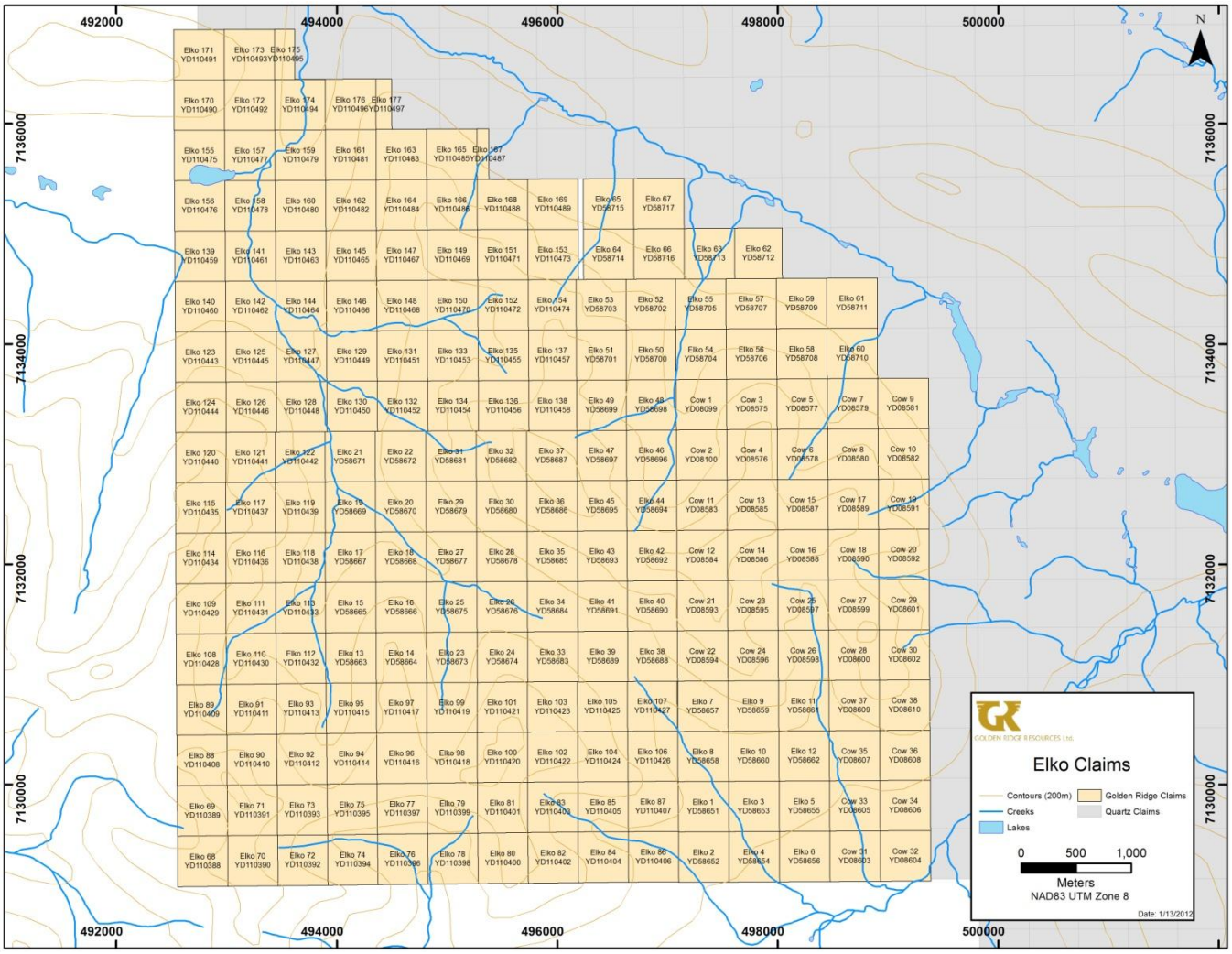

Figure 2 Elko claim map

3. ACCESS

The Elko project is accessible by helicopter from Mayo (90 km) or Keno City (45 km). The work program described in this report was accessed by helicopter from a road accessible base camp at McQuesten Lake, approximately 28 km southwest of the property (Figure 2). The Wind River Trail, a winter road, begins at McQuesten Lake and passes within 6 km of the north side of the Elko property (Figure 2).

4. PREVIOUS WORK

In 2010 a five-day program of silt sampling, soil sampling and prospecting was conducted over property with a focus toward the centre of the property. The program was successful in identifying Au, As, Sb, and Hg anomalies in silts, soils and rocks in an area underlain by shales, siltstones and calcareous sedimentary rocks (Cathro, 2010).

A careful review of government records including assessment reports identified no known mineral occurrences, nor any record of previous exploration prior to 2010 in the area of the Elko property.

The available government regional stream silt geochemistry shows that one drainage is strongly anomalous for gold (80 ppb; sample 106D775380) and several other adjacent drainages are moderately to highly anomalous in gold, arsenic, antimony, molybdenum and tungsten (Figure 3). This pathfinder assemblage is similar to that at Rau (Cathro, 2010).

5. REGIONAL GEOLOGY AND MINERAL DEPOSITS

The Property is underlain by Upper Proterozoic/Paleozoic rocks of ancestral North America (PCH; Hyland Group) and is located directly south of, adjacent to and in the hangingwall of the regionally important Dawson Thrust (Figure 3). Mississippian aged rocks just to the east of the claims (MK; Keno Hill Quartzite) and Upper Cambrian- Lower Devonian rocks are immediately north of the claims on the Rau Property (CDB1; Bouvette Formation).

Figure 3 shows the regional geological mapping by the Geological Survey of Canada (L. Green and J.A. Roddick, GSC Map 15-1962). The Elko area is shown as being underlain primarily by Paleozoic unit 3.

Unit 3 (now known as the Hyland Group) is described as Precambrian and/or Cambrian buff, brown and rusty weathering gritty quartzite, sandstone and quartz pebble conglomerate; black, maroon and green shales and slates, schistose quartzite, quartz chlorite schist, quartz mica schist, and phyllite with minor limestone and black chert. In some places thin to medium-bedded limestone can be mapped. It is important to note that Hyland Group is an important host to gold mineralization at Brewery Creek and elsewhere in the region.

The emerging Rau belt falls along the thrust-faulted margin of the Selwyn Basin and Mackenzie platform. Mainly underlain by Paleozoic carbonate and silicicalstic rocks, this area has been explored in the past for Keno-Hill type Ag-Pb-Zn veins and stratabound Pb-Zn-Ag replacement and Mississippi Valley type mineralization, although gold exploration has been minimal.

According to information released by ATAC, the Tiger Zone mineralization at Rau consists of stratabound lenses replacing dolomitized and decalcified limestone of the Upper Cambrian to Lower Devonian Bouvette Formation. Gold mineralization has been outlined over a 650 m long, 150 m wide area and averages about 40 m thick. Mineralization occurs beneath a volcaniclastic horizon, which may have acted as an impermeable cap. The Rau trend mineralization is closely associated with a northwest- trending zone of structural disruption coincident with the hinge zone of a regional anticlinal fold closure occurring between the regional scale Dawson and Robert Service Thrusts.

Both high-grade oxide (limonite) and low to moderate-grade sulphide (pyrite- arsenopyrite-pyrrhotite) zones are hosted in fractured, brecciated and altered carbonate rocks of the Bouvette Formation (Unit CDB1). Highlighted drill intersections include 24.08 m grading 24.07 g/t Au and 24.47 m grading 19.59 g/t Au in oxide, and 70.8 m grading 5.11 g/t Au and 78.54 m grading 1.71 g/t Au (sulphide). The Tiger zone is reported to have been discovered by following up an anomalous government stream sediment sample (150 ppb Au, 6.8 ppm As, 44 ppb Pb, 19 ppb W). Mineralization has been described as "Nevada-Style" and similarities with sediment-hosted (Carlin-type) and Ketza River, Yukon deposits have been noted. A genetic association with a nearby Late Cretaceous (?) dyke swarm has also been inferred.

The Rau belt occurs north of the important Tombstone gold belt, which includes the important Fairbanks, Fort Knox, and Pogo intrusion-related gold deposits in Alaska, and the Brewery Creek, Clear Creek, and Eagle Gold (Dublin Gulch) deposits in Yukon. The Eagle Gold deposit, owned by Victoria Gold Corp. is located west southwest of the Elko property area and has an Indicated Resource of 2.7 million ounces of gold (98.6 million tonnes grading 0.85 g/t).

The prolific and high-grade Keno Hill silver-lead-zinc mining camp (Alexco Resources Corp.) is located approximately 45 kilometres south of Elko. Between 1913 and 1990 this district is reported to have produced more than 217 million ounces of silver at an average grade of 40.5 oz/ton, along with significant quantities lead and zinc. Other important deposits in the immediate area include the carbonate-hosted Blende deposit of Blind Creek Resources, located 25 km northeast of Elko, with an inferred resource of 19.6 Mt grading 3.04% Zn, 2.8% Pb and 55.9 g/t Ag.

6. REGIONAL GEOPHYSICS

The regional government total field aeromagnetic map (Figure 4) shows subtle aeromagnetic highs to the NW and SE of the Property, suggestive of possible un-mapped or buried intrusive bodies which are indicative of Tombstone-style gold deposits, and which may also be important at Rau (red colour on the map indicates relative magnetic high and on the other end of the spectrum, the blue colour indicates relative magnetic low).

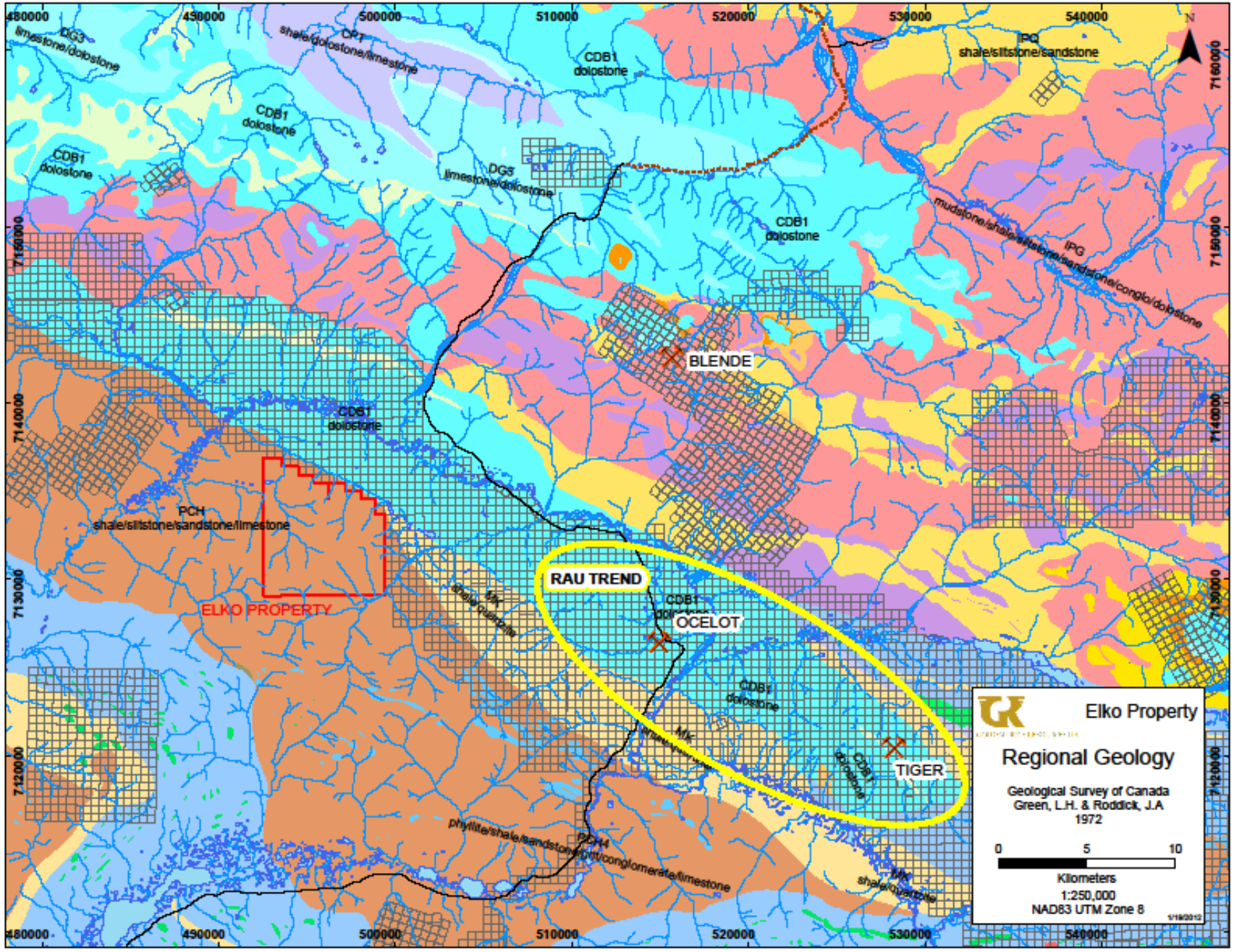

Figure 3 Elko regional geology

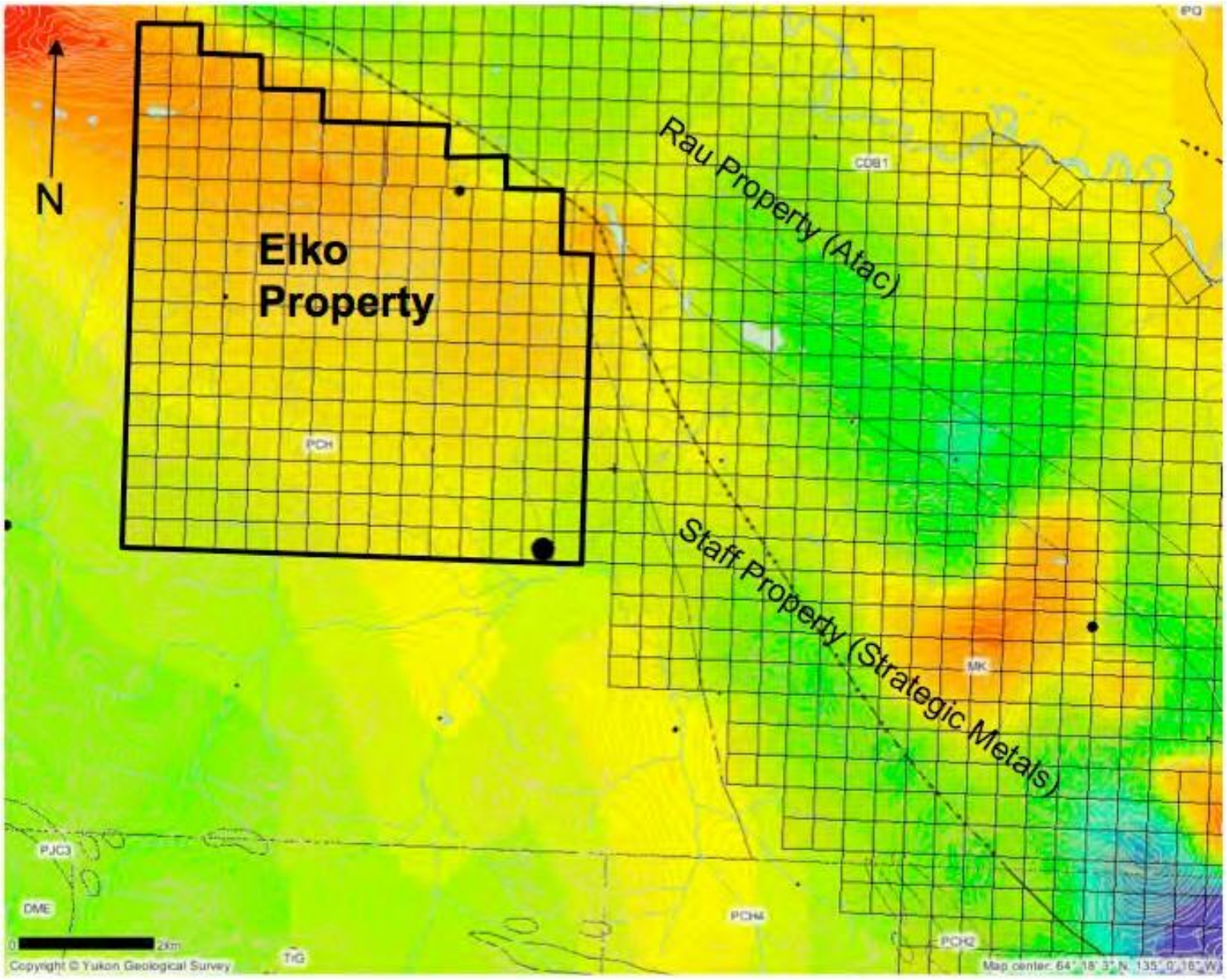

Figure 4 Elko regional total field aeromagnetics (from Yukon Geological Survey)

7. 2011 WORK PROGRAM

Fugro Airborne Surveys Corp was contracted to complete a DIGHEM V survey covering the entire Elko project area. This survey was completed from August 8th to August 12th, 2011. A total of 246 line-km was flown orientated NE-SW (30°/210°) with a line spacing of 200m. Tie lines were flown orthogonal to traverse lines with 2000 m line spacing. Further details of equipment used and data processing techniques are available in Appendix 1.

In addition, staking of additional claims was completed by contractor Coureur des Bois on and January 26, 2011 (Elko 68-177 claims).

8. RESULTS AND INTERPRETATION

The results of the DIGHEM V survey have clearly identified at least five NW-SE trending resistivity low zones (Figure 5). Three of these zones are consistent with higher elevation and are considered to be bedrock responses that may represent sulphide bearing zones.

The magnetic responses also highlight the NW-SE trending stratigraphy that is prevalent throughout the region. Results from the Residual Magnetic Intensity survey do not have a strong correlation with the conductive zones but do however show an increase of magnetic susceptibility toward the NE. Close to the NE corner of the Elko property (approximately the northern extent of 2010 soil sampling) 2-3 magnetic highs have been identified (in correlation to resistivity high) and appear to be plug like intrusions with potential skarn-type mineralization associated with them (Figure 6).

These magnetic plugs are very interesting as soil sample ESA018, collected in 2010, reported 156 ppb Au, 6.2 ppm Ag and 238.6 ppm Cu and is described in the field as calcareous material with strong Fe-oxide weathering. These “plugs” are broadly along strike of a N-S trending break identified in the magnetics and the topography. This break intersects one of the identified conductive zones where the majority of the sampling took occurred in 2010. This is very encouraging as sampling from the 2010 field program reported anomalous Au and pathfinder elements.

View Appendix 1 for the complete Fugro Airborne Surveys DIGHEM V report.

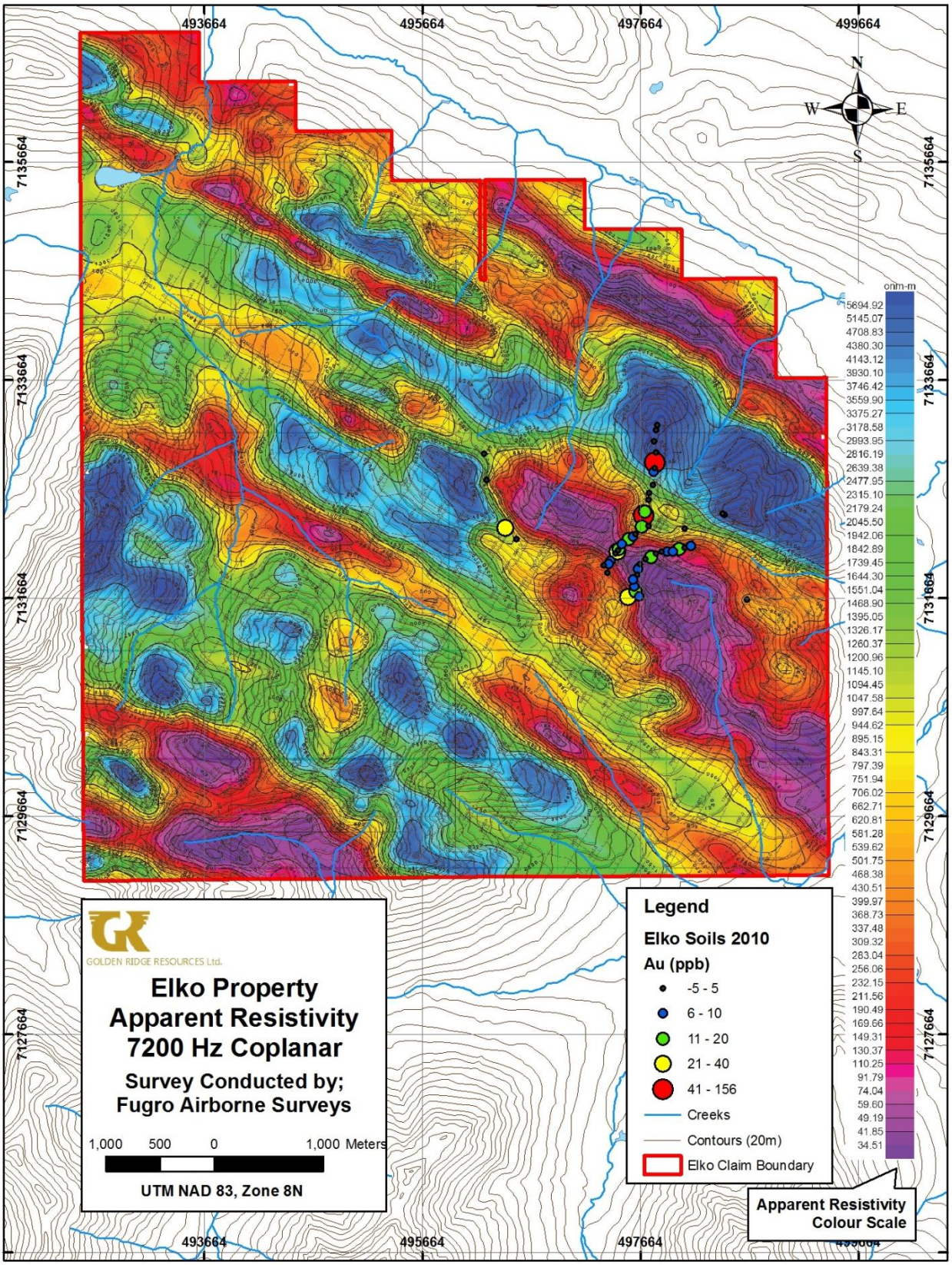

Figure 5 Elko apparent resistivity, 7200 coplanar

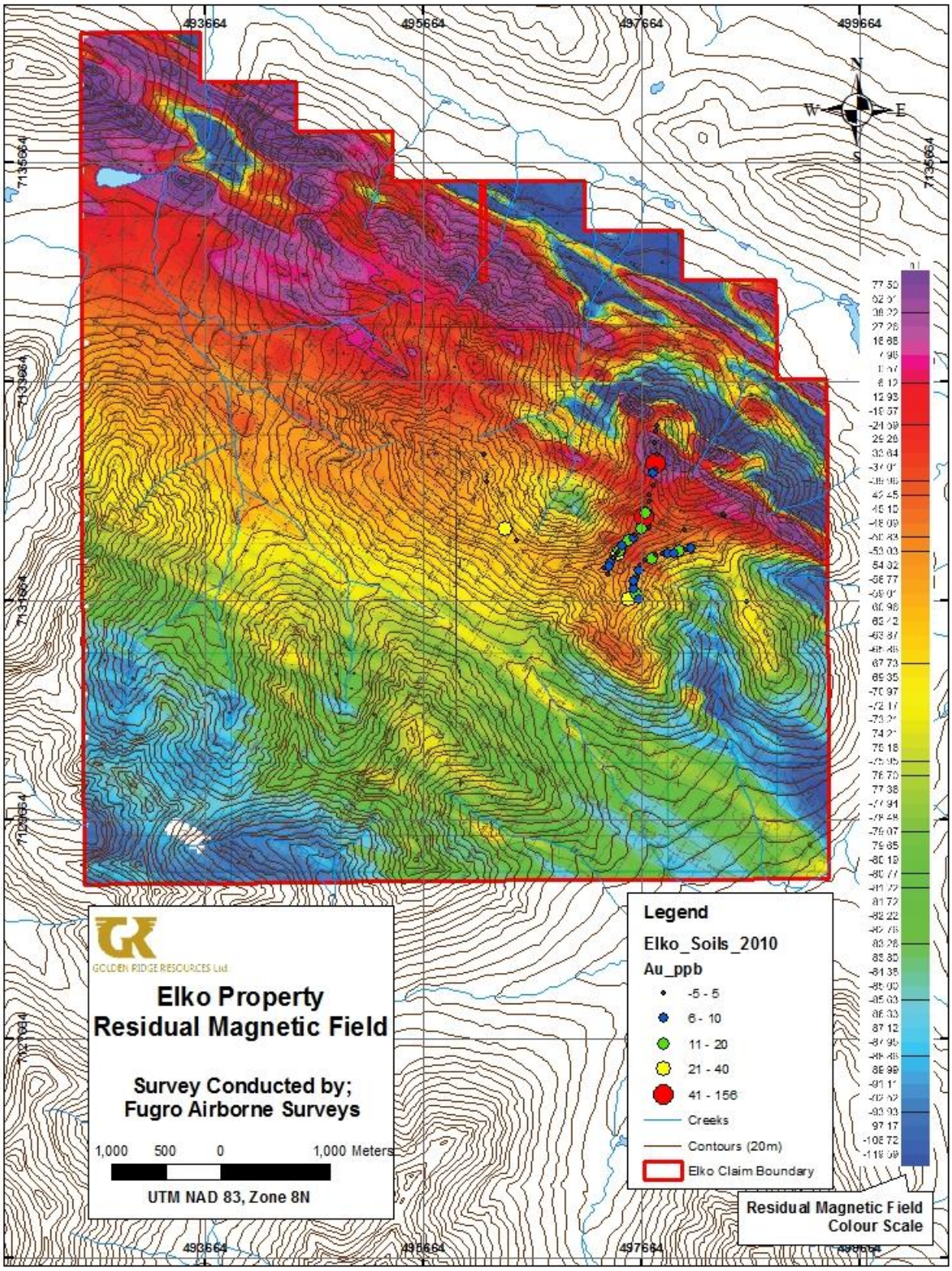

Figure 6 Elko residual magnetic field

9. SUMMARY AND RECOMMENDATIONS

A DIGHEM V electromagnetic/resistivity/magnetic survey, conducted by Fugro Airborne Surveys Corp, was flown over the Elko property between August 8th and August 12th 2011. The objective of the 2011 program was to follow up on encouraging geochemical sampling completed in 2010. The survey was successful in delineating several conductive and magnetic trends similar to that of the known Rau Trend (Figure 5 & 6). Three of these conductive zones are consistent with higher elevation and are considered to be bedrock responses that may represent sulphide bearing zones. Residual Magnetic lows are also considered important, especially toward the NE. Based on field mapping and analytical results from 2010 sampling there appears to be mineralization associated with these magnetic lows.

To date, the Elko Property still remains largely unexplored. It is recommended that a follow-up field sampling program be undertaken to further investigate the conductive units and magnetic units identified from the DIGHEM V survey as outlined by Fugro Airborne Surveys, especially in the NE where previous sampling identified encouraging Au and Au pathfinder samples.

Completing several traverses across each geophysical anomaly in order to collect geological, geochemical and structural data is recommended as a minimum work program. Continued ridge and spur sampling along with contour sampling totaling approximately 20 line km of soil sampling at 25 m sample intervals is recommended. Chip/channel samples are also recommended whenever possible. 300 chip/channel samples have been budgeted for (table. 2). This program would ideally result in high priority trench and/or drill targets to further advance the project into the next stage of development.

Table 2 Recommended budget for 2012

	Quantity	Cost	Amount	Total	Subtotals
Personal					
Sr. Geologist	1	$600	25	$15,000	
Geologist	1	$350	25	$8,750	
Sampler	2	$275	25	$13,750	$37,500
Expenses					
Truck rental	1	$100	20	$2,000	
Fuel	1	$150	10	$1,500	
Hotel	5	$100	20	$10,000	
Food	5	$75	20	$7,500	$21,000
Sampling					
Chip/trench	1	$33	300	$9,900	
Soil	1	$33	800	$26,400	
Silt	1	$33	10	$330	$36,630
Other					
Helicopter	1	$1,500	15	$22,500	$22,500
Supplies	1	$1	15000	$15,000	$15,000
GIS/Reporting	1	$500	10	$5,000	$5,000
Subtotal					**$137,630**
Contingency	20%	$137,630		$27,526	
			Total	***$165,156***	

10. STATEMENT OF EXPENDITURES

Professional Services

Fugro Airborne Surveys	246 Line km	$65,041
Mobilization/demobilization		$5,000
Total		$70,041

Note: Expenditures are bases on a percentage of line km completed by Fugro Airborne Surveys as the survey was flown in conjunction with Golden Ridge Resources' Nash project ~20km NE.

11. STATEMENT OF QUALIFICATIONS

I, Kevin E Piepgrass, of 2781 Lakeridge Road, West Kelowna, British Columbia, hereby certify that:

- I am a graduate of the University of Alberta, Edmonton Alberta, with a B.Sc. with specialization in Geology (2005).
- I am presently employed as a consulting geologist with Fieldgrass Consulting.
- I have been working as a Geologist in Training in mineral exploration and mineral exploration management and geological research since 2004.
- I have gained experience in precious and base metal exploration with a strong focus on gold. I have worked on and managed mineral exploration programs in Western Ethiopia, Guyana, Surinam, Peru, Nevada and Minnesota, USA and Yukon and NWT, Canada.
- I have conducted geological exploration on intrusion related gold deposits (IRGS), Skarn deposits (W-Sn-Au and Cu-Au), Epithermal deposits, mesothermal deposit, Au porphyry deposit, Carlin type deposits, Fe-Ti in oxide-bearing ultramafic intrusions (OUI) and a diamond mine.

_____

Kevin E Piepgrass, BSc. Geology

January 16, 2012

12. REFERENCES

Fugro Airborne Surveys, **2011**. DIGHEM V Survey for Golden Ridge Resources Inc. Elko and Nash Mayo Area, Yukon Territory, Summary Report

Cathro, M, 2011. Assessment Report on Geochemical Prospecting on the Elko Property Comprised of, Cow 1-38, and Elko 1-67 Claims. Mayo Mining District, Yukon Territory. NTS 106D/07

Appendix 1

Fugro Airborne Survey

DIGHEM V Survey

Complete Report

Report # 11058

DIGHEM ^{V} SURVEY
FOR
GOLDEN RIDGE RESOURCES INC.
ELKO and NASH PROPERTIES
MAYO AREA, YUKON TERRITORY

NTS: 106 D/6,7,10

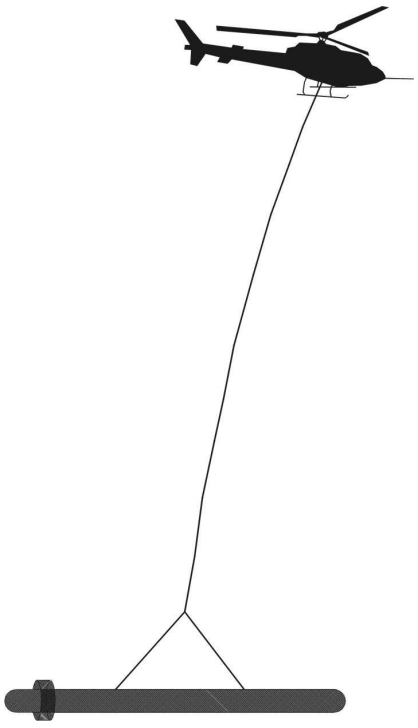

Fugro Airborne Surveys Corp.
Mississauga, Ontario

December 15, 2011

Fugro Airborne Surveys, 2505 Meadowvale Boulevard, Mississauga, Ontario, Canada, L5N 5S2
Phone: 1 905 812 0212, Fax: 1 905 812 1504

SUMMARY

This report describes the logistics, data acquisition, and processing of a DIGHEM^{V} electromagnetic and magnetic airborne geophysical survey carried out for Golden Ridge Resources Inc., over two properties near Mayo, Yukon Territory. Total coverage of the survey blocks amounted to 314 km. The survey was flown between August 8th and August 12th, 2011.

The purpose of the survey was to locate Carlin-type, sediment-hosted, auriferous mineralization, to determine the geophysical signatures over any known zones of mineralization, and to provide information that could be used to map the geology and structure of the survey areas. Data were acquired using a DIGHEM electromagnetic system, supplemented by a high-sensitivity cesium magnetometer. The information from these sensors was processed to produce maps and images that display the magnetic and conductive properties of the survey areas. A GPS electronic navigation system ensured accurate positioning of the geophysical data with respect to the base map coordinates.

The survey properties host numerous anomalous features, some of which are considered to be of moderate priority as exploration targets. Although auriferous targets in this area might be associated with resistive units, rather than conductive units, there are several inferred bedrock conductors that may warrant further investigation using appropriate surface exploration techniques. Areas of interest may be assigned priorities on the basis of supporting geophysical, geochemical and/or geological information. After initial investigations have been carried out, it may be necessary to re-evaluate the remaining anomalous responses based on information acquired from the follow-up program.

CONTENTS

1. INTRODUCTION 1.1

2. SURVEY OPERATIONS 2.1

3. SURVEY EQUIPMENT 3.1
   - Electromagnetic System 3.1
   - In-Flight EM System Calibration 3.2
   - Magnetometer 3.3
   - Magnetic Base Station 3.3
   - Navigation (Global Positioning System) 3.5
   - Radar Altimeter 3.7
   - Barometric Pressure and Temperature Sensors 3.7
   - Digital Data Acquisition System 3.7
   - Video Flight Path Recording System 3.8

4. QUALITY CONTROL AND IN-FIELD PROCESSING 4.1

5. DATA PROCESSING 5.1
   - Flight Path Recovery 5.1
   - Electromagnetic Data 5.2
   - Altitude Data 5.2
   - Base Station Diurnal Correction 5.3
   - Apparent Resistivity 5.3
   - Resistivity-depth Sections (optional) 5.4
   - Residual Magnetic Intensity 5.5
   - Calculated Vertical Magnetic Gradient 5.6
   - Magnetic Derivatives (optional) 5.6
   - Contour, Colour and Shadow Map Displays 5.7
   - Digital Elevation (optional) 5.7

6. PRODUCTS 6.1
   - Base Maps 6.1
   - Final Products 6.2

7. SURVEY RESULTS 7.1
   - General Discussion 7.1
   - Magnetic Data 7.2
   - Apparent Resistivity 7.4
   - Electromagnetic Anomalies 7.9

Bedrock Conductors 7.11

8. CONCLUSIONS AND RECOMMENDATIONS 8.1

APPENDICES

A. List of Personnel
B. Data Processing Flowcharts
C. Background Information
D. Data Archive Description
E. EM Anomaly List
F. Glossary

1. INTRODUCTION

A DIGHEM V electromagnetic/resistivity/magnetic survey was flown for Golden Ridge Resources Inc., over two properties near Mayo, Yukon Territory. The survey was flown from August 8 to August 12, 2011. The survey areas can be located on NTS map sheets 106 D/6.7 (Elko) and 106 D/10 (Nash).

Survey coverage consisted of approximately 246 line-km in the Elko area, and 68 line-km in the Nash area, for a total of 314 line-km, including tie lines. Flight lines were flown NE-SW (30°/210°) on the Elko property, and N-S (360°/180°) on the Nash property, with a line separation of 200 metres. Tie lines were flown orthogonal to the traverse lines with a line separation of 2000 metres.

The survey employed the DIGHEM ^{V} electromagnetic system. Ancillary equipment consisted of an optically pumped, high-sensitivity cesium magnetometer, radar and barometric altimeters, a video camera, digital recorders, and an electronic navigation system. The instrumentation was installed in an AS350-B2 turbine helicopter (Registration C-GJIX) that was provided by Questral Helicopters Ltd. The helicopter flew at an average airspeed of 100 km/h with an EM sensor height of approximately 35 metres.

Figure 1: Fugro Airborne Surveys DIGHEM ^{V} EM bird with AS350-B2

2. SURVEY OPERATIONS

The base of operations for the survey was established at Keno with a remote fuel cache at the McQuesten Camp. Table 2-1 lists the corner coordinates of the survey areas in NAD83, UTM Zone 8N, central meridian 135°W.

TABLE 2-1

Nad83 Utm zone 8N

Block	Corners	X-UTM (E)	Y-UTM (N)
11058-1	1	492520	7136852
Elko	2	493616	7136858
Property	3	493618	7136401
	4	494497	7136404
	5	494499	7135948
	6	495378	7135951
	7	495380	7135495
	8	497148	7135505
	9	497151	7135048
	10	498040	7135052
	11	498042	7134595
	12	498902	7134599
	13	498907	7133686
	14	499365	7133688
	15	499389	7129124
	16	492558	7129071
11058-2	1	507212	7154983
Nash	2	507229	7153614
Property	3	507687	7153619
	4	507698	7152707
	5	508156	7152713
	6	508156	7152668
	7	508227	7152322
	8	508165	7151961
	9	508167	7151800
Block	Corners	X-UTM (E)	Y-UTM (N)

	10	509083	7151811
	11	509077	7152268
	12	512738	7152314
	13	512724	7153463
	14	512591	7153378
	15	512561	7153336
	16	512542	7153383
	17	512477	7153410
	18	512327	7153415
	19	512266	7153449
	20	512216	7153477
	21	512152	7153544
	22	512074	7153674
	23	511951	7153976
	24	511884	7154084
	25	511834	7154128
	26	511799	7154156
	27	511601	7154249
	28	511438	7154412
	29	511338	7154439
	30	510983	7154415
	31	510897	7154437
	32	510830	7154493
	33	510550	7154463
	34	510492	7154469
	35	510414	7154495
	36	510341	7154565
	37	509048	7154549
	38	509042	7155005

Table 2-2

:

Survey specifications were as follows:

Parameter	Specifications
Traverse line direction (Elko/Nash) Traverse line spacing(Elko/Nash) Tie line direction(Elko/Nash) Tie line spacing(Elko/Nash) Sample interval Aircraft mean terrain clearance EM & mag sensors mean terrain clearance Average speed Navigation (guidance) Post-survey flight path	NE-SW (30°); N-S (360°) 200 m; 200 m; NW-SE (120°); E-W (90°) 2000 m; 2000 m 10 Hz, 2.75 m @ 100 km/h 65 m 35m 100 km/h ±5 m, Real-time GPS ±2 m, Differential GPS

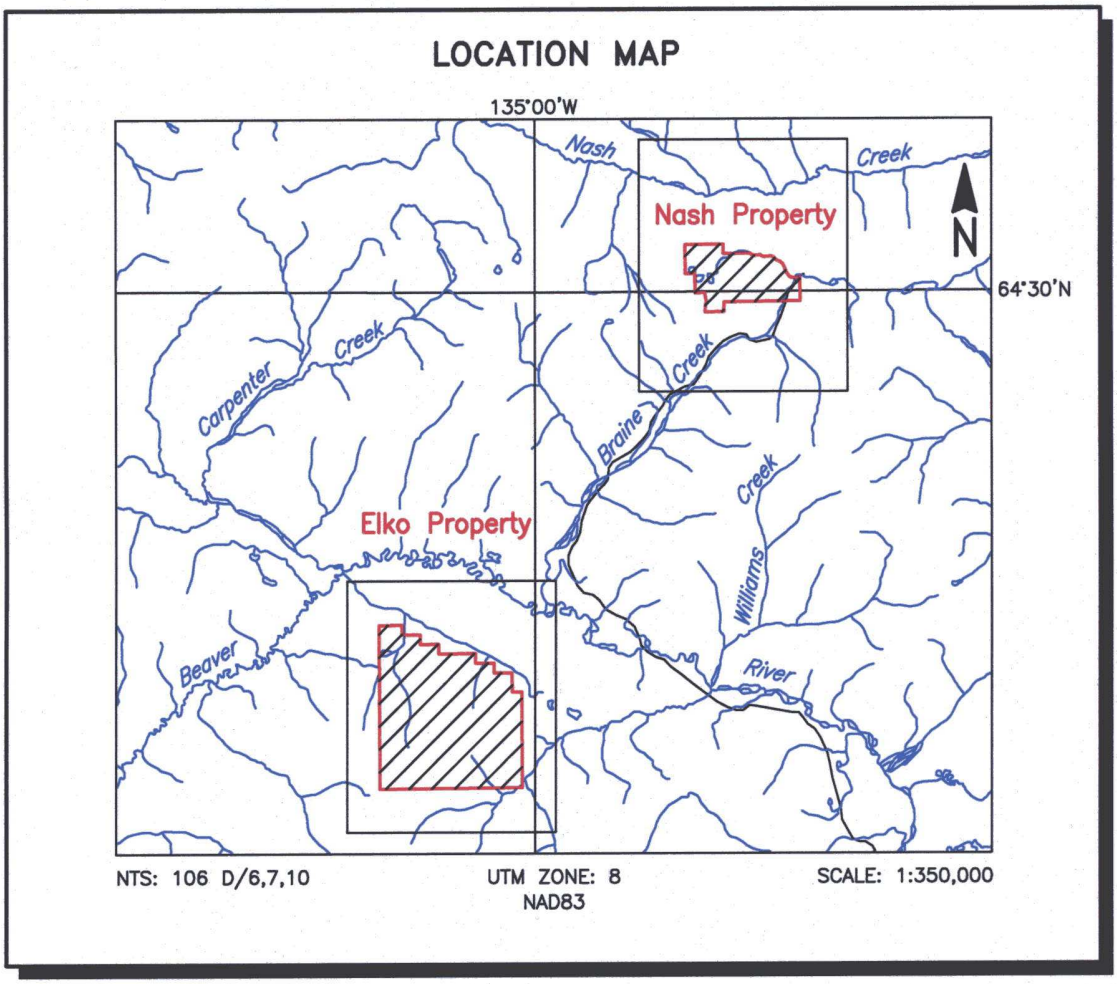

Figure 2-2
Location Map and Sheet Layout
Elko and Nash Properties
Job # 11058

3. SURVEY EQUIPMENT

This section provides a brief description of the geophysical instruments used to acquire the survey data and the calibration procedures employed. The geophysical equipment was installed in an AS350-B2 helicopter. This aircraft provides a safe and efficient platform for surveys of this type.

Electromagnetic System

Model: DIGHEM ^{V}-BKS 55

Type: Towed bird, symmetric dipole configuration operated at a nominal survey altitude of 30 metres. Coil separation is 8 metres for 900 Hz, 1000 Hz, 5500 Hz and 7200 Hz, and 6.3 metres for the 56,000 Hz coil-pair.

Coil orientations, frequencies and dipole moments

Atm^2	orientation		nominal	actual
211	coaxial	/	1000 Hz	1117 Hz
211	coplanar	/	900 Hz	883 Hz
67	coaxial	/	5500 Hz	5909 Hz
56	coplanar	/	7200 Hz	7490 Hz
15	coplanar	/	56,000 Hz	55270 Hz

Channels recorded:
5 in-phase channels
5 quadrature channels
2 monitor channels

Sensitivity:
0.06 ppm at 1000 Hz Cx
0.12 ppm at 900 Hz Cp
0.12 ppm at 5,500 Hz Cx
0.24 ppm at 7,200 Hz Cp
0.60 ppm at 56,000 Hz Cp

Sample rate: 10 per second, equivalent to 1 sample every 2.75 m, at a survey speed of 100 km/h.

The electromagnetic system utilizes a multi-coil coaxial/coplanar technique to energize conductors in different directions. The coaxial coils are vertical with their axes in the flight direction. The coplanar coils are horizontal. The secondary fields are sensed simultaneously by means of receiver coils that are maximum-coupled to their respective transmitter coils. The system yields an in-phase and a quadrature channel from each transmitter-receiver coil-pair.

In-Flight EM System Calibration

Calibration of the system during the survey uses the Fugro AutoCal automatic, internal calibration process. At the beginning and end of each flight, and at intervals during the flight, the system is flown up to high altitude to remove it from any “ground effect” (response from the earth). Any remaining signal from the receiver coils (base level) is measured as the zero level, and is removed from the data collected until the time of the next calibration. Following the zero level setting, internal calibration coils, for which the response phase and amplitude have been determined at the factory, are automatically triggered – one for each frequency. The on-time of the coils is sufficient to determine an accurate response through any ambient noise. The receiver response to each calibration coil “event” is compared to the expected response (from the factory calibration) for both phase angle and amplitude, and any phase and gain corrections are automatically applied to bring the data to the correct value.

In addition, the outputs of the transmitter coils are continuously monitored during the survey, and the gains are adjusted to correct for any change in transmitter output.

Because the internal calibration coils are calibrated at the factory (on a resistive half-space) ground calibrations using external calibration coils on-site are not necessary for system calibration. A check calibration may be carried out on-site to ensure all systems are working correctly. All system calibrations will be carried out in the air, at sufficient altitude that there will be no measurable response from the ground.

The internal calibration coils are rigidly positioned and mounted in the system relative to the transmitter and receiver coils. In addition, when the internal calibration coils are calibrated at the factory, a rigid jig is employed to ensure accurate response from the external coils.

Using real time Fast Fourier Transforms and the calibration procedures outlined above, the data are processed in real time, from measured total field at a high sampling rate, to in-phase and quadrature values at 10 samples per second.

Magnetometer

Model:	Scintrex CS-3 sensor with a Fugro D1344 counter.
Type:	Optically pumped cesium vapour
Sensitivity:	0.01 nT
Sample rate:	10 per second

The magnetometer sensor is housed in the HEM bird, which is flown 28 m below the helicopter.

Magnetic Base Station

Primary

Model:	Fugro CF1 base station with timing provided by integrated GPS	
Sensor type:	Scintrex CS-3	
Counter specifications:	Accuracy:	±0.1 nT
	Resolution:	0.01 nT
	Sample rate	1 Hz

GPS specifications:	Model:	Marconi Allstar
	Type:	Code and carrier tracking of L1 band, 12-channel, C/A code at 1575.42 MHz
	Sensitivity:	-90 dBm, 1.0 second update
	Accuracy:	Manufacturer's stated accuracy for differential corrected GPS is 2 metres

Environmental Monitor specifications: Temperature:

- Accuracy: ±1.5ºC max
- Resolution: 0.0305ºC
- Sample rate: 1 Hz
- Range: -40ºC to +75ºC

Barometric pressure:

- Model: Motorola MPXA4115AP
- Accuracy: ±3.0º kPa max (-20ºC to 105ºC temp. ranges)
- Resolution: 0.013 kPa
- Sample rate: 1 Hz
- Range: 55 kPa to 108 kPa

Backup

Model:	GEM Systems GSM-19T
Type:	Digital recording proton precession
Sensitivity:	0.10 nT
Sample rate:	3 second intervals

A digital recorder is operated in conjunction with the base station magnetometer to record the diurnal variations of the earth's magnetic field. The clock of the base station is

synchronized with that of the airborne system, using GPS time, to permit subsequent removal of diurnal drift. The Fugro CF1 was the primary magnetic base station

Magnetic Base Station Locations

Status	Location Name	WGS84 Latitude (deg-min-sec)	WGS84 Longitude (deg-min-sec)
Primary	Fuel Cache	64°03' 27.1796" N	135°20' 49.6 272" W
Secondary	Fuel Cache	64°03' 27.3364" N	135°20' 49.3321" W

Navigation (Global Positioning System)

Airborne Receiver for Real-time Navigation & Guidance

Model:	NovAtel OEM4.
Type:	Code and carrier tracking of L1-C/A code at 1575.42 MHz and L2-P code at 1227.0 MHz. Dual frequency, 24-channel. WAAS enabled.
Sensitivity:	-132 dBm, 10 Hz update.
Accuracy:	Manufacturer's stated accuracy is better than 2 metres, real time.
Antenna:	Aero AT1675; Mounted on tail of aircraft.

Primary Base Station for Post-Survey Differential Correction

Model:	NovAtel OEM4
Type:	Code and carrier tracking of L1-C/A code at 1575.42 MHz and L2-P code at 1227.0 MHz. Dual frequency, 24-channel.
Sample rate:	10 Hz update.
Accuracy:	Better than 1 metre in differential mode.

Secondary GPS Base Station

Model:	Marconi Allstar, CMT-1200
Type:	Code and carrier tracking of L1 band, 12-channel, C/A code at 1575.42 MHz
Sensitivity:	-90 dBm, 1.0 second update
Accuracy:	Manufacturer's stated accuracy for differential corrected GPS is better than 2 metres.

The Wide Area Augmentation System (WAAS enabled) NovAtel OEM4 is a line of sight, satellite navigation system that utilizes time-coded signals from at least four of forty-eight available satellites. Both GLONASS and NAVSTAR satellite constellations are used to calculate the position and to provide real time guidance to the helicopter. For flight path processing, a similar NovAtel system was used as the primary base station receiver. The mobile and base station raw XYZ data were recorded, thereby permitting post-survey differential corrections for theoretical accuracies of better than 2 metres. A Marconi Allstar GPS unit, part of the CF-1, was used as a secondary (back-up) base station.

Each base station receiver is able to calculate its own latitude and longitude. For this survey, both the primary and secondary GPS stations were located at the fuel cache.

Status	Location	WGS84 Latitude (deg-min-sec)	WGS84 Longitude (deg-min-sec)	Orthometric Height (m)
Primary	Fuel Cache	64°03' 27.3664" N	135°20' 49.3 321" W	706.306
Secondary	Fuel Cache	64°03' 27.1796" N	135°20' 49 .6272" W	703.370

The GPS records data relative to the WGS84 ellipsoid, which is the basis of the revised North American Datum (NAD83). Conversion software is used to transform the WGS84 Lat/Lon coordinates to the UTM Zone 8N system displayed on the maps.

Radar Altimeter

Manufacturer:	Honeywell/Sperry
Model:	RT300
Type:	Short pulse modulation, 4.3 GHz
Sensitivity:	0.3 m
Sample rate:	10 per second

The radar altimeter measures the vertical distance between the helicopter and the ground except in areas of dense tree cover. This information is used in the processing algorithm that determines conductor depth.

Barometric Pressure and Temperature Sensors

Model:	DIGHEM D 1300	
Type:	Motorola MPX4115AP analog pressure sensor	
	AD592AN high-impedance remote temperature sensors	
Sensitivity:	Pressure:	150 mV/kPa
	Temperature:	100 mV/℃ or 10 mV/℃ (selectable)
Sample rate:	10 per second	

The D1300 circuit is used in conjunction with one barometric sensor and up to three temperature sensors. Two sensors (baro and temp) are installed in the EM console in the aircraft, to monitor pressure (KPA) and internal operating temperatures (TEMP_INT).

Digital Data Acquisition System

Manufacturer:	Fugro
Model:	HeliDAS – Integrated Data Acquisition System
Recorder:	SanDisk compact flash card (PCMCIA)

The stored data are downloaded to the field workstation PC at the survey base, for verification, backup and preparation of in-field products.

Video Flight Path Recording System

Type:	Panasonic WVCD/32 Camera
Recorder:	Axis 241S Video Server and Tablet Computer
Format:	BIN/BDX

Fiducial numbers are recorded continuously and are displayed on the margin of each image. This procedure ensures accurate correlation of data with respect to visible features on the ground.

4. QUALITY CONTROL AND IN-FIELD PROCESSING

Digital data for each flight were transferred to the field workstation, in order to verify data quality and completeness. A database was created and updated using Geosoft Oasis Montaj and proprietary Fugro Atlas software. This allowed the field personnel to calculate, display and verify both the positional (flight path) and geophysical data on a screen or printer. Records were examined as a preliminary assessment of the data acquired for each flight.

In-field processing of Fugro survey data consists of differential corrections to the airborne GPS data, verification of the flight path, verification of EM calibrations, drift correction of the raw airborne EM data, spike rejection and filtering of all geophysical and ancillary data, verification of the flight videos, calculation of preliminary resistivity data, diurnal correction, and preliminary leveling of magnetic data.

All data, including base station records, were checked on a daily basis, to ensure compliance with the survey contract specifications. Reflights were required if any of the following specifications were not met.

Navigation - Positional (x,y) accuracy of better than 10 m, with a CEP (circular error of probability) of 95%.

Flight Path - No lines to exceed ±25 % departure from nominal line spacing over a continuous distance of more than 1 km, except for reasons of safety.

Clearance - Mean terrain sensor clearance of 35 m, ±10 m, except where precluded by safety considerations, e.g., restricted or populated areas, severe topography, obstructions, tree canopy, aerodynamic limitations, etc.

Airborne Mag - Aerodynamic magnetometer noise envelope not to exceed 0.5 nT over a distance of more than 1 km. The non-normalized 4th

difference not to exceed 1.6 nT over a continuous distance of 1 kilometre excluding areas where this specification is exceeded due to natural anomalies.

Base Mag - Diurnal variations not to exceed 10 nT over a straight-line time chord of 1 minute.

EM - Spheric pulses may occur having strong peaks but narrow widths. The EM data area considered acceptable when their occurrence is less than 10 spheric events exceeding the stated noise specification for a given frequency per 100 samples continuously over a distance of 2,000 metres.

Frequency	**Coil Orientation**	**Peak to Peak Noise Envelope (ppm)**
1000Hz	vertical coaxial	5.0
900 Hz	horizontal coplanar	10.0
5500 Hz	vertical coaxial	10.0
7200 Hz	horizontal coplanar	20.0
56,000 Hz	horizontal coplanar	40.0

5. DATA PROCESSING

Flight Path Recovery

The quality of the GPS navigation was controlled on a daily basis by recovering the flight path of the aircraft. The correction procedure used the raw ranges from the base station to create improved models of clock error, atmospheric error, satellite orbit, and selective availability. These models were used to improve the conversion of aircraft raw ranges to differentially corrected aircraft position.

The raw range data from at least four satellites are simultaneously recorded by both the base and mobile GPS units. The geographic positions of both units, relative to the model ellipsoid, are calculated from this information. Differential corrections, which are obtained from the base station, are applied to the mobile unit data to provide a post-flight track of the aircraft, accurate to within 2 m.

To check the quality of the positional data, the speed of the bird was calculated using the differentially corrected x, y and z data. Any sharp changes in the speed were used to flag possible problems with the positional data. If speed jumps were evident, the data were inspected to determine the source of the error. The erroneous data were deleted and splined if less than two seconds in length. If the error was greater than two seconds the raw data were examined and, if acceptable, could be used to replace the bad data. The GPS-Z component is the most common source of error. When it shows problems that cannot be corrected by recalculating the differential correction, the barometric altimeter is used as a guide to assist in making the appropriate correction.

The corrected WGS84 latitude/longitude coordinates are transformed to the UTM coordinate system used on the final maps. Images or plots are then created to provide a visual check of the flight path.

Electromagnetic Data

EM data are processed at the recorded sample rate of 10 samples/second. Spheric rejection median and Hanning filters are then applied to reduce noise to acceptable levels. EM test profiles are then created to allow the interpreter to select the most appropriate EM anomaly picking controls for a given survey area. The EM picking parameters depend on several factors but are primarily based on the dynamic range of the resistivities within the survey area, and the types and expected geophysical responses of the targets being sought.

The interpretation geophysicist determines initial anomaly picking parameters and thresholds. Anomalous electromagnetic responses that meet the specific criteria are then automatically selected and analysed by computer to provide a preliminary electromagnetic anomaly map. The automatic selection algorithm is intentionally oversensitive to assure that no meaningful responses are missed. Using the preliminary maps in conjunction with the multi-parameter stacked profiles, the interpreter then classifies the anomalies according to their source and eliminates those that are not substantiated by the data. The final interpreted EM anomaly map will include bedrock, surficial and cultural conductors. A map containing only bedrock conductors can be generated, if desired.

Altitude Data

Radar altimeter data were despiked by applying a 1.5 second median filter and smoothed using a 1.5 second Hanning filter. The radar altimeter data were then subtracted from the GPS elevation to create a digital elevation grid, that was used in conjunction with profiles of the radar altimeter and flight path video, to detect any spurious values. The ALTBIRD_M channel is the corrected height of the bird above the ground, except in areas where erroneous results are caused by dense tree canopies.

Base Station Diurnal Correction

The raw diurnal data were sampled at 1 Hz and imported into a database. The data were filtered with a 51-point median filter and then a 51-point Hanning filter to remove spikes and smooth short wavelength variations. A non linear variation was then calculated and a flag channel was created to indicate any areas where the variation might have exceeded the survey tolerance. Acceptable diurnal data were interpolated to a 10 Hz sample rate and the local regional field value, calculated from the average of the first day's diurnal data, was removed to leave the diurnal variation. This diurnal variation was then used in the processing of the airborne magnetic data.

Apparent Resistivity

The apparent resistivities in ohm-m are generated from the in-phase and quadrature EM components for all of the coplanar frequencies, using a pseudo-layer half-space model. The inputs to the resistivity algorithm are the in-phase and quadrature amplitudes of the secondary field. The algorithm calculates the apparent resistivity in ohm-m, and the apparent height of the bird above the conductive source. Any difference between the apparent height and the true height, as measured by the radar altimeter, is called the pseudo-layer and reflects the difference between the real geology and a homogeneous half-space. This difference is often attributed to the presence of a highly resistive upper layer. Any errors in the altimeter reading, caused by heavy tree cover, are included in the pseudo-layer and do not affect the resistivity calculation. The apparent depth estimates, however, will reflect the altimeter errors. Apparent resistivities calculated in this manner may differ from those calculated using other models.

In any areas where the effects of magnetic permeability or dielectric permittivity have suppressed the in-phase responses, the calculated resistivities will be erroneously high. Various algorithms and inversion techniques can be used to partially correct for the effects of permeability and permittivity.

Apparent resistivity maps portray all of the information for a given frequency over the entire survey area. This full coverage contrasts with the electromagnetic anomaly map, which provides information only over interpreted conductors. The large dynamic range afforded by the multiple frequencies makes the apparent resistivity parameter an excellent mapping tool.

The preliminary apparent resistivity maps and images are carefully inspected to identify any lines or line segments that might require base level adjustments. Subtle changes between in-flight calibrations of the system can result in line-to-line differences that are more recognizable in resistive (low signal amplitude) areas. If required, manual level adjustments are carried out to eliminate or minimize resistivity differences that can be attributed, in part, to changes in operating temperatures. These leveling adjustments are usually very subtle, and do not result in the degradation of discrete anomalies.

After the manual levelling process is complete, revised resistivity grids are created. The resulting grids can be subjected to a microlevelling technique in order to smooth the data for contouring. The coplanar resistivity parameter has a broad 'footprint' that requires very little filtering.

The calculated resistivities for the 900 Hz, 7200 Hz and 56kHz coplanar frequencies are included in the XYZ and grid archives. Apparent Resistivity maps have been created from the 7200 Hz and 56 kHz data. Values are in ohm-metres on all final products.

Resistivity-depth Sections (optional)

The apparent resistivities for all frequencies can be displayed simultaneously as coloured resistivity-depth sections. Usually, only the coplanar data are displayed as the close frequency separation between the coplanar and adjacent coaxial data tends to distort the section. The sections can be plotted using the topographic elevation profile as the surface. The digital elevations, in metres a.m.s.l., can be calculated from the GPS Z-value or barometric altimeter, minus the aircraft radar altimeter.

Resistivity-depth sections can be generated in three formats:

(1) Sengpiel resistivity sections, where the apparent resistivity for each frequency is plotted at the depth of the centroid of the in-phase current flow[1]; and,

(2) Differential resistivity sections, where the differential resistivity is plotted at the differential depth[2].

(3) Occam[3] or Multi-layer[4] inversion

Both the Occam and multi-layer inversions compute the layered earth resistivity model that would best match the measured EM data. The Occam inversion uses a series of thin, fixed layers (usually 20 x 5m and 10 x 10m layers) and computes resistivities to fit the EM data. The multi-layer inversion computes the resistivity and thickness for each of a defined number of layers (typically 3-5 layers) to best fit the data.

Residual Magnetic Intensity

The residual magnetic intensity (RMI) is derived from the total magnetic field (TMF) channels, the diurnal, and the regional magnetic field. The total magnetic intensity is recorded in the aircraft, the diurnal is measured from the ground base station, and the regional magnetic field is calculated from the updated IGRF (International Geomagnetic Reference Field).

A fourth difference editing routine is applied to the magnetic data to remove any spikes. The result is then corrected for diurnal variation using the magnetic base station data. The results can then be levelled using tie and traverse line intercepts. Manual adjustments are

---

1 Sengpiel, K.P., 1988, Approximate Inversion of Airborne EM Data from Multilayered Ground: Geophysical Prospecting 36, 446-459.

2 Huang, H. and Fraser, D.C., 1993, Differential Resistivity Method for Multi-frequency Airborne EM Sounding: presented at Intern. Airb. EM Workshop, Tucson, Ariz.

3 Constable et al, 1987, Occam's inversion: a practical algorithm for generating smooth models from electromagnetic sounding data: Geophysics, 52, 289-300.

4 Huang H., and Palacky, G.J., 1991, Damped least-squares inversion of time domain airborne EM data based on singular value decomposition: Geophysical Prospecting, 39, 827-844.

applied to any lines that require levelling, as indicated by shadowed images of the gridded magnetic data.

The IGRF calculated for the specific survey location and the time of the survey, is then removed from the levelled magnetic data to yield the residual magnetic intensity (RMI). The levelled data are then subjected to a microlevelling filter for gridding and contouring.

Calculated Vertical Magnetic Gradient

The diurnally-corrected residual magnetic field data are subjected to a processing algorithm that enhances the response of magnetic bodies in the upper 500 m and attenuates the response of deeper bodies. The resulting vertical gradient map provides better definition and resolution of near-surface magnetic units. It also identifies weak magnetic features that may not be evident on the total field or residual magnetic maps. However, regional magnetic variations and changes in lithology may be better defined on the total magnetic field or residual magnetic intensity maps.

Magnetic Derivatives (optional)

The total magnetic field data can be subjected to a variety of filtering techniques to yield maps or images of the following:

enhanced magnetics
second vertical derivative
reduction to the pole/equator
magnetic susceptibility with reduction to the pole
upward/downward continuations
analytic signal

All of these filtering techniques improve the recognition of near-surface magnetic bodies, with the exception of upward continuation. Any of these parameters can be produced on request.

Contour, Colour and Shadow Map Displays

The geophysical data are interpolated onto a regular grid using a modified Akima spline technique. The resulting grid is suitable for image processing and generation of contour maps. The grid cell size is 20% of the line interval.

Colour maps or images are produced by interpolating the grid down to the pixel size. The parameter is then incremented with respect to specific amplitude ranges to provide colour "contour" maps.

Monochromatic shadow maps or images can be generated by employing an artificial sun to cast shadows on a surface defined by the geophysical grid. There are many variations in the shadowing technique. These techniques can be applied to total field or enhanced magnetic data, magnetic derivatives, resistivity, etc. The shadowing technique is also used as a quality control method to detect subtle changes between lines.

Digital Elevation (optional)

The altimeter values (sensor to ground clearance) are subtracted from the differentially corrected and de-spiked GPS-Z values to produce profiles of the orthometric heights (a.m.s.l.) along the survey lines. These values are gridded to produce contour maps showing approximate elevations within the survey area. The calculated digital terrain data are then tie-line levelled and can be adjusted to any known benchmarks in the survey area. Any remaining subtle line-to-line discrepancies are manually removed. After the manual corrections are applied, the digital terrain data are filtered with a microlevelling algorithm.

The accuracy of the elevation calculation is directly dependent on the accuracy of the two input parameters, altimeter and GPS-Z. The altimeter values may be erroneous in areas of heavy tree cover, where the altimeter reflects the distance to the tree canopy rather than the ground. The GPS-Z value is primarily dependent on the number of

available satellites. Although post-processing of GPS data will yield X and Y accuracies in the order of 1-2 metres, the accuracy of the Z value is usually much less, sometimes in the ±10 metre range. Further inaccuracies might be introduced during the interpolation and gridding process.

The data archive contains the calculated digital elevations above the geoid (a.m.s.l.). Because of the inherent inaccuracies of this method, no guarantee is made or implied that the information displayed is a true representation of the height above sea level. Although this product may be of some use as a general reference, THIS PRODUCT MUST NOT BE USED FOR NAVIGATION PURPOSES.

6. PRODUCTS

This section lists the final maps and products that are provided under the terms of the survey agreement. Other products can be prepared from the existing dataset, if requested. These include stacked multi-parameter profiles, resistivity-depth sections, inversions, magnetic enhancements or derivatives, percent magnetite, and digital elevation. Most parameters can be displayed as contours, profiles, or in colour; or as digital images in PDF or other file formats.

Base Maps

Base maps of the survey area are produced by scanning published topographic maps to a bitmap (.bmp) format. This process provides a relatively accurate, distortion-free base that facilitates correlation of the navigation data to the map coordinate system. It should be noted that the (older) scanned topographic map shows UTM coordinate lines in the NAD 27 datum, whereas the smaller graticules (crosses) are in the newer NAD 83 system. The difference between the two coordinate systems is seen as a shift of about 180 m to the south and 100 m to the east for the NAD 83 relative to NAD 27. This is not a location error, as the NAD 83 geophysical data are properly positioned relative to the NAD 27 topography. The NAD 27 topographic files were combined with NAD 83 geophysical data for plotting the final maps. All maps were created using the following parameters:

Projection Description:

Datum:	NAD 83
Ellipsoid:	WGS 84; GRS 1980
Projection:	UTM (Zone: 8N)
Central Meridian:	135° W
False Northing:	0
False Easting:	500000
Scale Factor:	0.9996
WGS84 to Local Conversion:	Molodensky
Datum Shifts:	DX: 0 DY: 0 DZ: 0

Final Products

The following parameters are presented on single map sheets for each area at a scale of 1:20,000. All maps include flight lines and topography, unless otherwise indicated. Preliminary products are not listed.

	2 Map Sheets x 2 Sets*	
	Blackline	Colour
EM Anomalies		2x2
Residual Magnetic Intensity		2x2
Calculated Vertical Magnetic Gradient		2x2
Apparent Resistivity 7200 Hz		2x2
Apparent Resistivity 56 kHz		2x2

Additional Products

Digital Archive (see Archive Description)	1 DVD
Survey Report	2 copies + PDF version
Final Digital versions of all maps above	PDF files (+ DXF for the EM)
Flight Path Video Records	4 DVDs

7. SURVEY RESULTS

General Discussion

Table 7-1 summarizes the EM responses in the survey area, with respect to conductance grade and interpretation. For “discrete” conductors (B, D, or T), the apparent conductance and depth values shown in the EM Anomaly list appended to this report have been calculated from “local” in-phase and quadrature amplitudes of the Coaxial 5500 Hz frequency, using a near-vertical, half plane model. Conductance values for the broader (S, H, or E) types have been calculated from absolute amplitudes using a horizontal half-space model.

Wide bedrock conductors or flat-lying conductive units, (S, H, or E) whether from surficial or bedrock sources, may give rise to very broad anomalous responses on the EM profiles. These may not appear on the electromagnetic anomaly map if they have a regional character rather than a locally anomalous character. These broad conductors, which more closely approximate a half-space model, will be maximum coupled to the horizontal (coplanar) coil-pair and should be more evident on the resistivity parameters. Resistivity maps, therefore, may be more valuable than the electromagnetic anomaly maps, in areas where broad or flat-lying conductors are considered to be of importance. All three coplanar resistivity grids are included on the final data archive.

The picking and interpretation procedure relies on several parameters and calculated functions. For this survey, the Coaxial 5500 Hz responses and the mid-frequency difference channels were used as two of the main picking criteria. The 7200 Hz coplanar results were also weighted to provide picks over wider or flat-dipping sources. The quadrature channels provided picks in any areas where the in-phase responses might have been suppressed by magnetite.

Excellent resolution and discrimination of conductors was accomplished by using a fast sampling rate of 0.1 sec and by employing a “common” frequency (5500Hz / 7200Hz) on

two orthogonal coil-pairs (coaxial and coplanar). The resulting difference channel parameters often permit differentiation of bedrock and surficial conductors, even though they may exhibit similar conductance values. Because of the poorly conductive nature of the expected mineralization in the area, the difference calculations were based on the mid frequencies rather than the low frequencies. The lower frequencies tend to “see deeper” in conductive environments, but the higher frequencies respond better to weaker conductors and resistive units, and are probably better suited to this specific target.

Magnetic Data

A Fugro CF-1 cesium vapour magnetometer was operated at the survey base to record diurnal variations of the earth's magnetic field. The clock of the base station was synchronized with that of the airborne system to permit subsequent removal of diurnal drift. A GEM Systems GSM-19T proton precession magnetometer was also operated as a backup unit.

The residual magnetic field data (IGRF removed) have been presented as contours on the base maps using a contour interval of 5 nT where gradients permit. The maps show the magnetic properties of the rock units underlying the survey areas.

The residual magnetic field data were also subjected to a processing algorithm to produce maps of the calculated vertical gradient. This procedure enhances near-surface magnetic units and suppresses regional gradients. It also provides better definition and resolution of magnetic boundaries and displays weak magnetic features that may not be clearly evident on the residual magnetic intensity maps.

Magnetic relief is moderate, yielding a dynamic range of about 1424 nT on the Elko property, and 2123 nT on Nash. Strikes in the Elko are generally between 116° to 130°, and are intersected obliquely by at least three inferred breaks that strike NNW. On the Nash property, there is a well defined contact that trends ESE and then SSE along the NE edge of the strong magnetic unit that dominates the SW quadrant of the block. The 56kHz

resistivity patterns show weak correlation with this contact, which suggests that the two parameters are probably responding to similar (bedrock) causative sources in this area. In the northeast, however, the magnetic trends are ambiguous, while the prominent WNW trending resistivity low appears to be primarily reflecting the near-surface cover in the low-lying topography adjacent to the river valley. .

In the Elko area, the Residual Magnetic Intensity map shows a gradual increase in magnetic susceptibility towards the NE, up to the contact that runs along the NE property boundary. The CVG map, however, presents a much more complex image, suggesting the presence of several interbedded bands or upturned layers of weakly magnetic and slightly less magnetic units. The conductive zones on the property conform to this general SE strike (130°±10°), but the multi-conductor sources can be either magnetic or non-magnetic. The stronger conductors, however, generally appear to be non-magnetic, which suggests graphite, or argillaceous shales as likely contributing factors. Conversely, some of the less conductive, more magnetic, narrow bands might reflect increases in sulphide content.

Differences in the magnetic and resistivity patterns could also be influenced by changes in the thickness of overburden, a lack of magnetic contrast between the near-surface units, gradational changes in susceptibility due to metamorphism or alteration, or the presence of overlapping, flat-dipping layers that tend to yield averaged values. The magnetic parameter could also be reflecting deeper basement units that may not be exposed at surface.

There is strong evidence on the magnetic maps, particularly the calculated vertical gradient, which shows that the survey areas host several distinct units, some of which have been subjected to deformation and/or alteration. These structural complexities are evident on the colour contour maps as variations in magnetic intensity, irregular patterns, and as offsets or changes in strike direction.

If a specific magnetic intensity can be assigned to the rock type that is believed to host the auriferous mineralization, it may be possible to select areas of higher priority on the basis of the magnetic data. This is based on the assumption that the magnetite content of the host rocks will give rise to a limited range of contour values that will permit differentiation of the various lithological units.

The magnetic results have provided valuable information that can be used in conjunction with the other geophysical parameters, to help map the geology and structure in the survey areas.

Apparent Resistivity

Apparent resistivity grids, which display the conductive properties of the survey areas, were produced from the 900 Hz, 7200 Hz, and 56000 Hz coplanar data. The maximum resistivity values, which are calculated for each frequency, are 1080, 8,640 and 30,000 ohm-m respectively. These cut-offs eliminate the erratic higher resistivities that could result from unstable ratios of very small EM amplitudes. All coplanar resistivity data are included on the final data archive.

It is not known if the sedimentary units in these areas have undergone sufficient alteration and porosity to cause a measureable change in resistivity. If true, these changes could be very subtle, and would likely be more evident on the high frequency (56kHz) maps. Both resistive and weakly conductive trends are evident on the near-surface 56 kHz maps. It is interesting to note that some of the well-defined magnetic lows are highly conductive, (e.g., Elko Anomaly 10270S) while other lows are resistive (at fiducial 2456 on line 10080). Conductor 11080D is non-magnetic, while the nearby response at 10080E is magnetic.

In any areas where the targets are expected to be highly silicified and non-porous, these should show as narrow resistive units. These non-magnetic, non-conductive linear

trends may prove to be the more attractive targets in the search for quartz-vein type mineralization. Conversely, increased porosity, (Carlin-type) alteration, or an increase in sulphide content associated with some shears or faults, could show as more conductive trends. Any plug-like intrusive features, either resistive or conductive, are also considered to be of interest as they could have influenced mineral deposition along their perimeters.. Any weak EM responses that are associated with the margins of these inferred intrusive units may also warrant further investigation.

As there is no consistent resistivity/magnetic correlation on the survey blocks, this indicates that the magnetic and resistivity parameters are sometimes responding to different causative sources; i.e., the EM-derived resistivity is responding to changes in the overburden and near-surface layers, while the magnetic data are reflecting changes in the deeper underlying basement units. It is also possible that the near-surface non-magnetic sediments contain enough graphite (or sulphides) to yield strong conductors within these non-magnetic host units.

If the sediments have been intruded by felsic (granitic) intrusions, one might expect to see little or no change in susceptibility, although the associated resistivity could be slightly higher. Conversely, intermediate or mafic intrusions or flows would likely yield a stronger magnetic signature with a probable decrease in resistivity. However, if the host units contain appreciable amounts of magnetite, the suppression of in-phase responses could yield (overstated) resistivity values that are higher than background.

Both resistivity highs and lows may therefore be of interest. The magnetic signatures can be also be quite complex in areas where the limestone units are interlayered with mafic flows. An attempt should be made to determine the geophysical signatures over the various rock types. The ATAC Resources web site suggests that the RAU (Tiger) zone is a Carlin-type, strata-bound, structurally controlled, dolomite/iron carbonate replacement zone, associated with both sulphide and oxide mineralization.

There are at least five main zones of low resistivity on the Elko property and one main zone on the Nash property. The more conductive portions of these zones have been outlined on the EM Anomaly maps. Although these conductive zones may be of minor exploration significance, there are high Au soil and rock sample values on the ridge near the northern edge of Zone D in Elko.

There are a few weak quadrature responses on both properties that are associated with relative resistivity highs. Elko anomaly 10360S is one weak example, while the magnetite-hosted (9.5% FeO) response at 20070D (Nash) is another. The very strong magnetic response on line10310 at fiducial 8035 is a classic example of high apparent resistivity that has been caused by magnetite suppression. This interesting magnetic feature contains more than 11.5% magnetite, but is non-conductive.

At least three of the conductive zones on **Elko** are also associated with creeks or low-lying areas, and may also be partially caused by surface (overburden) conductivity. However, it is interesting to note that at least three other zones are located on high ground, and have been attributed to conductive bedrock sources. These moderately strong multi-conductor units are considered to be of minor importance at this time, except in areas where they appear to be intruded, faulted or folded. North-south trending structures may be significant in this area

Apart from the several SE-trending resistivity lows, there are at least four resistivity highs that correlate loosely with magnetic lows. These are evident on line 10090 at fiducial 2746; line 10190 at fiducial 6767, at the north end of line 10270 at fiducials 1854 and possibly1883, line 10280 at 1655 along a ridge of high ground, line 10350 at 5513, and line 10370 at 4600. These subtle features could reflect sedimentary layers, faults, or non-magnetic intrusions. However, the very strong isolated, magnetite-induced resistivity high on line 10310 at fiducial 8035, and the weaker magnetite sources on 10330 at 6865 and 10350 at 5716, could possibly reflect skarns. The estimated magnetite content on line10310 at 8035 is about 11%. Although this plug-like isolated magnetic high is quite small, it is considered to be a potential target that warrants further

investigation. The resistive unit that strikes ESE from fiducial 6825 on line 10330 to fiducial 2204 on 10420 is at least partially due to magnetite suppression.

The conductive “zones” shown on the EM anomaly map, are based on the 7200 Hz resistivity outlines. Although these conductive zones are also evident on the near-surface 56kHz maps, it is interesting to note that most are stronger on the deeper 900Hz parameter. This indicates that these conductive zones are overlain by more resistive cover, and many may not all be exposed at surface. The low 900 Hz resistivities also indicate that the apparent conductance increases with depth. Lower resistivities on the 900 Hz are evident in most zones, including the anomalies at 10130D in ZoneA1, 10200N in Zone A2, 10210G in B1, 10250D in B2, 10250W in Zone C, and 10360N in Zone D.

There are also a few more isolated or less conductive zones that should also be investigated. Although it is not outlined on the EM anomaly map, there is a major resistivity low that strikes about 120° from 10190A to 10250G, and then swings SE (140°) through 10460A. This unit may be offset in the vicinity of 10260N..

There is also a moderately conductive zone, near the crest of a hill, which extends ESE (116°) from 10180M to 10230Q, a distance of about 1 km. This zone contains both thin and thick sources within in a non-magnetic host unit.

The close proximity of the multiple conductors in the Elko area often precludes accurate dip estimates. However, dips appear to vary from NE (anomalies 10130F in A1, 10190K in A2, and 10260C in B2) to SW (10230J in B1, and 10360D in Zone D). On line 10340, anomaly E suggests a possible SW dip, while anomaly I indicates an opposing dip to the NE.

Although the highly conductive sources in the Elko area may not necessarily be of economic interest, there are some areas where these zones appear to be intersected by possible faults or non-magnetic linear features that can be inferred from the CVG data.

As other sediment-hosted gold deposits in the general area are reportedly associated with structural breaks, these are the areas that are considered to be of greater significance. It is beyond the scope of this report to describe the 812 anomalous responses detected by the Elko survey, but any responses associated with these inferred faults, folds, or intrusions probably warrant further investigation, particularly if they occur in areas of favourable geology or geochemistry.

The single ESE-trending resistivity low on **Nash** is associated with a tributary of Nash Creek and may be partially due to conductive cover along the south side of the creek valley. However, this unit appears to lie south of the creek, and contains several strong conductors that have been attributed to bedrock sources. Line 20180 has defined at least five distinct conductive sources comprising the resistivity low at the north end of the survey block. All of these highly conductive sources are non-magnetic, so graphitic or argillaceous sediiments are considered to be possible causes. There are no distinct magnetic contacts associated with the boundaries of this conductive unit, although anomaly 20150B yields a weak 11 nT correlation. . This formational unit might warrant further work to determine the causative sources of the anomalous responses within, or near the perimeter of this zone, and also in any areas where the unit appears to have been faulted or folded.

A more significant resistivity contrast is the subtle low that is associated with the NW edge of the well-defined ESE-SSE trending magnetic contact in the SW quadrant of the property. This magnetic unit may be intersected by at least five structural breaks, which can be inferred from the CVG data. The magnetite content near the north contact, at anomaly 20070D, is estimated to be more than 9.5%. All of the weak responses associated with this contact, including 20060B, 20090C and 20090D, are considered to be high priority targets. In addition, any other responses that occur in close proximity to inferred breaks or contacts should also be subjected to further investigation, particularly those with magnetic correlation. The subtle arcuate resistivity low that includes 20120A, 20110A, and 20160B, could reflect an alteration halo, although it is associated with a

non-magnetic unit at the eastern contact of the strong magnetic high that dominates the SW quadrant. This weak zone is located within a basin-shaped topographic depression.

The other non-magnetic, weakly conductive zones on the property are also considered to be of potential interest, even if they are essentially “non-anomalous”. These zones are most evident on the 56kHz map, which measures a much larger dynamic range of resistivities. These should be checked, in order to determine if they are due to increased alteration or porosity associated with faults or sheared contacts. As the target mineralization can be associated with oxide hosts, resistivity contrasts that yield flanking or direct magnetic correlation will probably be of greater significance.

There are other resistivity lows and highs that might also be of interest. Some of these are quite extensive and appear to reflect "formational" conductors or layers that could be of minor interest as direct exploration targets. However, attention may be focused on areas where these zones appear to be faulted or folded or where anomaly characteristics differ along strike. The ESE-trending low resistivity zones that are evident on both properties appear to have been faulted or folded in several areas.

Other conductive zones are quite subtle, and could be due to changes in overburden thickness, rather than changes in rock type. However, those that are associated with linear magnetic breaks, contacts, or decreases in magnetite, are considered to be of slightly higher priority.

Electromagnetic Anomalies

Although the targets of interest in this area may be resistive, rather than conductive, discrete EM anomalies have been picked, in order to locate possible sulphide zones and to detect zones of alteration or clay-rich shears. As such zones are likely to be poorly conductive, anomaly picks were based primarily on the mid-frequency (5500 Hz) coaxial channel which responds better to weaker conductors than the lower 1000 Hz.

The EM anomalies resulting from this survey appear to fall within one of three general categories. The first type consists of discrete, well-defined anomalies that yield marked inflections on the difference channels. These anomalies are usually attributed to conductive sulphides or graphite, and are generally given a "B" or "D" interpretive symbol, denoting a bedrock source.

The second class of anomalies comprises moderately broad responses that exhibit the characteristics of a half-space and do not yield well-defined inflections on the difference channels. Anomalies in this category are usually given an "S" (at, or near surface) or "H" (buried half-space) interpretive symbol. The lack of a difference channel response usually implies a broad or flat-lying conductive source. Some of these anomalies could reflect buried flat-dipping conductive rock units, zones of alteration or deep weathering, or increased overburden thickness, all of which can yield “non-discrete” signatures. Anomalies in this category are generally considered to be of minor interest unless they occur in areas of favourable geology.

The effects of conductive overburden are evident over portions of both survey blocks. Although the difference channels (DIFI and DIFQ) are extremely valuable in detecting bedrock conductors that are partially masked by conductive overburden, sharp undulations in the bedrock/overburden interface can yield anomalies in the difference channels which may be interpreted as possible bedrock conductors. Such anomalies usually fall into the "S?" or "B?" classification but may also be given an "E" interpretive symbol, denoting a resistivity contrast at the edge of a conductive unit.

The "?" symbol does not question the validity of an anomaly, but instead indicates some degree of uncertainty as to which is the most appropriate EM source model. This ambiguity results from the combination of effects from two or more conductive sources, such as overburden and bedrock, gradational changes, or moderately shallow dips. The presence of a conductive upper layer has a tendency to mask or alter the characteristics

of bedrock conductors, making interpretation difficult. This problem is further exacerbated in the presence of magnetite.

The third anomaly category includes responses that are associated with magnetite. Magnetite can cause suppression or polarity reversals of the in-phase components, particularly at the lower frequencies in resistive areas. Conductive overburden tends to mask many of these negative excursions, particularly at the higher frequencies, but the effects of magnetite-rich rock units are occasionally evident on the EM profiles as suppressions or negative excursions of the lower frequency in-phase channels.

Poorly conductive magnetic features can give rise to resistivity anomalies that are only slightly below or slightly above background. If it is expected that poorly conductive economic mineralization could be associated with magnetite-rich units, most of these weakly anomalous features will also be of interest. In areas where magnetite causes the in-phase components to become negative, the apparent conductance and depth of EM anomalies will be unreliable. Magnetite effects usually give rise to overstated (higher) resistivity values and understated (too shallow) depth calculations.

Bedrock Conductors

As potential targets within the areas can be associated faults, alteration zones, or very weakly disseminated sulphides, which may be hosted by non-magnetic quartz-rich units, and which can be overlain by conductive overburden, it is impractical to assess the relative merits of EM anomalies on the basis of conductance. It is recommended that an attempt be made to compile a suite of geophysical "signatures" over any known areas of interest.

Broad zones of carbonate alteration, skarn-type mineralization or sediment-hosted auriferous mineralization would not normally give rise to discrete EM conductors, unless the gold was associated with conductive clay material or semi-massive to massive sulphides. Identifying weakly conductive zones on the 56kHz resistivity parameter will

probably be a more effective tool to locate alteration zones. However, electromagnetic anomalies have been picked for these survey areas in order to locate any possible conductive sulphide concentrations and any weakly conductive faults or shears that could serve as conduits or host units for auriferous mineralization. The electromagnetic anomaly maps show the anomaly locations with the interpreted conductor type, dip, and conductance being indicated by symbols. Direct magnetic correlation is also shown, if it exists.

Tables 7-1 and 7-2 show that nearly 81% of the anomalous responses in Elko and 60% of the responses in Nash have been attributed to possible bedrock sources. The anomalous EM responses detected by the survey have been assigned a simple colour code on the EM Anomaly maps, in order to facilitate source recognition. The thinner dyke-like (D) sources have been assigned a red colour, while the thicker (B) bedrock sources are shown in dark blue. Surficial (S) overburden responses or buried thick layers (H) are shown in green, as are edge effects (E).

Conductor axes have not been shown because of the large number of anomalies combined with the fact that most trends can be visually correlated from line to line with a reasonable degree of confidence. Most of the anomalous responses are of moderate to strong signal amplitude and they generally yield moderate to low conductance values of less than 10 Siemens (mhos). The conductance is based on the mid-frequency coaxial responses, so there could be higher conductance values than those shown on the map, particularly in areas where anomalies suggest an increase in conductivity at depth, as evidenced by the more conductive 900 Hz responses. Some zones comprise multi-conductor sources that may be buried beneath more resistive cover.

It is beyond the scope of this report to attempt to describe the 920 anomalous responses detected by the survey. Most of the “sulphide-type” responses that have been attributed to possible or probable bedrock sources are shown on the EM Anomaly map in red or blue colours. There is little merit in analysing the stronger EM conductors unless it can be determined that the auriferous mineralization is associated with

increases in graphite or sulphide content. Instead, an attempt should be made to determine the geophysical signatures over the more favourable (sedimentary) host units, and use the magnetic parameters to locate areas of structural deformation that may have influenced mineral deposition.

TABLE 7-1 EM ANOMALY STATISTICS

ELKO PROJECT AREA

CONDUCTOR GRADE	CONDUCTANCE RANGE SIEMENS (MHOS)	NUMBER OF RESPONSES
7	>100	3
6	50 - 100	7
5	20 - 50	33
4	10 - 20	47
3	5 - 10	79
2	1 - 5	475
1	<1	151
*	INDETERMINATE	17
TOTAL		812

CONDUCTOR MODEL	MOST LIKELY SOURCE	NUMBER OF RESPONSES
D	THIN BEDROCK CONDUCTOR	393
B	DISCRETE BEDROCK CONDUCTOR	250
S	CONDUCTIVE COVER	128
H	ROCK UNIT OR THICK COVER	17
E	EDGE OF WIDE CONDUCTOR	24
L	CULTURE	0
TOTAL		812

(SEE EM MAP LEGEND FOR EXPLANATIONS)

TABLE 7-2 EM ANOMALY STATISTICS

NASH PROJECT AREA

CONDUCTOR GRADE	CONDUCTANCE RANGE SIEMENS (MHOS)	NUMBER OF RESPONSES
7	>100	0
6	50 - 100	0
5	20 - 50	1
4	10 - 20	4
3	5 - 10	10
2	1 - 5	74
1	<1	12
*	INDETERMINATE	7
TOTAL		108

CONDUCTOR MODEL	MOST LIKELY SOURCE	NUMBER OF RESPONSES
D	THIN BEDROCK CONDUCTOR	16
B	DISCRETE BEDROCK CONDUCTOR	41
S	CONDUCTIVE COVER	42
H	ROCK UNIT OR THICK COVER	1
E	EDGE OF WIDE CONDUCTOR	8
L	CULTURE	0
TOTAL		108

(SEE EM MAP LEGEND FOR EXPLANATIONS)

Although many of these responses reflect sulphide-type targets, they do not necessarily represent the more economically attractive areas on the properties, given the non-conductive nature of the expected sediment-hosted (auriferous) target mineralization.

The magnetic parameter appears to have been more effective than the resistivity parameter in delineating rock units and areas of structural deformation that may have influenced local mineral deposition. The resistivity parameter, however, has outlined several conductive zones as well as resistive units. The two parameters are complementary, and when used together, should help to locate the more favourable areas for mineral deposition.

8. CONCLUSIONS AND RECOMMENDATIONS

This report provides a very brief description of the survey results and describes the equipment, data processing procedures and logistics of the airborne survey over the Elko and Nash project areas, near Mayo, Yukon Territory. The various products accompanying this report display the magnetic and conductive properties of the survey areas.

The magnetic results have provided valuable structural information that can be used to help locate the more favourable areas for strata-bound, structurally-controlled, sediment - hosted gold mineralization on the properties. In addition to locating several linear faults and shears, the vertical gradient data have outlined the contacts of both magnetic and non-magnetic units. The former could reflect mafic layers, intrusions, or units containing concentrations of oxide (magnetite) mineralization. The latter could reflect faults or shears, non-magnetic intrusions or sedimentary layers, alteration zones, or reducing environments that could host auriferous mineralization.

The resistivity parameters have outlined both conductive and resistive units. The former are generally attributed to rock units hosting multiple bedrock conductors, most of which are non-magnetic. The non-magnetic characteristics suggest that many of the conductors could be due to graphitic or argillaceous sediments, rather than magnetic sulphides such as pyrrhotite. The more subtle resistivity lows could reflect possible alteration zones or minor increases in sulphide content. The non-magnetic plug-like resistivity highs could be due to resistive intrusions (stocks), although some of the magnetic resistive zones are obviously due to rock units containing higher concentrations of magnetite.

There were more than 810 anomalous EM responses detected in the Elko area and about 108 in the Nash area, about 70% of which have been interpreted as possible or probable bedrock conductors. Some of these have been attributed to increases in conductive sulphide content or clay-altered shears. Most responses are of moderate to low

amplitude, but are quite well defined, yielding moderately low conductance values of less than 10 Siemens

In the Elko block, the magnetic data show a well-defined SWE-trending (120°) contact along the NE property boundary The south-flanking magnetic zone shows a gradual decrease in susceptibility towards the SW, but the CVG suggests that this unit actually comprises several interlayered units that exhibit subtle changes in susceptibility. Several faults can be inferred from the CVD data, and these zones of structural deformation or alteration are deemed to be favourable areas for mineral deposition.

The Elko resistivity patterns follow the same general (120°) strike direction, but do not show a consistent or direct correlation with the (deeper?) magnetic units. An attempt should be made to determine if some of the more subtle resistivity lows can be attributed to Carlin-type alteration/replacement zones. In addition, the magnetite-rich zones detected by the survey should be investigated in order to determine their causative sources. High gold soil/rock samples occur on the property, in moderately close proximity to magnetite-rich horizons. Auriferous mineralization ESE of the property is reportedly associated with both oxide and minor sulphide mineralization.

The magnetic data on the Nash property show a strong, well-defined magnetic unit in the southwestern quadrant. The vertical gradient patterns suggest the presence of a few inferred linear breaks, all of which are considered to be of interest as possible structural controls or conduits. Additional work is also recommended to check the causative sources of the weak conductors that are associated with the northern contact of this interesting plug-like feature, including the magnetite-rich conductor at 20070D.

The 650 m-wide conductive band that strikes ESE near the NE Nash property boundary hosts several bedrock conductors. Nearly all of these are non-magnetic so graphitic sediments are considered to be a likely cause. Additional work may be warranted to confirm the causative source of the responses near 20160E and 20220A, where very subtle breaks can be inferred from the vertical gradient data. The most conductive portion

of this zone is near anomaly 20260D, where values of less than 5 ohm-m are observed at depth.

The anomalous resistivity and magnetic targets defined by the survey should be subjected to further investigation, using appropriate surface exploration techniques. Any inferred contacts and structural breaks are considered to be of particular interest as they may have influenced or controlled mineral deposition within the survey areas. Anomalies that are currently considered to be of moderately low priority may require upgrading if follow-up results are favourable.

A detailed analysis of existing geophysical data is recommended, in conjunction with all available geological and geochemical data, in order to extract the maximum amount of information from the survey results. Current software and imaging techniques can often provide valuable information on structure and lithology, which may not be clearly evident on the colour maps and images provided with this report. These techniques can yield images that define subtle, but significant, structural details.

Respectfully submitted,

FUGRO AIRBORNE SURVEYS CORP.

R11058

APPENDIX A

LIST OF PERSONNEL

The following personnel were involved in the acquisition, processing, interpretation and presentation of data, relating to a DIGHEM airborne geophysical survey carried out over the Elko and Nash project areas, for Golden Ridge Resources Inc., near Mayo, YT.

Lesley Minty	Project Manager
Terry Lacey	Equipment Operator
Sarah Underhay	Data Processor/Crew Leader
Tayebe Hamzeh	Data Processor (Office)
Lyn Vanderstarren	Drafting Supervisor
Guy Lajoie	Pilot (Questral Helicopters Ltd.)

The survey consisted of 314 km of coverage, flown from August 8 to August 12, 2011.

All personnel are employees of Fugro Airborne Surveys, except for the pilot who is an employee of Questral Helicopters Ltd.

APPENDIX B

DATA PROCESSING FLOWCHARTS

APPENDIX B

Processing Flow Chart - Electromagnetic Data

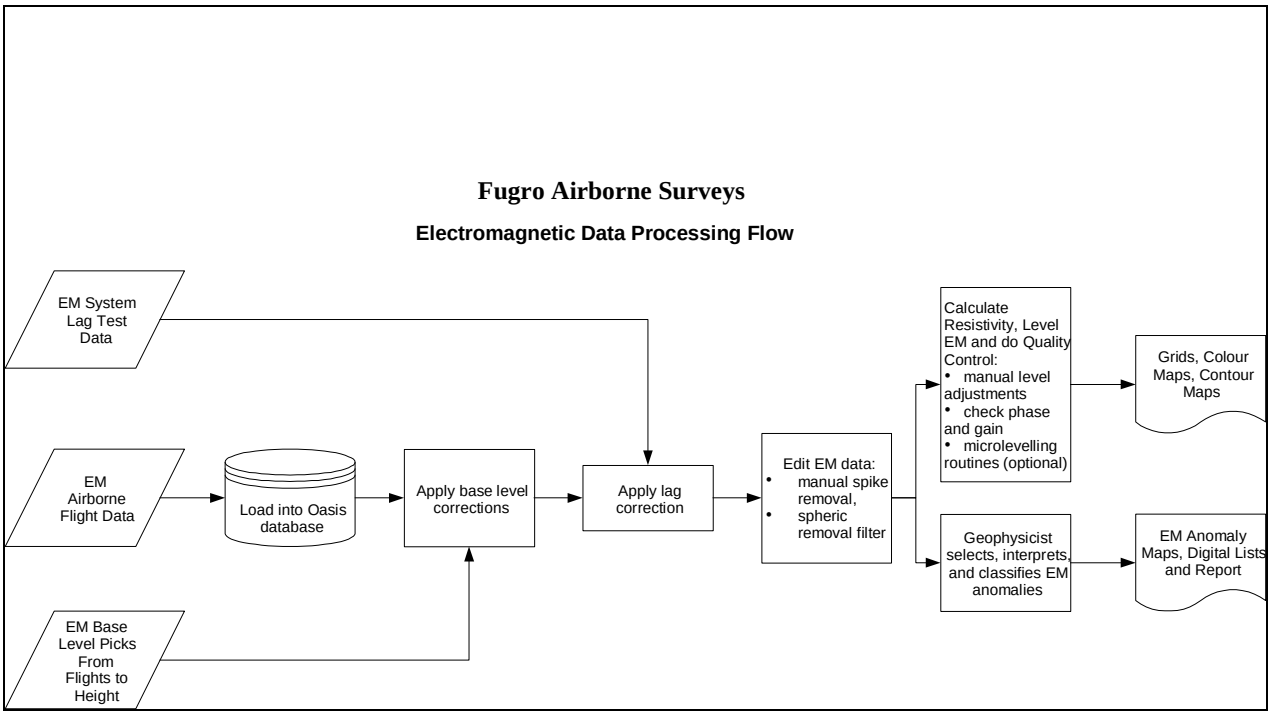

Processing Flow Chart - Magnetic Data

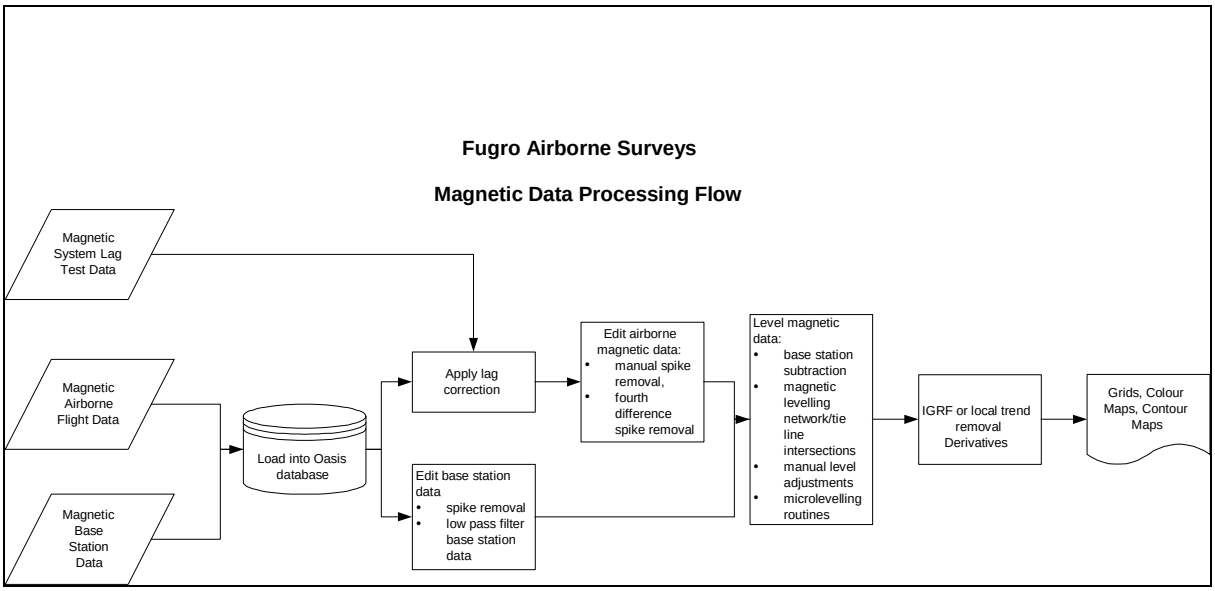

APPENDIX C

BACKGROUND INFORMATION

BACKGROUND INFORMATION

Electromagnetics

Fugro electromagnetic responses fall into two general classes, discrete and broad. The discrete class consists of sharp, well-defined anomalies from discrete conductors such as sulphide lenses and steeply dipping sheets of graphite and sulphides. The broad class consists of wide anomalies from conductors having a large horizontal surface such as flatly dipping graphite or sulphide sheets, saline water-saturated sedimentary formations, conductive overburden and rock, kimberlite pipes and geothermal zones. A vertical conductive slab with a width of 200 m would straddle these two classes.

The vertical sheet (half plane) is the most common model used for the analysis of discrete conductors. The B, D and T type are analyzed according to this model, with the conductance being calculated from the local amplitudes of the coaxial data.. The following section entitled **Discrete Conductor Analysis** describes this model in detail.

The conductive earth (half-space) model is more suitable for broad conductors that carry an S, H, or E type interpretation symbol. Conductance values for these anomalous responses are based on the absolute amplitudes of the selected coplanar channels. Resistivity maps result from the use of this model. A later section entitled **Resistivity Mapping** describes the method further.

Geometric Interpretation

The geophysical interpreter attempts to determine the geometric shape and dip of the conductor. Figure C-1 shows typical HEM anomaly shapes that are used to guide the geometric interpretation.

Discrete Conductor Analysis

The EM anomalies appearing on the electromagnetic map are analyzed by computer to give the conductance (i.e., conductivity-thickness product) in siemens (mhos). The B, D, and T type calculations are based on a vertical sheet model. This is not an unreasonable procedure, because the computed conductance increases as the electrical quality of the conductor increases, regardless of its true shape. HEM anomalies are divided into seven grades of conductance, as shown in Table C-1. The conductance in siemens (mhos) is the reciprocal of resistance in ohms.

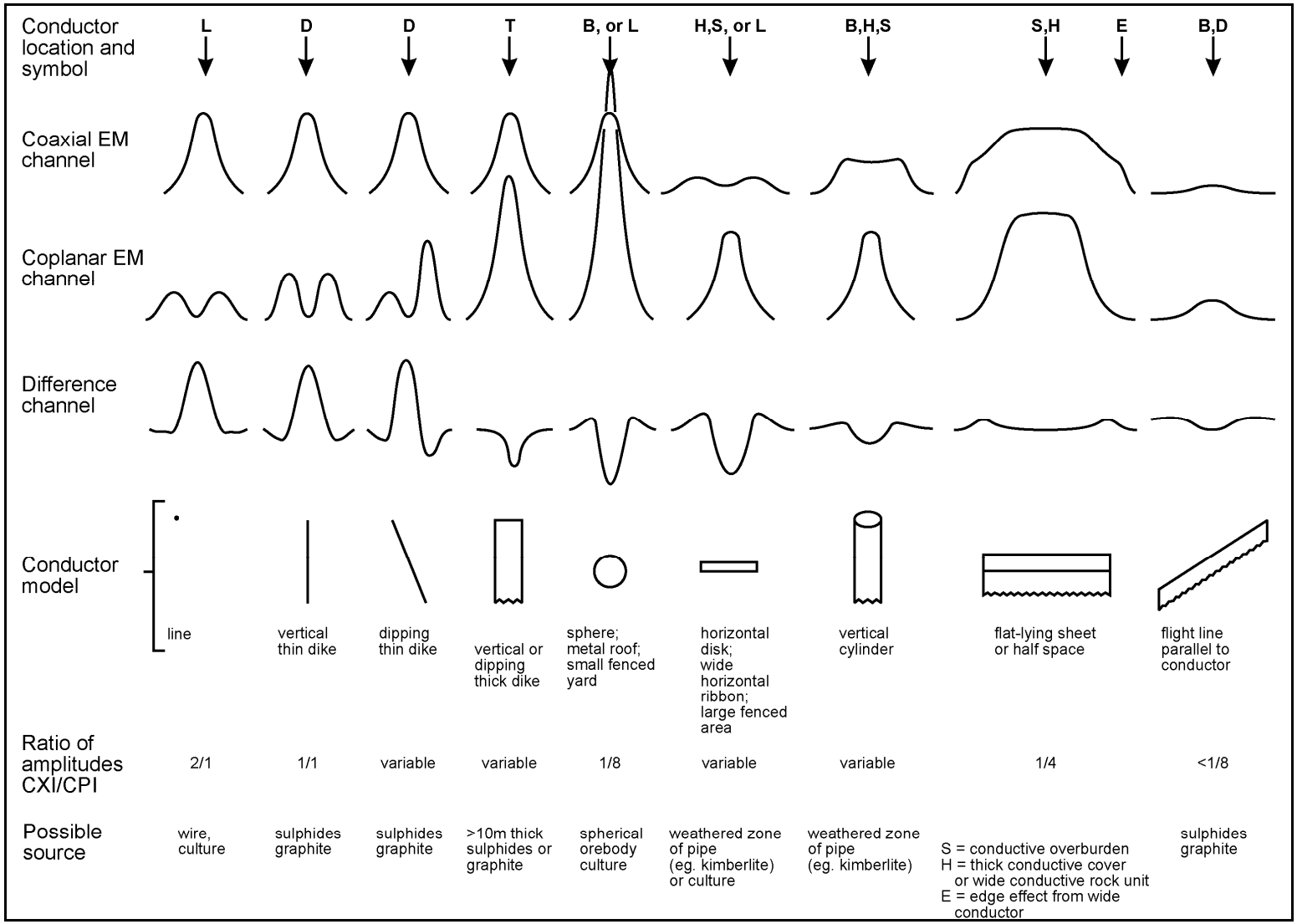

Typical HEM anomaly shapes
Figure C-1

The conductance value is a geological parameter because it is a characteristic of the conductor alone. It generally is independent of frequency, flying height or depth of burial, apart from the averaging over a greater portion of the conductor as height increases. Small anomalies from deeply buried strong conductors are not confused with small anomalies from shallow weak conductors because the former will have larger conductance values.

Table C-1. EM Anomaly Grades

Anomaly Grade	Siemens
7	> 100
6	50 - 100
5	20 - 50
4	10 - 20
3	5 - 10
2	1 - 5
1	< 1

Conductive overburden generally produces broad EM responses which may not be shown as anomalies on the geophysical maps. However, patchy conductive overburden in otherwise resistive areas can yield discrete anomalies with a conductance grade (cf. Table C-1) of 1, 2 or even 3 for conducting clays that have resistivities as low as 50 ohm-m. In areas where ground resistivities are less than 10 ohm-m, anomalies caused by weathering variations and similar causes can have any conductance grade. The anomaly shapes from the multiple coils often allow such conductors to be recognized, and these are indicated by the letters S, H, and sometimes E on the geophysical maps (see EM legend on maps).

For bedrock conductors, the higher anomaly grades indicate increasingly higher conductances. Examples: the New Insco copper discovery (Noranda, Canada) yielded a grade 5 anomaly, as did the neighbouring copper-zinc Magusi River ore body; Mattabi (copper-zinc, Sturgeon Lake, Canada) and Whistle (nickel, Sudbury, Canada) gave grade 6; and the Montcalm nickel-copper discovery (Timmins, Canada) yielded a grade 7 anomaly. Graphite and sulphides can span all grades but, in any particular survey area, field work may show that the different grades indicate different types of conductors.

Strong conductors (i.e., grades 6 and 7) are characteristic of massive sulphides or graphite. Moderate conductors (grades 4 and 5) typically reflect graphite or sulphides of a less massive character, while weak bedrock conductors (grades 1 to 3) can signify poorly connected graphite or heavily disseminated sulphides. Grades 1 and 2 conductors may not respond to ground EM equipment using frequencies less than 2000 Hz.

The presence of sphalerite or gangue can result in ore deposits having weak to moderate conductances. As an example, the three million ton lead-zinc deposit of Restigouche Mining Corporation near Bathurst, Canada, yielded a well-defined grade 2 conductor. The 10 percent by volume of sphalerite occurs as a coating around the fine-grained massive pyrite, thereby inhibiting electrical conduction. Faults, fractures and shear zones may

produce anomalies that typically have low conductances (e.g., grades 1 to 3). Conductive rock formations can yield anomalies of any conductance grade. The conductive materials in such rock formations can be salt water, weathered products such as clays, original depositional clays, and carbonaceous material.

For each interpreted electromagnetic anomaly on the geophysical maps, a letter identifier and an interpretive symbol are plotted beside the EM grade symbol. In areas where anomalies are crowded, the letter identifiers and interpretive symbols may be obliterated. The EM grade symbols, however, will always be discernible, and any obliterated information can be obtained from the anomaly listing appended to this report.

The conductance measurement is considered more reliable than the depth estimate. There are a number of factors that can produce an error in the depth estimate, including the averaging of topographic variations by the altimeter, overlying conductive overburden, and the location and attitude of the conductor relative to the flight line. Conductor location and attitude can provide an erroneous depth estimate because the stronger part of the conductor may be deeper or to one side of the flight line, or because it has a shallow dip. A heavy tree cover can also produce errors in depth estimates. This is because the depth estimate is computed as the distance of the bird from the conductor, minus the altimeter reading. The altimeter can lock onto the top of a dense forest canopy. This situation yields an erroneously large depth estimate but does not affect the conductance estimate.

Dip symbols are used to indicate the direction of dip of conductors. These symbols are used only when the anomaly shapes are unambiguous, which usually requires a fairly resistive environment.

A further interpretation is often presented on the EM map by means of the line-to-line correlation of bedrock anomalies, which is based on a comparison of anomaly shapes on adjacent lines. This provides conductor axes that may define the geological structure over portions of the survey area. The absence of conductor axes in an area implies that anomalies could not be correlated from line to line with reasonable confidence.

The electromagnetic anomalies are designed to provide a correct impression of conductor quality by means of the conductance grade symbols. The symbols can stand alone with geology when planning a follow-up program. The actual conductance values are printed in the attached anomaly list for those who wish quantitative data. The map provides an interpretation of conductors in terms of length, strike and dip, geometric shape, conductance, and thickness. The accuracy is comparable to an interpretation from a high quality ground EM survey having the same line spacing.

The appended EM anomaly list provides a tabulation of anomalies in ppm, conductance, and depth for the vertical sheet or horizontal sheet models. The vertical sheet model (B, D, and T types) uses the local coaxial amplitudes for the calculation. Values for the horizontal sheet model (S, H, and E types) are calculated from the absolute amplitudes of the selected coplanar channels. No conductance or depth estimates are shown for weak anomalous responses that are not of sufficient amplitude to yield reliable calculations, or where magnetite effects have caused negative in-phase responses.

Questionable Anomalies

The EM maps may contain anomalous responses that are displayed as asterisks (*). These responses denote weak anomalies of indeterminate conductance, which may reflect one of the following: a weak conductor near the surface, a strong conductor at depth (e.g., 100 to 120 m below surface) or to one side of the flight line, or aerodynamic noise. Those responses that have the appearance of valid bedrock anomalies on the flight profiles are indicated by appropriate interpretive symbols (see EM legend on maps). The others probably do not warrant further investigation unless their locations are of considerable geological interest.

The Thickness Parameter

A comparison of coaxial and coplanar shapes can provide an indication of the thickness of a steeply dipping conductor. The amplitude of the coplanar anomaly (e.g., CPI channel) increases relative to the coaxial anomaly (e.g., CXI) as the apparent thickness increases, i.e., the thickness in the horizontal plane. (The thickness is equal to the conductor width if the conductor dips at 90 degrees and strikes at right angles to the flight line.) This report refers to a conductor as thin when the thickness is likely to be less than 5 m, and thick when in excess of 10 m. Thick conductors are indicated on the EM map by parentheses "( )". For base metal exploration in steeply dipping geology, thick conductors can be high priority targets because many massive sulphide ore bodies are thick. The system cannot sense the thickness when the strike of the conductor is subparallel to the flight line, when the conductor has a shallow dip, when the anomaly amplitudes are small, or when the resistivity of the environment is less than 100 ohm-m.

Resistivity Mapping

Resistivity mapping is useful in areas where broad or flat lying conductive units are of interest. One example of this is the clay alteration that is associated with Carlin-type deposits in the southwest United States. The resistivity parameter was able to identify the clay alteration zone over the Cove deposit. The alteration zone appeared as a strong resistivity low on the 900 Hz resistivity parameter. The 7,200 Hz and 56,000 Hz resistivities showed more detail in the covering sediments, and delineated a range front fault. This is typical in many areas of the southwest United States, where conductive near surface sediments, which may sometimes be alkalic, attenuate the higher frequencies.

Resistivity mapping has proven successful for locating diatremes in diamond exploration. Weathering products from relatively soft kimberlite pipes produce a resistivity contrast with the unaltered host rock. In many cases weathered kimberlite pipes were associated with thick conductive layers that contrasted with overlying or adjacent relatively thin layers of lake bottom sediments or overburden.

Areas of widespread conductivity are commonly encountered during surveys. These conductive zones may reflect alteration zones, shallow-dipping sulphide or graphite-rich units, saline ground water, or conductive overburden. In such areas, EM amplitude changes can be generated by decreases of only 5 m in survey altitude, as well as by increases in conductivity. The typical flight record in conductive areas is characterized by in-phase and quadrature channels that are continuously active. Local EM peaks reflect either increases in conductivity of the earth or decreases in survey altitude. For such conductive areas, apparent resistivity profiles and contour maps are necessary for the correct interpretation of the airborne data. The advantage of the resistivity parameter is that anomalies caused by altitude changes are virtually eliminated, so the resistivity data reflect only those anomalies caused by conductivity changes. The resistivity analysis also helps the interpreter to differentiate between conductive bedrock and conductive overburden. For example, discrete conductors will generally appear as narrow lows on the contour map and broad conductors (e.g., overburden) will appear as wide lows.

The apparent resistivity is calculated using the pseudo-layer (or buried) half-space model defined by Fraser (1978)[5]. This model consists of a resistive layer overlying a conductive half-space. The depth channels give the apparent depth below surface of the conductive material. The apparent depth is simply the apparent thickness of the overlying resistive layer. The apparent depth (or thickness) parameter will be positive when the upper layer is more resistive than the underlying material, in which case the apparent depth may be quite close to the true depth.

The apparent depth will be negative when the upper layer is more conductive than the underlying material, and will be zero when a homogeneous half-space exists. The apparent depth parameter must be interpreted cautiously because it will contain any errors that might exist in the measured altitude of the EM bird (e.g., as caused by a dense tree cover). The inputs to the resistivity algorithm are the in-phase and quadrature components of the coplanar coil-pair. The outputs are the apparent resistivity of the conductive half-space (the source) and the sensor-source distance. The flying height is not an input variable, and the output resistivity and sensor-source distance are independent of the flying height when the conductivity of the measured material is sufficient to yield significant in-phase as well as quadrature responses. The apparent depth, discussed above, is simply the sensor-source distance minus the measured altitude or flying height. Consequently, errors in the measured altitude will affect the apparent depth parameter but not the apparent resistivity parameter.

The apparent depth parameter is a useful indicator of simple layering in areas lacking a heavy tree cover. Depth information has been used for permafrost mapping, where positive apparent depths were used as a measure of permafrost thickness. However, little quantitative use has been made of negative apparent depths because the absolute value of the negative depth is not a measure of the thickness of the conductive upper layer and,

[5] Resistivity mapping with an airborne multicoil electromagnetic system: Geophysics, v. 43, p.144-172

therefore, is not meaningful physically. Qualitatively, a negative apparent depth estimate usually shows that the EM anomaly is caused by conductive overburden. Consequently, the apparent depth channel can be of significant help in distinguishing between overburden and bedrock conductors.

Interpretation in Conductive Environments

Environments having low background resistivities (e.g., below 30 ohm-m for a 900 Hz system) yield very large responses from the conductive ground. This usually prohibits the recognition of discrete bedrock conductors. However, Fugro data processing techniques produce three parameters that contribute significantly to the recognition of bedrock conductors in conductive environments. These are the in-phase and quadrature difference channels (DIFI and DIFQ, which are available only on systems with "common" frequencies on orthogonal coil pairs), and the resistivity and depth channels (RES and DEP) for each coplanar frequency.

The EM difference channels (DIFI and DIFQ) eliminate most of the responses from conductive ground, leaving responses from bedrock conductors, cultural features (e.g., telephone lines, fences, etc.) and edge effects. Edge effects often occur near the perimeter of broad conductive zones. This can be a source of geologic noise. While edge effects yield anomalies on the EM difference channels, they do not produce resistivity anomalies. Consequently, the resistivity channel aids in eliminating anomalies due to edge effects. On the other hand, resistivity anomalies will coincide with the most highly conductive sections of conductive ground, and this is another source of geologic noise. The recognition of a bedrock conductor in a conductive environment therefore is based on the anomalous responses of the two difference channels (DIFI and DIFQ) and the resistivity channels (RES). The most favourable situation is where anomalies coincide on all channels.

The DEP channels, which give the apparent depth to the conductive material, also help to determine whether a conductive response arises from surficial material or from a conductive zone in the bedrock. When these channels ride above the zero level on the depth profiles (i.e., depth is negative), it implies that the EM and resistivity profiles are responding primarily to a conductive upper layer, i.e., conductive overburden. If the DEP channels are below the zero level, it indicates that a resistive upper layer exists, and this usually implies the existence of a bedrock conductor. If the low frequency DEP channel is below the zero level and the high frequency DEP is above, this suggests that a bedrock conductor occurs beneath conductive cover.

Reduction of Geologic Noise

Geologic noise refers to unwanted geophysical responses. For purposes of airborne EM surveying, geologic noise refers to EM responses caused by conductive overburden and magnetic permeability. It was mentioned previously that the EM difference channels (i.e., channel DIFI for in-phase and DIFQ for quadrature) tend to eliminate the response of conductive overburden.

Magnetite produces a form of geological noise on the in-phase channels. Rocks containing less than 1% magnetite can yield negative in-phase anomalies caused by magnetic permeability. When magnetite is widely distributed throughout a survey area, the in-phase EM channels may continuously rise and fall, reflecting variations in the magnetite percentage, flying height, and overburden thickness. This can lead to difficulties in recognizing deeply buried bedrock conductors, particularly if conductive overburden also exists. However, the response of broadly distributed magnetite generally vanishes on the in-phase difference channel DIFI. This feature can be a significant aid in the recognition of conductors that occur in rocks containing accessory magnetite.

EM Magnetite Mapping

The information content of HEM data consists of a combination of conductive eddy current responses and magnetic permeability responses. The secondary field resulting from conductive eddy current flow is frequency-dependent and consists of both in-phase and quadrature components, which are positive in sign. On the other hand, the secondary field resulting from magnetic permeability is independent of frequency and consists of only an in-phase component which is negative in sign. When magnetic permeability manifests itself by decreasing the measured amount of positive in-phase, its presence may be difficult to recognize. However, when it manifests itself by yielding a negative in-phase anomaly (e.g., in the absence of eddy current flow), its presence is assured. In this latter case, the negative component can be used to estimate the percent magnetite content.

A magnetite mapping technique, based on the low frequency coplanar data, can be complementary to magnetometer mapping in certain cases. Compared to magnetometry, it is far less sensitive but is more able to resolve closely spaced magnetite zones, as well as providing an estimate of the amount of magnetite in the rock. The method is sensitive to 1/4% magnetite by weight when the EM sensor is at a height of 30 m above a magnetitic half-space. It can individually resolve steep dipping narrow magnetite-rich bands that are separated by 60 m. Unlike magnetometry, the EM magnetite method is unaffected by remanent magnetism or magnetic latitude.

The EM magnetite mapping technique provides estimates of magnetite content that are usually correct within a factor of 2 when the magnetite is fairly uniformly distributed. EM magnetite maps can be generated when magnetic permeability is evident as negative in-phase responses on the data profiles.

Like magnetometry, the EM magnetite method maps only bedrock features, provided that the overburden is characterized by a general lack of magnetite. This contrasts with resistivity mapping which portrays the combined effect of bedrock and overburden.

The Susceptibility Effect

When the host rock is conductive, the positive conductivity response will usually dominate the secondary field, and the susceptibility effect[6] will appear as a reduction in the in-phase, rather than as a negative value. The in-phase response will be lower than would be predicted by a model using zero susceptibility. At higher frequencies the in-phase conductivity response also gets larger, so a negative magnetite effect observed on the low frequency might not be observable on the higher frequencies, over the same body. The susceptibility effect is most obvious over discrete magnetite-rich zones, but also occurs over uniform geology such as a homogeneous half-space.

High magnetic susceptibility will affect the calculated apparent resistivity, if only conductivity is considered. Standard apparent resistivity algorithms use a homogeneous half-space model, with zero susceptibility. For these algorithms, the reduced in-phase response will, in most cases, make the apparent resistivity higher than it should be. It is important to note that there is nothing wrong with the data, nor is there anything wrong with the processing algorithms. The apparent difference results from the fact that the simple geological model used in processing does not match the complex geology.

Measuring and Correcting the Magnetite Effect

Theoretically, it is possible to calculate (forward model) the combined effect of electrical conductivity and magnetic susceptibility on an EM response in all environments. The difficulty lies, however, in separating out the susceptibility effect from other geological effects when deriving resistivity and susceptibility from EM data.

Over a homogeneous half-space, there is a precise relationship between in-phase, quadrature, and altitude. These are often resolved as phase angle, amplitude, and altitude. Within a reasonable range, any two of these three parameters can be used to calculate the half space resistivity. If the rock has a positive magnetic susceptibility, the in-phase component will be reduced and this departure can be recognized by comparison to the other parameters.

The algorithm used to calculate apparent susceptibility and apparent resistivity from HEM data, uses a homogeneous half-space geological model. Non half-space geology, such as horizontal layers or dipping sources, can also distort the perfect half-space relationship of the three data parameters. While it may be possible to use more complex models to calculate both rock parameters, this procedure becomes very

---

[6] Magnetic susceptibility and permeability are two measures of the same physical property. Permeability is generally given as relative permeability, μ_r, which is the permeability of the substance divided by the permeability of free space ($4 \pi \times 10^{-7}$). Magnetic susceptibility k is related to permeability by $k=\mu^r-1$. Susceptibility is a unitless measurement, and is usually reported in units of 10^{-6}. The typical range of susceptibilities is –1 for quartz, 130 for pyrite, and up to 5×10^5 for magnetite, in 10^{-6} units (Telford et al, 1986).

complex and time-consuming. For basic HEM data processing, it is most practical to stick to the simplest geological model.

Magnetite reversals (reversed in-phase anomalies) have been used for many years to calculate an “FeO” or magnetite response from HEM data (Fraser, 1981). However, this technique could only be applied to data where the in-phase was observed to be negative, which happens when susceptibility is high and conductivity is low.

Applying Susceptibility Corrections

Resistivity calculations done with susceptibility correction may change the apparent resistivity. High-susceptibility conductors, which were previously masked by the susceptibility effect in standard resistivity algorithms, may become evident. In this case the susceptibility corrected apparent resistivity is a better measure of the actual resistivity of the earth. However, other geological variations, such as a deep resistive layer, can also reduce the in-phase by the same amount. In this case, susceptibility correction would not be the best method. Different geological models can apply in different areas of the same data set. The effects of susceptibility, and other effects that can create a similar response, must be considered when selecting the resistivity algorithm.

Susceptibility from EM vs Magnetic Field Data

The response of the EM system to magnetite may not match that from a magnetometer survey. First, HEM-derived susceptibility is a rock property measurement, like resistivity. Magnetic data show the total magnetic field, a measure of the potential field, not the rock property. Secondly, the shape of an anomaly depends on the shape and direction of the source magnetic field. The electromagnetic field of HEM is much different in shape from the earth’s magnetic field. Total field magnetic anomalies are different at different magnetic latitudes; HEM susceptibility anomalies have the same shape regardless of their location on the earth.

In far northern latitudes, where the magnetic field is nearly vertical, the total magnetic field measurement over a thin vertical dike is very similar in shape to the anomaly from the HEM-derived susceptibility (a sharp peak over the body). The same vertical dike at the magnetic equator would yield a negative magnetic anomaly, but the HEM susceptibility anomaly would show a positive susceptibility peak.

Effects of Permeability and Dielectric Permittivity

Resistivity algorithms that assume free-space magnetic permeability and dielectric permittivity, do not yield reliable values in highly magnetic or highly resistive areas. Both magnetic polarization and displacement currents cause a decrease in the in-phase component, often resulting in negative values that yield erroneously high apparent resistivities. The effects of magnetite occur at all frequencies, but are most evident at

the lowest frequency. Conversely, the negative effects of dielectric permittivity are most evident at the higher frequencies, in resistive areas.

The table below shows the effects of varying permittivity over a resistive (10,000 ohm-m) half space, at frequencies of 56,000 Hz (DIGHEM^V) and 140,000 Hz (RESOLVE).

Apparent Resistivity Calculations
Effects of Permittivity on In-phase/Quadrature/Resistivity

Freq (Hz)	Coil	Sep (m)	Thres (ppm)	Alt (m)	In Phase	Quad Phase	App Res	App Depth (m)	Permittivity
56,000	CP	6.3	0.1	30	7.3	35.3	10118	-1.0	1 Air
56,000	CP	6.3	0.1	30	3.6	36.6	19838	-13.2	5 Quartz
56,000	CP	6.3	0.1	30	-1.1	38.3	81832	-25.7	10 Epidote
56,000	CP	6.3	0.1	30	-10.4	42.3	76620	-25.8	20 Granite
56,000	CP	6.3	0.1	30	-19.7	46.9	71550	-26.0	30 Diabase
56,000	CP	6.3	0.1	30	-28.7	52.0	66787	-26.1	40 Gabbro
140,000	CP	7.94	0.1	30	52.1	159.1	8710	0.2	1 Air
140,000	CP	7.94	0.1	30	16.1	180.4	29215	-18.5	5 Quartz
140,000	CP	7.94	0.1	30	-27.0	211.9	102876	-26.9	10 Epidote
140,000	CP	7.94	0.1	30	-103.6	287.0	84044	-27.2	20 Granite
140,000	CP	7.94	0.1	30	-166.0	371.5	70766	-27.5	30 Diabase
140,000	CP	7.94	0.1	30	-215	459.3	61433	-27.6	40 Gabbro

Methods have been developed (Huang and Fraser, 2000, 2001) to correct apparent resistivities for the effects of permittivity and permeability. The corrected resistivities yield more credible values than if the effects of permittivity and permeability are disregarded.

Recognition of Culture

Cultural responses include all EM anomalies caused by man-made metallic objects. Such anomalies may be caused by inductive coupling or current gathering. The concern of the interpreter is to recognize when an EM response is due to culture. Points of consideration used by the interpreter, when coaxial and coplanar coil-pairs are operated at a common frequency, are as follows:

1. The CPPL channel monitors 60 Hz radiation. An anomaly on this channel shows that the conductor is radiating power. Such an indication is normally a guarantee that the conductor is cultural. However, care must be taken to ensure that the conductor is not a geologic body that strikes across a power line, carrying leakage currents.

2. A flight that crosses a "line" (e.g., fence, telephone line, etc.) yields a centre-peaked coaxial anomaly and an m-shaped coplanar anomaly.[7] When the flight crosses the cultural line at a high angle of intersection, the amplitude ratio of coaxial/coplanar response is 2. Such an EM anomaly can only be caused by a line. The geologic body that yields anomalies most closely resembling a line is the vertically dipping thin dike. Such a body, however, yields an amplitude ratio of 1 rather than 2. Consequently, an m-shaped coplanar anomaly with a CXI/CPI amplitude ratio of 2 is virtually a guarantee that the source is a cultural line.

3. A flight that crosses a sphere or horizontal disk yields centre-peaked coaxial and coplanar anomalies with a CXI/CPI amplitude ratio (i.e., coaxial/coplanar) of 1/8. In the absence of geologic bodies of this geometry, the most likely conductor is a metal roof or small fenced yard.[8] Anomalies of this type are virtually certain to be cultural if they occur in an area of culture.

4. A flight that crosses a horizontal rectangular body or wide ribbon yields an m-shaped coaxial anomaly and a centre-peaked coplanar anomaly. In the absence of geologic bodies of this geometry, the most likely conductor is a large fenced area.[5] Anomalies of this type are virtually certain to be cultural if they occur in an area of culture.

5. EM anomalies that coincide with culture, as seen on the video display, are usually caused by culture. However, care is taken with such coincidences because a geologic conductor could occur beneath a fence, for example. In this example, the fence would be expected to yield an m-shaped coplanar anomaly as in case #2 above. If, instead, a centre-peaked coplanar anomaly occurred, there would be concern that a thick geologic conductor coincided with the cultural line.

6. Thee above description of anomaly shapes is valid when the culture is not conductively coupled to the environment. In this case, the anomalies arise from inductive coupling to the EM transmitter. However, when the environment is quite conductive (e.g., less than 100 ohm-m at 900 Hz), the cultural conductor may be conductively coupled to the environment. In this latter case, the anomaly shapes tend to be governed by current gathering. Current gathering can completely distort the anomaly shapes, thereby complicating the identification of cultural anomalies. In such circumstances, the interpreter can only rely on the radiation channel and the video records

Magnetic Responses

---

[7] See Figure C-1 presented earlier.

[8] It is a characteristic of EM that geometrically similar anomalies are obtained from: (1) a planar conductor, and (2) a wire that forms a loop having dimensions identical to the perimeter of the equivalent planar conductor.

The measured total magnetic field provides information on the magnetic properties of the earth materials in the survey area. This information can be used to locate magnetic bodies of direct interest for exploration, and for structural and lithological mapping.

The total magnetic field response reflects the abundance of magnetic material in the source. Magnetite is the most common magnetic mineral. Other minerals such as ilmenite, pyrrhotite, franklinite, chromite, hematite, arsenopyrite, limonite and pyrite are also magnetic, but to a lesser extent than magnetite on average.

In some geological environments, an EM anomaly with magnetic correlation has a greater likelihood of being produced by sulphides than one that is non-magnetic. However, sulphide ore bodies may be non-magnetic (e.g., the Kidd Creek deposit near Timmins, Canada) as well as magnetic (e.g., the Mattabi deposit near Sturgeon Lake, Canada).

Iron ore deposits will be anomalously magnetic in comparison to surrounding rock due to the concentration of iron minerals such as magnetite, ilmenite and hematite.

Changes in magnetic susceptibility often allow rock units to be differentiated based on the total magnetic field. Geophysical classifications may differ from geological classifications if various magnetite levels exist within one general geological classification. Geometric considerations of the source such as shape, dip and depth, inclination of the earth's field and remanent magnetization will complicate such an analysis.

In general, mafic lithologies contain more magnetite and are therefore more magnetic than many sediments which tend to be weakly magnetic. Metamorphism and alteration can also increase or decrease the magnetization of a rock unit.

Textural differences on a total field magnetic contour, colour or shadow map due to the frequency of activity of the magnetic parameter resulting from inhomogeneities in the distribution of magnetite within the rock, may define certain lithologies. For example, near surface volcanics may display highly complex contour patterns with little line-to-line correlation.

Rock units may be differentiated based on the plan shapes of their total or residual magnetic field responses. Mafic intrusive plugs can appear as isolated "bulls-eye" anomalies. Granitic intrusives appear as sub-circular zones, and may have contrasting rings due to contact metamorphism. Generally, granitic terrain will lack a pronounced strike direction, although granite gneiss may display strike.

Linear north-south units are theoretically not well defined on total magnetic field maps in equatorial regions, due to the low inclination of the earth's magnetic field. However, most stratigraphic units will have variations in composition along strike that will cause the units to appear as a series of alternating magnetic highs and lows.

Faults and shear zones may be characterized by alteration that causes destruction of magnetite (e.g., weathering) that produces a contrast with surrounding rock. Structural

breaks may be filled by magnetite-rich, fracture filling material, as is the case with diabase dikes, or by non-magnetic felsic material.

Faulting can also be identified by patterns in the magnetic contours or colours. Faults and dikes tend to appear as lineaments and often have strike lengths of several kilometres. Offsets in narrow, magnetic, stratigraphic trends also delineate structure. Sharp contrasts in magnetic lithologies may arise due to large displacements along strike-slip or dip-slip faults.

APPENDIX D

DATA ARCHIVE DESCRIPTION

APPENDIX D

ARCHIVE DESCRIPTION

Job # 11058

The DVD accompanying this report contains FINAL archived data and grids from an airborne Dighem^{V} electromagnetic and magnetic geophysical survey over the ELKO and NASH Properties, near Mayo YT, conducted by FUGRO AIRBORNE SURVEYS CORP, from August 8 to August 12, 2011, on behalf of GOLDEN RIDGE RESOURCES INC.,

The "READ ME" file on the DVD describes the contents of the final data archive, which includes the following for both properties:

\GRIDS Grids in Geosoft format

CVG_.GRD	- Calculated Vertical Magnetic Gradient nT/m
MAG_.GRD	- Residual Magnetic Intensity nT
RES900_RD	- Apparent Resistivity 900 Hz ohm·m
RES7200_GRD	- Apparent Resistivity 7200 Hz ohm·m
RES56K_GRD	- Apparent Resistivity 56k Hz ohm·m

\LINEDATA

GDB	- Data archive in Geosoft GDB format
XYZ	- Data archive in Geosoft ASCII format
AEM_.XYZ	- Anomaly archive in ASCII format

\MAPS Final colour maps in PDF format: (AEM in DXF format)

AEM_	- Electromagnetic Anomalies *
CVG_	- Calculated Vertical Magnetic Gradient (nT/m) *
MAG_	- Residual Magnetic Intensity (nT)*
RES900	- Apparent Resistivity 900 Hz (ohm·m)
RES7200	- Apparent Resistivity 7200 Hz (ohm·m)
RES56kHz	- Apparent Resistivity 56000 Hz (ohm·m)*

\REPORT

11058-.PDF	- Survey Report

****

GEOSOFT GDB and XYZ ARCHIVE SUMMARY

#	CHANNEL NAME	TIME	UNITS	DESCRIPTION
1	x	0.1	m	eastings NAD83 (Zone 10N)
2	y	0.1	m	northings NAD83 (Zone 10N)
3	fid	0.1		synchronization counter
4	longitude	0.1	degrees	longitude WGS84
5	latitude	0.1	degrees	latitude WGS84
6	flight	0.1		flight number
7	date	0.1		flight date (yyyy/mm/dd)
8	altrad_bird	0.1	m	calculated bird height above ground from radar altimeter
9	altlas_bird	0.1	m	measured bird height above ground from laser altimeter

10 gpsz	0.1	m	survey height above spheroid
11 dtm	0.1	m	terrain with respect to ellipsoid
12 diurnal_filt	0.1	nT	ground magnetic intensity
13 diurnal_cor	0.1	nT	diurnal correction - base removed
14 mag_raw	0.1	nT	total magnetic field - spike rejected
15 mag_lag	0.1	nT	total magnetic field - corrected for lag
16 mag_diu	0.1	nT	total magnetic field - diurnal variation removed
17 igrf	0.1	nT	international geomagnetic reference field
18 mag_rmi	0.1	nT	residual magnetic intensity - final
19 cpi900_filt	0.1	ppm	coplanar inphase 900 Hz - unlevelled
20 cpq900_filt	0.1	ppm	coplanar quadrature 900 Hz - unlevelled
21 cxi1000_filt	0.1	ppm	coaxial inphase 1000 Hz - unlevelled
22 cxq1000_filt	0.1	ppm	coaxial quadrature 1000 Hz - unlevelled
23 cxi5500_filt	0.1	ppm	coaxial inphase 5500 Hz - unlevelled
24 cxq5500_filt	0.1	ppm	coaxial quadrature 5500 Hz - unlevelled
25 cpi7200_filt	0.1	ppm	coplanar inphase 7200 Hz - unlevelled
26 cpq7200_filt	0.1	ppm	coplanar quadrature 7200 Hz -unlevelled
27 cpi56k_filt	0.1	ppm	coplanar inphase 56 kHz - unlevelled
28 cpq56k_filt	0.1	ppm	coplanar quadrature 56 kHz - unlevelled
29 cpi900	0.1	ppm	coplanar inphase 900 Hz
30 cpq900	0.1	ppm	coplanar quadrature 900 Hz
31 cxi1000	0.1	ppm	coaxial inphase 1000 Hz
32 cxq1000	0.1	ppm	coaxial quadrature 1000 Hz
33 cxi5500	0.1	ppm	coaxial inphase 5500 Hz
34 cxq5500	0.1	ppm	coaxial quadrature 5500 Hz
35 cpi7200	0.1	ppm	coplanar inphase 7200 Hz
36 cpq7200	0.1	ppm	coplanar quadrature 7200 Hz
37 cpi56k	0.1	ppm	coplanar inphase 56 kHz
38 cpq56k	0.1	ppm	coplanar quadrature 56 kHz
39 res900	0.1	ohm·m	apparent resistivity - 900 Hz
40 res7200	0.1	ohm·m	apparent resistivity - 7200 Hz
41 res56k	0.1	ohm·m	apparent resistivity - 56 kHz
42 dep900	0.1	m	apparent depth - 900 Hz
43 dep7200	0.1	m	apparent depth - 7200 Hz
44 dep56k	0.1	m	apparent depth - 56 kHz
45 difi	0.1		difference channel based on cxi5500/cpi7200
46 difq	0.1		difference channel based on cxq5500/cpq7200
47 cppl	0.1		coplanar powerline monitor
48 cxsp	0.1		coaxial spherics monitor
49 cpsp	0.1		coplanar spherics monitor

FUGRO ANOMALY SUMMARY

# CHANNEL NAME	TIME	UNITS	DESCRIPTION
1 Easting	0.10	m	easting NAD83 (Zone 10N)
2 Northing	0.10	m	northing NAD83 (Zone 10N)
3 FID	1.00		Synchronization Counter
4 FLT	0.10		Flight
5 MHOS	0.10	siemens	Conductance (see report for model used)
6 DEPTH	0.10	m	Depth (see report for model used)
7 MAG	0.10	nT	Mag Correlation, local amplitude
8 CXI1	0.10	ppm	Inphase Coaxial 1000 Hz, local amplitude
9 CXQ1	0.10	ppm	Quadrature Coaxial 1000 Hz, local amplitude
10 CPI1	0.10	ppm	Inphase Coplanar 900 Hz, absolute amplitude
11 CPQ1	0.10	ppm	Quadrature Coplanar 900 Hz, absolute amplitude
12 CPI2	0.10	ppm	Inphase Coplanar 7200 Hz, absolute amplitude
13 CPQ2	0.10	ppm	Quadrature Coplanar 7200 Hz, absolute amplitude
14 LET	0.10		Anomaly Identifier
15 SYM	0.10		Anomaly Interpretation Symbol
16 GRD	0.10		Anomaly Grade

- Appendix D. 3 -

The coordinate system for all grids and the data archive is projected as follows

Datum	NAD83	
Spheroid	GRS80	
Central meridian	135 West (Z8N)	
False easting	500000	
False northing	0	
Scale factor	0.9996	
Northern parallel	N/A	
Base parallel	N/A	
WGS84 to local conversion method		Molodensky
Delta X shift	0	
Delta Y shift	0	
Delta Z shift	0	

If you have any problems with this archive please contact

Processing Manager
FUGRO AIRBORNE SURVEYS CORP.
2505 Meadowvale Blvd.
Mississauga, Ontario
Canada L5N 5S2
Tel (905) 812-0212
Fax (905) 812-1504
E-mail toronto@fugroairborne.com

APPENDIX E

EM ANOMALY LIST

NOTE: Because of the large number of EM anomalies, the EM anomaly list has been included on the Final Data Archive, but the pages have not been printed and appended to this report.

APPENDIX F

GLOSSARY

APPENDIX F

GLOSSARY

Note: The definitions given in this glossary refer to the common terminology as used in airborne geophysics.

altitude attenuation: the absorption of gamma rays by the atmosphere between the earth and the detector. The number of gamma rays detected by a system decreases as the altitude increases.

apparent- : the ***physical parameters*** of the earth measured by a geophysical system are normally expressed as apparent, as in "apparent ***resistivity*****"**. This means that the measurement is limited by assumptions made about the geology in calculating the response measured by the geophysical system. Apparent resistivity calculated with ***HEM***, for example, generally assumes that the earth is a ***homogeneous half-space*** – not layered.

amplitude: The strength of the total electromagnetic field. In ***frequency domain*** it is most often the sum of the squares of ***in-phase*** and ***quadrature*** components. In multi-component electromagnetic surveys it is generally the sum of the squares of all three directional components.

analytic signal: The total amplitude of all the directions of magnetic ***gradient***. Calculated as the sum of the squares.

anisotropy: Having different ***physical parameters*** in different directions. This can be caused by layering or fabric in the geology. Note that a unit can be anisotropic, but still **homogeneous**.

anomaly: A localized change in the geophysical data characteristic of a discrete source, such as a conductive or magnetic body: something locally different from the **background**.

B-field: In time-domain **electromagnetic** surveys, the magnetic field component of the (electromagnetic) **field**. This can be measured directly, although more commonly it is calculated by integrating the time rate of change of the magnetic field **dB/dt**, as measured with a receiver coil.

background: The "normal" response in the geophysical data – that response observed over most of the survey area. **Anomalies** are usually measured relative to the background. In airborne gamma-ray spectrometric surveys the term defines the **cosmic**, radon, and aircraft responses in the absence of a signal from the ground.

base-level: The measured values in a geophysical system in the absence of any outside signal. All geophysical data are measured relative to the system base level.

base frequency: The frequency of the pulse repetition for a ***time-domain electromagnetic*** system. Measured between subsequent positive pulses.

bird: A common name for the pod towed beneath or behind an aircraft, carrying the geophysical sensor array.

bucking: The process of removing the strong ***signal*** from the ***primary field*** at the ***receiver*** from the data, to measure the ***secondary field***. It can be done electronically or mathematically. This is done in ***frequency-domain EM***, and to measure ***on-time*** in ***time-domain EM***.

calibration coil: A wire coil of known size and dipole moment, which is used to generate a field of known ***amplitude*** and ***phase*** in the receiver, for system calibration. Calibration coils can be external, or internal to the system. Internal coils may be called Q-coils.

coaxial coils: **[CX]** Coaxial coils in an HEM system are in the vertical plane, with their axes horizontal and collinear in the flight direction. These are most sensitive to vertical conductive objects in the ground, such as thin, steeply dipping conductors perpendicular to the flight direction. Coaxial coils generally give the sharpest anomalies over localized conductors. (See also ***coplanar coils***)

coil: A multi-turn wire loop used to transmit or detect electromagnetic fields. Time varying ***electromagnetic*** fields through a coil induce a voltage proportional to the strength of the field and the rate of change over time.

compensation: Correction of airborne geophysical data for the changing effect of the aircraft. This process is generally used to correct data in ***fixed-wing time-domain electromagnetic*** surveys (where the transmitter is on the aircraft and the receiver is moving), and magnetic surveys (where the sensor is on the aircraft, turning in the earth's magnetic field.

component: In ***frequency domain electromagnetic*** surveys this is one of the two **phase** measurements – ***in-phase or quadrature***. In "multi-component" electromagnetic surveys it is also used to define the measurement in one geometric direction (vertical, horizontal in-line and horizontal transverse – the Z, X and Y components).

Compton scattering: gamma ray photons will bounce off electrons as they pass through the earth and atmosphere, reducing their energy and then being detected by ***radiometric*** sensors at lower energy levels. See also ***stripping***.

conductance: See ***conductivity thickness***

conductivity: [σ] The facility with which the earth or a geological formation conducts electricity. Conductivity is usually measured in milli-Siemens per metre (mS/m). It is the reciprocal of ***resistivity***.

conductivity-depth imaging: see ***conductivity-depth transform***.

conductivity-depth transform: A process for converting electromagnetic measurements to an approximation of the conductivity distribution vertically in the earth, assuming a ***layered earth***. (Macnae and Lamontagne, 1987; Wolfgram and Karlik, 1995)

conductivity thickness: [σt] The product of the ***conductivity***, and thickness of a large, tabular body. (It is also called the "conductivity-thickness product") In electromagnetic geophysics, the response of a thin plate-like conductor is proportional to the conductivity multiplied by thickness. For example a 10 metre thickness of 20 Siemens/m mineralization will be equivalent to 5 metres of 40 S/m; both have 200 S conductivity thickness. Sometimes referred to as **conductance**.

conductor: Used to describe anything in the ground more conductive than the surrounding geology. Conductors are most often clays or graphite, or hopefully some type of mineralization, but may also be man-made objects, such as fences or pipelines.

coplanar coils: **[CP]** In HEM, the coplanar coils lie in the horizontal plane with their axes vertical, and parallel. These coils are most sensitive to massive conductive bodies, horizontal layers, and the ***halfspace***.

cosmic ray: High energy sub-atomic particles from outer space that collide with the earth's atmosphere to produce a shower of gamma rays (and other particles) at high energies.

counts (per second): The number of ***gamma-rays*** detected by a gamma-ray ***spectrometer*****.** The rate depends on the geology, but also on the size and sensitivity of the detector.

culture: A term commonly used to denote any man-made object that creates a geophysical anomaly. Includes, but not limited to, power lines, pipelines, fences, and buildings.

current channelling: See current gathering.

current gathering: The tendency of electrical currents in the ground to channel into a conductive formation. This is particularly noticeable at higher frequencies or early time channels when the formation is long and parallel to the direction of current flow. This tends to enhance anomalies relative to inductive currents (see also ***induction***). Also known as current channelling.

daughter products: The radioactive natural sources of gamma-rays decay from the original "parent" element (commonly potassium, uranium, and thorium) to one or more lower-energy "daughter" elements. Some of these lower energy elements are also radioactive and decay further. ***Gamma-ray spectrometry*** surveys may measure the gamma rays given off by the original element or by the decay of the daughter products.

dB/dt: As the ***secondary electromagnetic field*** changes with time, the magnetic field [**B**] component induces a voltage in the receiving ***coil***, which is proportional to the rate of change of the magnetic field over time.

decay: In ***time-domain electromagnetic*** theory, the weakening over time of the ***eddy currents*** in the ground, and hence the ***secondary field*** after the ***primary field*** electromagnetic pulse is turned off. In ***gamma-ray spectrometry***, the radioactive breakdown of an element, generally potassium, uranium, thorium, or one of their ***daughter*** products.

decay constant: see time constant.

decay series: In ***gamma-ray spectrometry***, a series of progressively lower energy ***daughter products*** produced by the radioactive breakdown of uranium or thorium.

depth of exploration: The maximum depth at which the geophysical system can detect the target. The depth of exploration depends very strongly on the type and size of the target, the contrast of the target with the surrounding geology, the homogeneity of the surrounding geology, and the type of geophysical system. One measure of the maximum depth of exploration for an electromagnetic system is the depth at which it can detect the strongest conductive target – generally a highly conductive horizontal layer.

differential resistivity: A process of transforming ***apparent resistivity*** to an approximation of layer resistivity at each depth. The method uses multi-frequency HEM data and approximates the effect of shallow layer ***conductance*** determined from higher frequencies to estimate the deeper conductivities (Huang and Fraser, 1996)

dipole moment: [NIA] For a transmitter, the product of the area of a ***coil***, the number of turns of wire, and the current flowing in the coil. At a distance significantly larger than the size of the coil, the magnetic field from a coil will be the same if the dipole moment product is the same. For a receiver coil, this is the product of the area and the number of turns. The sensitivity to a magnetic field (assuming the source is far away) will be the same if the dipole moment is the same.

diurnal: The daily variation in a natural field, normally used to describe the natural fluctuations (over hours and days) of the earth's magnetic field.

dielectric permittivity: **[ε]** The capacity of a material to store electrical charge, this is most often measured as the relative permittivity [ε_r], or ratio of the material dielectric to

that of free space. The effect of high permittivity may be seen in HEM data at high frequencies over highly resistive geology as a reduced or negative ***in-phase***, and higher ***quadrature*** data.

drape: To fly a survey following the terrain contours, maintaining a constant altitude above the local ground surface. Also applied to re-processing data collected at varying altitudes above ground to simulate a survey flown at constant altitude.

drift: Long-time variations in the base-level or calibration of an instrument.

eddy currents: The electrical currents induced in the ground, or other conductors, by a time-varying ***electromagnetic field*** (usually the ***primary field***). Eddy currents are also induced in the aircraft's metal frame and skin; a source of ***noise*** in EM surveys.

electromagnetic: **[EM]** Comprised of a time-varying electrical and magnetic field. Radio waves are common electromagnetic fields. In geophysics, an electromagnetic system is one which transmits a time-varying ***primary field*** to induce ***eddy currents*** in the ground, and then measures the ***secondary field*** emitted by those eddy currents.

energy window: A broad spectrum of ***gamma-ray*** energies measured by a spectrometric survey. The energy of each gamma-ray is measured and divided up into numerous discrete energy levels, called windows.

equivalent (thorium or uranium): The amount of radioelement calculated to be present, based on the gamma-rays measured from a **daughter** element. This assumes that the ***decay series*** is in equilibrium – progressing normally.

exposure rate: in radiometric surveys, a calculation of the total exposure rate due to gamma rays at the ground surface. It is used as a measurement of the concentration of all the **radioelements** at the surface. See also: **natural exposure rate**.

fiducial, or fid: Timing mark on a survey record. Originally these were timing marks on a profile or film; now the term is generally used to describe 1-second interval timing records in digital data, and on maps or profiles.

Figure of Merit: **(FOM)** A sum of the 12 distinct magnetic noise variations measured by each of four flight directions, and executing three aircraft attitude variations (yaw, pitch, and roll) for each direction. The flight directions are generally parallel and perpendicular to planned survey flight directions. The FOM is used as a measure of the **manoeuvre noise** before and after **compensation.**

fixed-wing: Aircraft with wings, as opposed to "rotary wing" helicopters.

footprint: This is a measure of the area of sensitivity under the aircraft of an airborne geophysical system. The footprint of an ***electromagnetic*** system is dependent on the altitude of the system, the orientation of the transmitter and receiver and the separation

between the receiver and transmitter, and the conductivity of the ground. The footprint of a ***gamma-ray spectrometer*** depends mostly on the altitude. For all geophysical systems, the footprint also depends on the strength of the contrasting ***anomaly***.

frequency domain: An ***electromagnetic*** system which transmits a ***primary field*** that oscillates smoothly over time (sinusoidal), inducing a similarly varying electrical current in the ground. These systems generally measure the changes in the ***amplitude*** and ***phase*** of the ***secondary field*** from the ground at different frequencies by measuring the **in-phase** and **quadrature** phase components. See also ***time-domain***.

full-stream data: Data collected and recorded continuously at the highest possible sampling rate. Normal data are stacked (see ***stacking***) over some time interval before recording.

gamma-ray: A very high-energy photon, emitted from the nucleus of an atom as it undergoes a change in energy levels.

gamma-ray spectrometry: Measurement of the number and energy of natural (and sometimes man-made) gamma-rays across a range of photon energies.

gradient: In magnetic surveys, the gradient is the change of the magnetic field over a distance, either vertically or horizontally in either of two directions. Gradient data is often measured, or calculated from the total magnetic field data because it changes more quickly over distance than the ***total magnetic field***, and so may provide a more precise measure of the location of a source. See also ***analytic signal***.

ground effect: The response from the earth. A common calibration procedure in many geophysical surveys is to fly to altitude high enough to be beyond any measurable response from the ground, and there establish ***base levels*** or ***backgrounds***.

half-space: A mathematical model used to describe the earth – as infinite in width, length, and depth below the surface. The most common halfspace models are ***homogeneous*** and ***layered earth***.

heading error: A slight change in the magnetic field measured when flying in opposite directions.

HEM: Helicopter ElectroMagnetic, This designation is most commonly used for helicopter-borne, ***frequency-domain*** electromagnetic systems. At present, the transmitter and receivers are normally mounted in a ***bird*** carried on a sling line beneath the helicopter.

herringbone pattern: A pattern created in geophysical data by an asymmetric system, where the **anomaly** may be extended to either side of the source, in the direction of flight. Appears like fish bones, or like the teeth of a comb, extending either side of centre, each tooth an alternate flight line.

homogeneous: This is a geological unit that has the same ***physical parameters*** throughout its volume. This unit will create the same response to an HEM system anywhere, and the HEM system will measure the same apparent ***resistivity*** anywhere. The response may change with system direction (see ***anisotropy***).

HTEM: Helicopter Time-domain ElectroMagnetic, This designation is used for the new generation of helicopter-borne, ***time-domain*** electromagnetic systems.

in-phase: the component of the measured ***secondary field*** that has the same phase as the transmitter and the ***primary field***. The in-phase component is stronger than the ***quadrature*** phase over relatively higher ***conductivity***.

induction: Any time-varying electromagnetic field will induce (cause) electrical currents to flow in any object with non-zero ***conductivity***. (see ***eddy currents***)

induction number: also called the "response parameter", this number combines many of the most significant parameters affecting the ***EM*** response into one parameter against which to compare responses. For a ***layered earth*** the response parameter is $\mu\omega\sigma h^2$ and for a large, flat, ***conductor*** it is $\mu\omega\sigma$**th**, where μ is the ***magnetic permeability***, ω is the angular ***frequency***, σ is the **conductivity**, t is the thickness (for the flat conductor) and h is the height of the system above the conductor.

inductive limit: When the frequency of an EM system is very high, or the **conductivity** of the target is very high, the response measured will be entirely **in-phase** with no **quadrature** (**phase** angle =0). The in-phase response will remain constant with further increase in conductivity or frequency. The system can no longer detect changes in conductivity of the target.

infinite: In geophysical terms, an "infinite' dimension is one much greater than the ***footprint*** of the system, so that the system does not detect changes at the edges of the object.

International Geomagnetic Reference Field: **[IGRF]** An approximation of the smooth magnetic field of the earth, in the absence of variations due to local geology. Once the IGRF is subtracted from the measured magnetic total field data, any remaining variations are assumed to be due to local geology. The IGRF also predicts the slow changes of the field up to five years in the future.

inversion, or **inverse modeling**: A process of converting geophysical data to an earth model, which compares theoretical models of the response of the earth to the data measured, and refines the model until the response closely fits the measured data (Huang and Palacky, 1991)

layered earth: A common geophysical model which assumes that the earth is horizontally layered – the ***physical parameters*** are constant to ***infinite*** distance horizontally, but change vertically.

magnetic permeability: **[μ]** This is defined as the ratio of magnetic induction to the inducing magnetic field. The relative magnetic permeability [μ_r] is often quoted, which is the ratio of the rock permeability to the permeability of free space. In geology and geophysics, the ***magnetic susceptibility*** is more commonly used to describe rocks.

magnetic susceptibility: **[k]** A measure of the degree to which a body is magnetized. In SI units this is related to relative ***magnetic permeability*** by $k=\mu_r-1$, and is a dimensionless unit. For most geological material, susceptibility is influenced primarily by the percentage of magnetite. It is most often quoted in units of 10^{-6}. In HEM data this is most often apparent as a negative ***in-phase*** component over high susceptibility, high ***resistivity*** geology such as diabase dikes.

manoeuvre noise: variations in the magnetic field measured caused by changes in the relative positions of the magnetic sensor and magnetic objects or electrical currents in the aircraft. This type of noise is generally corrected by magnetic **compensation**.

model: Geophysical theory and applications generally have to assume that the geology of the earth has a form that can be easily defined mathematically, called the model. For example steeply dipping **conductor**s are generally modeled as being **infinite** in horizontal and depth extent, and very thin. The earth is generally modeled as horizontally layered, each layer infinite in extent and uniform in characteristic. These models make the mathematics to describe the response of the (normally very complex) earth practical. As theory advances, and computers become more powerful, the useful models can become more complex.

natural exposure rate: in radiometric surveys, a calculation of the total exposure rate due to natural-source gamma rays at the ground surface. It is used as a measurement of the concentration of all the natural **radioelements** at the surface. See also: **exposure rate**.

noise: That part of a geophysical measurement that the user does not want. Typically this includes electronic interference from the system, the atmosphere (***sferics***), and man-made sources. This can be a subjective judgment, as it may include the response from geology other than the target of interest. Commonly the term is used to refer to high frequency (short period) interference. See also ***drift***.

Occam's inversion: an ***inversion*** process that matches the measured ***electromagnetic*** data to a theoretical model of many, thin layers with constant thickness and varying resistivity (Constable et al, 1987).

off-time: In a ***time-domain electromagnetic*** survey, the time after the end of the ***primary field pulse***, and before the start of the next pulse.

on-time: In a ***time-domain electromagnetic*** survey, the time during the ***primary field pulse***.

overburden: In engineering and mineral exploration terms, this most often means the soil on top of the unweathered bedrock. It may be sand, glacial till, or weathered rock.

Phase, phase angle: The angular difference in time between a measured sinusoidal electromagnetic field and a reference – normally the primary field. The phase is calculated from $\tan^{-1}$(***in-phase*** / ***quadrature***).

physical parameters: These are the characteristics of a geological unit. For electromagnetic surveys, the important parameters are ***conductivity***, ***magnetic permeability*** (or ***susceptibility***) and ***dielectric permittivity***; for magnetic surveys the parameter is magnetic susceptibility, and for gamma ray spectrometric surveys it is the concentration of the major radioactive elements: potassium, uranium, and thorium.

permittivity: see ***dielectric permittivity***.

permeability: see ***magnetic permeability***.

primary field: the EM field emitted by a transmitter. This field induces ***eddy currents*** in (energizes) the conductors in the ground, which then create their own ***secondary* fields**.

pulse: In time-domain EM surveys, the short period of intense ***primary*** field transmission. Most measurements (the ***off-time***) are measured after the pulse. **On-time** measurements may be made during the pulse.

quadrature: that component of the measured ***secondary field*** that is phase-shifted 90° from the ***primary field***. The quadrature component tends to be stronger than the ***in-phase*** over relatively weaker ***conductivity***.

Q-coils: see ***calibration coil***.

radioelements: This normally refers to the common, naturally-occurring radioactive elements: potassium (K), uranium (U), and thorium (Th). It can also refer to man-made radioelements, most often cobalt (Co) and cesium (Cs)

radiometric: Commonly used to refer to ***gamma ray*** spectrometry.

radon: A radioactive daughter product of uranium and thorium, radon is a gas which can leak into the atmosphere, adding to the non-geological background of a gamma-ray spectrometric survey.

receiver: the ***signal*** detector of a geophysical system. This term is most often used in active geophysical systems – systems that transmit some kind of signal. In airborne ***electromagnetic*** surveys it is most often a ***coil***. (see also, ***transmitter***)

resistivity: **[ρ]** The strength with which the earth or a geological formation resists the flow of electricity, typically the flow induced by the ***primary field*** of the electromagnetic transmitter. Normally expressed in ohm-metres, it is the reciprocal of ***conductivity***.

resistivity-depth transforms: similar to ***conductivity depth transforms***, but the calculated ***conductivity*** has been converted to ***resistivity***.

resistivity section: an approximate vertical section of the resistivity of the layers in the earth. The resistivities can be derived from the ***apparent resistivity***, the ***differential resistivities***, ***resistivity-depth transforms***, or ***inversions***.

Response parameter: another name for the **induction number**.

secondary field: The field created by conductors in the ground, as a result of electrical currents induced by the ***primary field*** from the ***electromagnetic*** transmitter. Airborne ***electromagnetic*** systems are designed to create and measure a secondary field.

Sengpiel section: a ***resistivity section*** derived using the ***apparent resistivity*** and an approximation of the depth of maximum sensitivity for each frequency.

sferic: Lightning, or the ***electromagnetic*** signal from lightning, it is an abbreviation of "atmospheric discharge". These appear to magnetic and electromagnetic sensors as sharp "spikes" in the data. Under some conditions lightning storms can be detected from hundreds of kilometres away. (see ***noise***)

signal: That component of a measurement that the user wants to see – the response from the targets, from the earth, etc. (See also ***noise***)

skin depth: A measure of the depth of penetration of an electromagnetic field into a material. It is defined as the depth at which the primary field decreases to 1/e of the field at the surface. It is calculated by approximately 503 x $\sqrt{}$(resistivity/frequency). Note that depth of penetration is greater at higher ***resistivity*** and/or lower ***frequency***.

spectrometry: Measurement across a range of energies, where ***amplitude*** and energy are defined for each measurement. In gamma-ray spectrometry, the number of gamma rays are measured for each energy ***window***, to define the ***spectrum***.

spectrum: In ***gamma ray spectrometry***, the continuous range of energy over which gamma rays are measured. In ***time-domain electromagnetic*** surveys, the spectrum is the energy of the **pulse** distributed across an equivalent, continuous range of frequencies.

spheric: see ***sferic***.

stacking: Summing repeat measurements over time to enhance the repeating ***signal***, and minimize the random ***noise***.
stripping: Estimation and correction for the gamma ray photons of higher and lower energy that are observed in a particular ***energy window***. See also ***Compton scattering***.

susceptibility: See ***magnetic susceptibility***.

tau: [τ] Often used as a name for the ***time constant***.

TDEM: ***time domain electromagnetic***.

thin sheet: A standard model for electromagnetic geophysical theory. It is usually defined as a thin, flat-lying conductive sheet, ***infinite*** in both horizontal directions. (see also ***vertical plate***)

tie-line: A survey line flown across most of the ***traverse lines***, generally perpendicular to them, to assist in measuring ***drift*** and ***diurnal*** variation. In the short time required to fly a tie-line it is assumed that the drift and/or diurnal will be minimal, or at least changing at a constant rate.

time constant: The time required for an ***electromagnetic*** field to decay to a value of 1/e of the original value. In ***time-domain*** electromagnetic data, the time constant is proportional to the size and ***conductance*** of a tabular conductive body. Also called the decay constant.

Time channel: In ***time-domain electromagnetic*** surveys the decaying ***secondary field*** is measured over a period of time, and the divided up into a series of consecutive discrete measurements over that time.

time-domain: ***Electromagnetic*** system which transmits a pulsed, or stepped ***electromagnetic*** field. These systems induce an electrical current (***eddy current***) in the ground that persists after the ***primary field*** is turned off, and measure the change over time of the ***secondary field*** created as the currents ***decay***. See also ***frequency-domain***.

total energy envelope: The sum of the squares of the three ***components*** of the ***time-domain electromagnetic secondary field***. Equivalent to the ***amplitude*** of the secondary field.

transient: Time-varying. Usually used to describe a very short period pulse of ***electromagnetic*** field.

transmitter: The source of the ***signa***l to be measured in a geophysical survey. In airborne ***EM*** it is most often a **coil** carrying a time-varying electrical current, transmitting the ***primary field***. (see also ***receiver***)

traverse line: A normal geophysical survey line. Normally parallel traverse lines are flown across the property in spacing of 50 m to 500 m, and generally perpendicular to the target geology.

vertical plate: A standard model for electromagnetic geophysical theory. It is usually defined as thin conductive sheet, ***infinite*** in horizontal dimension and depth extent. (see also ***thin shee***t)

waveform: The shape of the ***electromagnetic pulse*** from a ***time-domain*** electromagnetic transmitter.

window: A discrete portion of a ***gamma-ray spectrum*** or ***time-domain electromagnetic decay***. The continuous energy spectrum or ***full-stream*** data are grouped into windows to reduce the number of samples, and reduce ***noise***.

Version 1.5, November 29, 2005
Greg Hodges,
Chief Geophysicist
Fugro Airborne Surveys, Toronto

Common Symbols and Acronyms

k Magnetic susceptibility
ε Dielectric permittivity
μ, μ_r Magnetic permeability, relative permeability
ρ, ρ_a Resistivity, apparent resistivity
σ,σ_a Conductivity, apparent conductivity
σt Conductivity thickness
τ Tau, or time constant
Ωm ohm-metres, units of resistivity
AGS Airborne gamma ray spectrometry.
CDT Conductivity-depth transform, conductivity-depth imaging (Macnae and Lamontagne, 1987; Wolfgram and Karlik, 1995)
CPI, CPQ Coplanar in-phase, quadrature
CPS Counts per second
CTP Conductivity thickness product
CXI, CXQ Coaxial, in-phase, quadrature
FOM Figure of Merit
fT femtoteslas, normal unit for measurement of B-Field
EM Electromagnetic
keV kilo electron volts – a measure of gamma-ray energy
MeV mega electron volts – a measure of gamma-ray energy 1MeV = 1000keV
NIA dipole moment: turns x current x Area
nT nanotesla, a measure of the strength of a magnetic field
nG/h nanoGreys/hour – gamma ray dose rate at ground level
ppm parts per million – a measure of secondary field or noise relative to the primary or radioelement concentration.
pT/s picoteslas per second: Units of decay of secondary field, dB/dt
S siemens – a unit of conductance
x: the horizontal component of an EM field parallel to the direction of flight.
y: the horizontal component of an EM field perpendicular to the direction of flight.
z: the vertical component of an EM field.

References:

Constable, S.C., Parker, R.L., And Constable, C.G., 1987, Occam's inversion: a practical algorithm for generating smooth models from electromagnetic sounding data: Geophysics, 52, 289-300

Huang, H. and Fraser, D.C, 1996. The differential parameter method for muiltifrequency airborne resistivity mapping. Geophysics, 55, 1327-1337

Huang, H. and Palacky, G.J., 1991, Damped least-squares inversion of time-domain airborne EM data based on singular value decomposition: Geophysical Prospecting, v.39, 827-844

Macnae, J. and Lamontagne, Y., 1987, Imaging quasi-layered conductive structures by simple processing of transient electromagnetic data: Geophysics, v52, 4, 545-554.

Sengpiel, K-P. 1988, Approximate inversion of airborne EM data from a multi-layered ground. Geophysical Prospecting, 36, 446-459

Wolfgram, P. and Karlik, G., 1995, Conductivity-depth transform of GEOTEM data: Exploration Geophysics, 26, 179-185.

Yin, C. and Fraser, D.C. (2002), The effect of the electrical anisotropy on the responses of helicopter-borne frequency domain electromagnetic systems, Submitted to *Geophysical Prospecting*

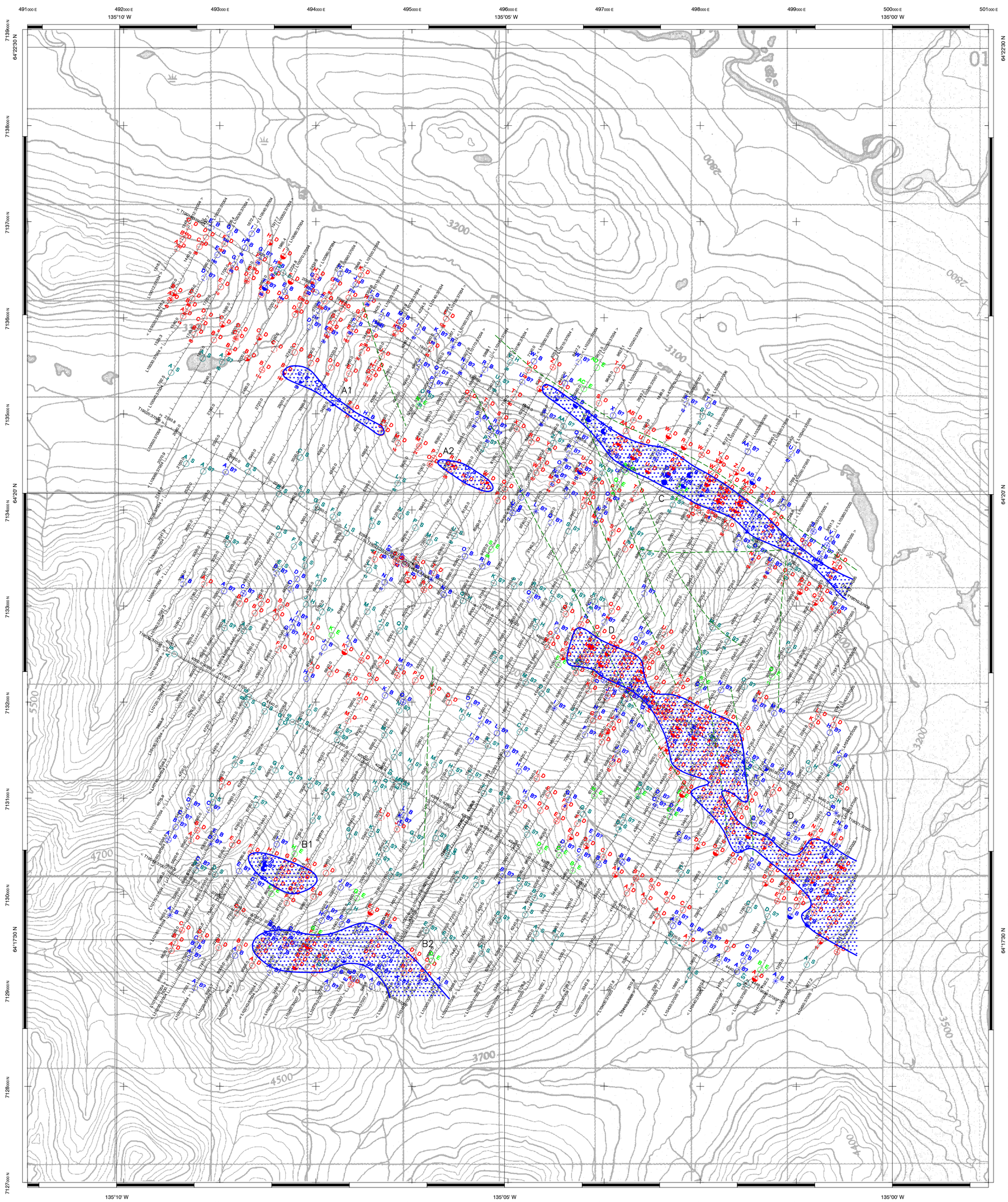

TECHNICAL SUMMARY

Navigation	Differentially-corrected GPS
Data reduction grid interval	40 metres
Terrain clearance	Helicopter 60 m Electromagnetic sensor 35 m Magnetometer 35 m
Data sampling interval	0.1 second
Magnetometer / sensitivity	Cesium / 0.01 nT
Electromagnetic system	DIGHEM^V

Frequency	Sensitivity	Coil Orientation
1000 Hz	.06 ppm	Vertical coaxial
5500 Hz	.12 ppm	Vertical coaxial
900 Hz	.12 ppm	Horizontal coplanar
7200 Hz	.24 ppm	Horizontal coplanar
56000 Hz	.60 ppm	Horizontal coplanar

ELECTROMAGNETIC ANOMALIES

Grade	Anomaly	Conductance
7	●	>100 siemens
6	◕	50–100 siemens
5	◑	20–50 siemens
4	◔	10–20 siemens
3	⊕	5–10 siemens
2	○	1–5 siemens
1	◌	< 1 siemens
–	✳	Questionable anomaly

Anomaly identifier: C1-H

Interpretive symbol

Interpretive symbol		Conductor model
	B	Bedrock conductor
	D	Narrow bedrock conductor ("thin dike")
	S	Conductive cover ("horizontal thin sheet")
	H	Broad conductive rock unit, deep conductive weathering, thick conductive cover ("half-space")
	E	Edge of broad conductor ("edge of half space")
□	L	Culture, e.g. power line, metal building or fence
△	M	Magnetite

FLIGHT LINES WITH EM ANOMALIES

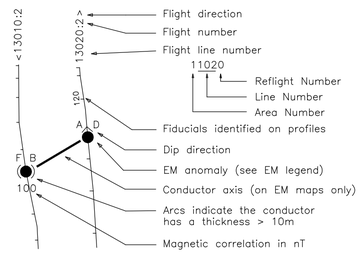

INTERPRETATION LEGEND

Inferred fault or contact

Conductive zone

LOCATION MAP

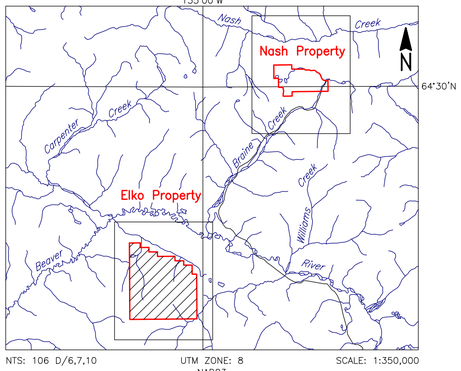

GOLDEN RIDGE RESOURCES INC.

ELKO PROPERTY, YUKON

ELECTROMAGNETIC ANOMALIES

FUGRO DIGHEM^V SURVEY	NTS: 106 D/6	GEOPHYSICIST:
DATE: OCTOBER, 2011	JOB: 11058	SHEET: 1
Fugro Airborne Surveys		

0 1 2 Km

0 1 Mi

Scale 1:20 000

FUGRO AIRBORNE SURVEYS

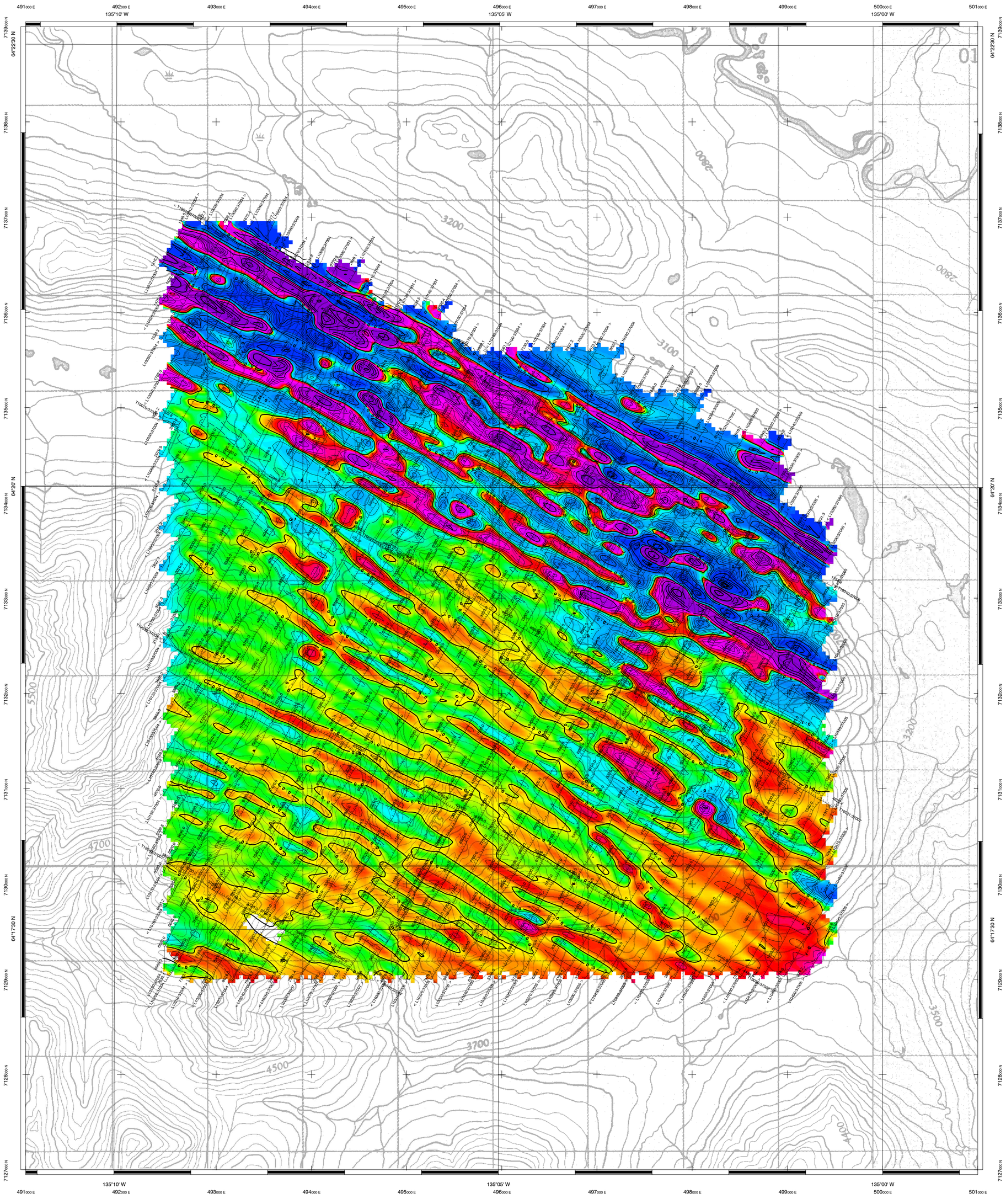

TECHNICAL SUMMARY

Navigation	Differentially–corrected GPS
Data reduction grid interval	40 metres
Terrain clearance	Helicopter 60 m Electromagnetic sensor 35 m Magnetometer 35 m
Data sampling interval	0.1 second
Magnetometer / sensitivity	Cesium / 0.01 nT
Electromagnetic system	DIGHEM^V

Frequency	Sensitivity	Coil Orientation
1000 Hz	.06 ppm	Vertical coaxial
5500 Hz	.12 ppm	Vertical coaxial
900 Hz	.12 ppm	Horizontal coplanar
7200 Hz	.24 ppm	Horizontal coplanar
56000 Hz	.60 ppm	Horizontal coplanar

nT/m

0.932
0.587
0.412
0.311
0.237
0.184
0.142
0.110
0.091
0.077
0.068
0.059
0.053
0.049
0.044
0.040
0.037
0.033
0.031
0.028
0.025
0.022
0.020
0.018
0.015
0.013
0.011
0.008
0.006
0.004
0.002
0.000
-0.002
-0.003
-0.005
-0.007
-0.009
-0.011
-0.013
-0.015
-0.017
-0.019
-0.021
-0.024
-0.027
-0.030
-0.033
-0.038
-0.044
-0.050
-0.059
-0.070
-0.084
-0.102
-0.126
-0.152
-0.185
-0.220
-0.272
-0.345
-0.431
-0.551
-0.723

FLIGHT LINES

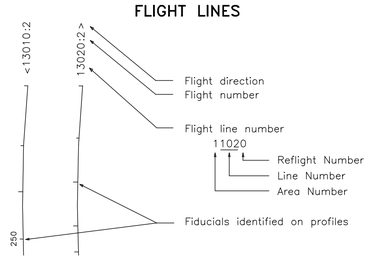

CALCULATED VERTICAL GRADIENT CONTOURS

- 2.5 nT/metre
- 0.5 nT/metre
- 0.1 nT/metre
- 0.05 nT/metre

LOCATION MAP

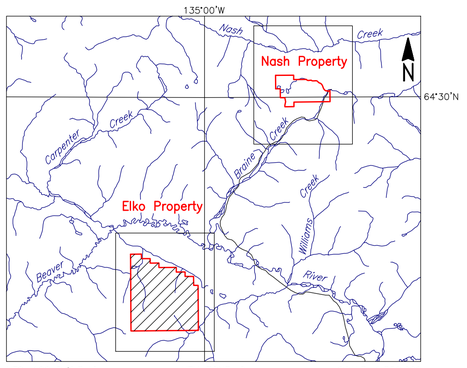

NTS: 106 D/6,7,10 | UTM ZONE: 8 NAD83 | SCALE: 1:350,000

GOLDEN RIDGE RESOURCES INC.

ELKO PROPERTY, YUKON

CALCULATED VERTICAL MAGNETIC GRADIENT

FUGRO DIGHEM^V SURVEY	NTS: 106 D/6	GEOPHYSICIST:
DATE: OCTOBER, 2011	JOB: 11058	SHEET: 1

Fugro Airborne Surveys

0 1 2 Km
0 1 Mi
Scale 1:20 000

FUGRO AIRBORNE SURVEYS

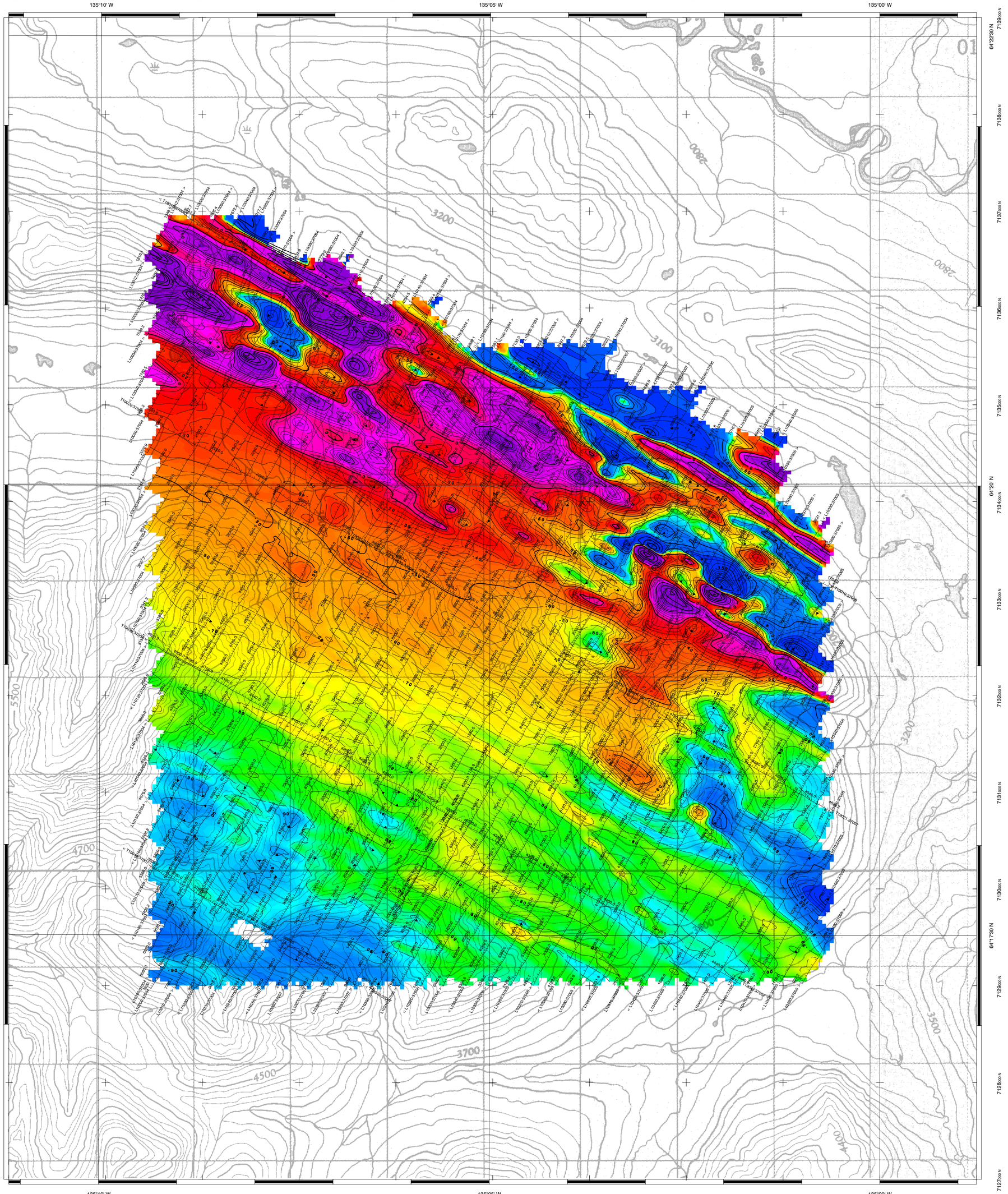

TECHNICAL SUMMARY

Navigation	Differentially–corrected GPS
Data reduction grid interval	40 metres
Terrain clearance	Helicopter 60 m Electromagnetic sensor 35 m Magnetometer 35 m
Data sampling interval	0.1 second
Magnetometer / sensitivity	Cesium / 0.01 nT
Electromagnetic system	DIGHEM^V

Frequency	Sensitivity	Coil Orientation
1000 Hz	.06 ppm	Vertical coaxial
5500 Hz	.12 ppm	Vertical coaxial
900 Hz	.12 ppm	Horizontal coplanar
7200 Hz	.24 ppm	Horizontal coplanar
56000 Hz	.60 ppm	Horizontal coplanar

nT
77.50
52.51
38.22
27.26
16.68
7.96
0.57
-6.12
-12.93
-19.57
-24.59
-29.28
-33.64
-37.01
-39.96
-42.45
-45.10
-48.09
-50.83
-53.03
-54.82
-56.77
-59.01
-60.96
-62.42
-63.87
-65.86
-67.73
-69.35
-70.97
-72.17
-73.21
-74.21
-75.16
-75.95
-76.70
-77.36
-77.94
-78.48
-79.07
-79.65
-80.19
-80.77
-81.22
-81.72
-82.22
-82.76
-83.26
-83.80
-84.38
-85.00
-85.63
-86.33
-87.12
-87.95
-88.86
-89.99
-91.11
-92.52
-93.93
-97.17
-106.72
-119.59

FLIGHT LINES

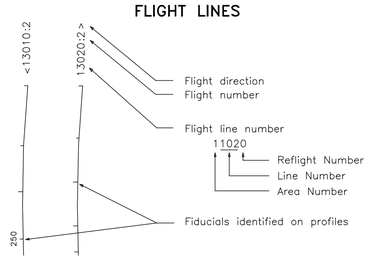

RESIDUAL MAGNETIC FIELD CONTOURS

- 250 nT
- 50 nT
- 10 nT
- 5 nT
- magnetic low

Magnetic inclination within the survey area: 79 degrees N
Magnetic declination within the survey area: 24 degrees E

LOCATION MAP

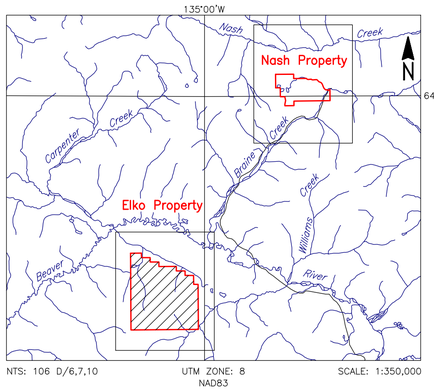

GOLDEN RIDGE RESOURCES INC.

ELKO PROPERTY, YUKON

RESIDUAL MAGNETIC FIELD

IGRF Removed

FUGRO DIGHEM^V SURVEY	NTS: 106 D/6	GEOPHYSICIST:
DATE: OCTOBER, 2011	JOB: 11058	SHEET: 1

Fugro Airborne Surveys

0 1 2 Km
0 1 Mi
Scale 1:20 000

FUGRO AIRBORNE SURVEYS

TECHNICAL SUMMARY

Navigation	Differentially-corrected GPS
Data reduction grid interval	40 metres
Terrain clearance	Helicopter 60 m Electromagnetic sensor 35 m Magnetometer 35 m
Data sampling interval	0.1 second
Magnetometer / sensitivity	Cesium / 0.01 nT
Electromagnetic system	DIGHEM^V

Frequency	Sensitivity	Coil Orientation
1000 Hz	.06 ppm	Vertical coaxial
5500 Hz	.12 ppm	Vertical coaxial
900 Hz	.12 ppm	Horizontal coplanar
7200 Hz	.24 ppm	Horizontal coplanar
56000 Hz	.60 ppm	Horizontal coplanar

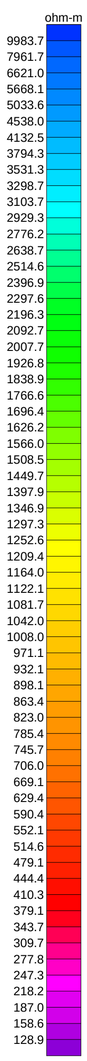

FLIGHT LINES

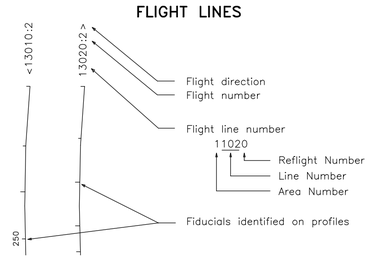

RESISTIVITY CONTOURS

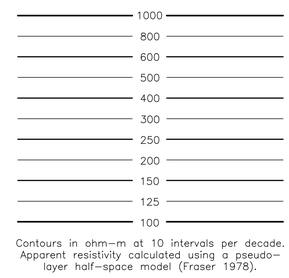

Contours in ohm-m at 10 intervals per decade. Apparent resistivity calculated using a pseudo-layer half-space model (Fraser 1978).

LOCATION MAP

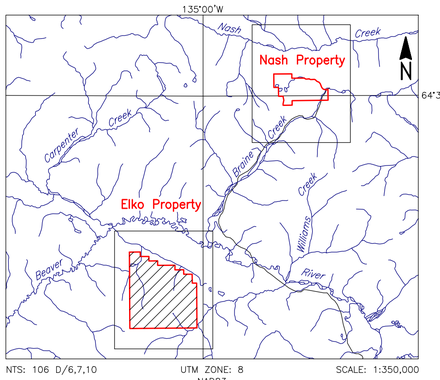

NTS: 106 D/6,7,10 UTM ZONE: 8 NAD83 SCALE: 1:350,000

GOLDEN RIDGE RESOURCES INC.

ELKO PROPERTY, YUKON

APPARENT RESISTIVITY
56,000 Hz COPLANAR

FUGRO DIGHEM^V SURVEY	NTS: 106 D/6	GEOPHYSICIST:
DATE: OCTOBER, 2011	JOB: 11058	SHEET: 1

Fugro Airborne Surveys

0 1 2 Km
0 1 Mi
Scale 1:20 000

FUGRO AIRBORNE SURVEYS

TECHNICAL SUMMARY

Navigation	Differentially-corrected GPS
Data reduction grid interval	40 metres
Terrain clearance	Helicopter 60 m Electromagnetic sensor 35 m Magnetometer 35 m
Data sampling interval	0.1 second
Magnetometer / sensitivity	Cesium / 0.01 nT
Electromagnetic system	DIGHEM^V

Frequency	Sensitivity	Coil Orientation
1000 Hz	.06 ppm	Vertical coaxial
5500 Hz	.12 ppm	Vertical coaxial
900 Hz	.12 ppm	Horizontal coplanar
7200 Hz	.24 ppm	Horizontal coplanar
56000 Hz	.60 ppm	Horizontal coplanar

ohm-m

5694.92
5145.07
4708.83
4380.30
4143.12
3930.10
3746.42
3559.90
3375.27
3178.58
2993.95
2816.19
2639.38
2477.95
2315.10
2179.24
2045.50
1942.06
1842.89
1739.45
1644.30
1551.04
1468.90
1395.05
1326.17
1260.37
1200.96
1145.10
1094.45
1047.58
997.64
944.62
895.15
843.31
797.39
751.94
706.02
662.71
620.81
581.28
539.62
501.75
468.38
430.51
399.97
368.73
337.48
309.32
283.04
256.06
232.15
211.56
190.49
169.66
149.31
130.37
110.25
91.79
74.04
59.60
49.19
41.85
34.51

FLIGHT LINES

<13010-2

13020-2>

Flight direction
Flight number
Flight line number
11020
Reflight Number
Line Number
Area Number
Fiducials identified on profiles
250

RESISTIVITY CONTOURS

1000
800
600
500
400
300
250
200
150
125
100

Contours in ohm-m at 10 intervals per decade. Apparent resistivity calculated using a pseudo-layer half-space model (Fraser 1978).

LOCATION MAP

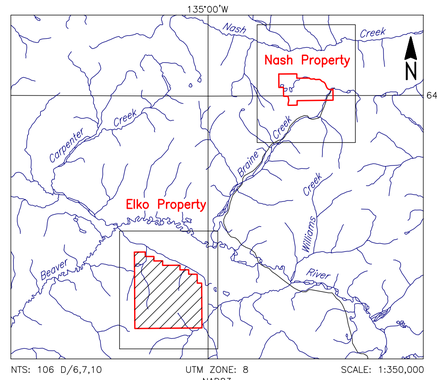

NTS: 106 D/6,7,10 UTM ZONE: 8 NAD83 SCALE: 1:350,000

GOLDEN RIDGE RESOURCES INC.

ELKO PROPERTY, YUKON

APPARENT RESISTIVITY
7200 Hz COPLANAR

FUGRO DIGHEM^V SURVEY	NTS: 106 D/6	GEOPHYSICIST:
DATE: OCTOBER, 2011	JOB: 11058	SHEET: 1

Fugro Airborne Surveys

0 1 2 Km
0 1 Mi
Scale 1:20 000

FUGRO AIRBORNE SURVEYS

TECHNICAL SUMMARY

Navigation	Differentially-corrected GPS
Data reduction grid interval	40 metres
Terrain clearance	Helicopter 60 m Electromagnetic sensor 35 m Magnetometer 35 m
Data sampling interval	0.1 second
Magnetometer / sensitivity	Cesium / 0.01 nT
Electromagnetic system	DIGHEM^V

Frequency	Sensitivity	Coil Orientation
1000 Hz	.06 ppm	Vertical coaxial
5500 Hz	.12 ppm	Vertical coaxial
900 Hz	.12 ppm	Horizontal coplanar
7200 Hz	.24 ppm	Horizontal coplanar
56000 Hz	.60 ppm	Horizontal coplanar

ohm-m

1079.98
1079.95
1079.80
1079.43
1078.56
1076.89
1074.27
1070.07
1063.77
1055.87
1045.25
1031.42
1016.81
997.70
976.15
952.93
926.69
901.68
872.78
839.47
808.07
773.73
739.71
707.79
673.24
638.44
603.92
572.12
538.44
507.44
475.79
445.17
413.52
383.66
353.41
325.93
298.70
273.60
250.38
227.31
205.67
186.47
169.98
153.31
138.73
125.09
112.12
99.86
89.03
77.66
68.65
59.76
50.77
43.89
37.43
32.06
26.44
21.90
18.23
15.45
13.29
11.22
9.22

FLIGHT LINES

<13010-2
13020-2>
250

Flight direction
Flight number
Flight line number
11020
Reflight Number
Line Number
Area Number
Fiducials identified on profiles

RESISTIVITY CONTOURS

1000
800
600
500
400
300
250
200
150
125
100

Contours in ohm-m at 10 intervals per decade. Apparent resistivity calculated using a pseudo-layer half-space model (Fraser 1978).

LOCATION MAP

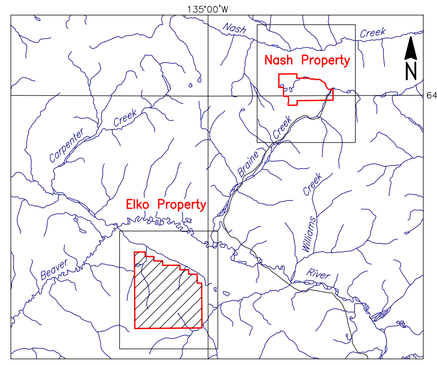

NTS: 106 D/6,7,10 UTM ZONE: 8 NAD83 SCALE: 1:350,000

GOLDEN RIDGE RESOURCES INC.

ELKO PROPERTY, YUKON

APPARENT RESISTIVITY
900 Hz COPLANAR

FUGRO DIGHEM^V SURVEY	NTS: 106 D/6	GEOPHYSICIST:
DATE: OCTOBER, 2011	JOB: 11058	SHEET: 1

Fugro Airborne Surveys

0 1 2 Km
0 1 Mi
Scale 1:20 000

FUGRO

FUGRO AIRBORNE SURVEYS